

Mechanistic aspects of DNA uptake in naturally competent *Vibrio cholerae*

THÈSE N° 6164 (2014)

PRÉSENTÉE LE 23 MAI 2014

À LA FACULTÉ DES SCIENCES DE LA VIE

UNITÉ DE LA PROF. BLOKESCH

PROGRAMME DOCTORAL EN APPROCHES MOLÉCULAIRES DU VIVANT

ÉCOLE POLYTECHNIQUE FÉDÉRALE DE LAUSANNE

POUR L'OBTENTION DU GRADE DE DOCTEUR ÈS SCIENCES

PAR

Patrick Martin SEITZ

acceptée sur proposition du jury:

Prof. N. Harris, présidente du jury
Prof. M. Blokesch, directrice de thèse
Prof. S. Cole, rapporteur
Prof. C. Dehio, rapporteur
Prof. P. Polard, rapporteur



ÉCOLE POLYTECHNIQUE
FÉDÉRALE DE LAUSANNE

Suisse
2014

Parts of this thesis are published in:

Seitz, P., Pezeshgi Modarres, H, Borgeaud, S, Bulushev, R. D, Steinbock, L. J, Radenovic, A, Dal Peraro, M, & Blokesch, M. (2014) ComEA is essential for the transfer of external DNA into the periplasm in naturally transformable *Vibrio cholerae* cells. *PLoS Genet* 10, e1004066.

Seitz, P. & Blokesch, M. (2013) DNA-uptake machinery of naturally competent *Vibrio cholerae*. *Proc Natl Acad Sci U S A* 110, 17987-17992.

Seitz, P. & Blokesch, M. (2013) Cues and regulatory pathways involved in natural competence and transformation in pathogenic and environmental Gram-negative bacteria. *FEMS Microbiol Rev* 37, 336-363.

Suckow, G, **Seitz, P.** & Blokesch, M. (2011) Quorum sensing contributes to natural transformation of *Vibrio cholerae* in a species-specific manner. *J Bacteriol* 193, 4914-4924.

Abstract

The physiological state of competence for natural transformation allows bacteria to take up free DNA from the environment and recombine it into their genome. As one of three modes of horizontal gene transfer, natural transformation has hence contributed substantially to the enormous diversity and plasticity of bacterial genomes. With its potential to promote the spread of antibiotic resistances and virulence factors of a variety of pathogens, natural transformation also has an important impact on human health. Even though conserved components required to undergo natural transformation have been identified in many bacterial species, our knowledge on the underlying mechanism of DNA transport remains very limited. To better understand this aspect, we established a first model of DNA uptake in the naturally competent human pathogen *Vibrio cholerae*. We showed that at least twenty proteins are required for efficient uptake, protection and recombination of transforming DNA in a non-species-specific manner. 14 of these proteins are needed to produce a type IV pilus, which we were able to visualize for the first time. We showed that this competence pilus is not restricted to cell poles, as has been shown for other competent bacterial species (e.g. *Bacillus subtilis*). Furthermore, we compared the position of this pilus to the localization of other competence proteins and determined their role in the assembly of a surface exposed pilus fiber. While this type IV pilus is important for efficient DNA uptake, we also observed rare transformation events in its absence. In contrast, three pilus-unrelated proteins that are likely involved in the transport process were absolutely required for transformation. Two of them were implicated in DNA transport across the inner membrane. Deletion of the corresponding genes led to a strong accumulation of transforming DNA within the periplasm. However, one of them, ComEA, was essential for DNA uptake across the outer membrane, independently of competence pili. We further characterized the role of this protein by showing that it is localized to the periplasm of competent *V. cholerae* cells and that it binds to DNA *in vivo*. Based on our results, we proposed that ComEA directly contributes to DNA transport. Although we showed that DNA uptake across the outer membrane and translocation of DNA into the cytoplasm are functionally uncoupled, our results suggest that the two events coincide spatially. In summary, these findings allow us to present a first mechanistic model of the DNA uptake process in *V. cholerae*. Many aspects of this model likely apply to other naturally competent bacteria, and therefore represent an important contribution to the general understanding of this basic biological process.

Keywords: Horizontal gene transfer, natural competence, transformation, DNA uptake, protein localization, type IV pilus, *Vibrio cholerae*, ComEA protein

Zusammenfassung

Natürliche Kompetenz für Transformation ist ein physiologischer Zustand, in welchem Bakterien freie DNA aus ihrer Umgebung aufnehmen und in ihr Genom integrieren können. Als eine von drei bekannten Formen des horizontalen Gentransfers hat natürliche Transformation wesentlich zur enormen Diversität und Plastizität bakterieller Genome beigetragen. Von medizinischer Bedeutung ist dieser Vorgang vor allem durch sein Potential zur Verbreitung von Antibiotika-Resistenzen und Virulenzfaktoren in zahlreichen Krankheitserregern. Obwohl einige konservierte Proteine, welche für die natürliche Transformation unterschiedlicher Bakterien benötigt werden, bereits identifiziert wurden, bleiben die zugrunde liegenden molekularen Mechanismen unklar. Dies trifft insbesondere auf die DNA-Aufnahme zu. Um diesen Aspekt besser zu verstehen, haben wir den Mechanismus der DNA-Aufnahme zum ersten Mal im natürlich kompetenten Humanpathogen *Vibrio cholerae* untersucht. Es hat sich gezeigt, dass mindestens zwanzig Proteine zur effizienten Aufnahme, zum Schutz und zur Rekombination von transformierender DNA benötigt werden. Die Herkunft der DNA war dabei nicht entscheidend für deren Aufnahme. Wie wir zum ersten Mal nachweisen konnten, sind 14 der identifizierten Proteine an der Produktion eines Typ IV Pilus beteiligt. Im Gegensatz zu Studien in anderen Bakterien (z.B. in *B. subtilis*) war die Lokalisation dieses Kompetenz-Pilus nicht auf den Zellpol beschränkt. Ausserdem wurde die Position des Pilus in Bezug auf bestimmte kompetenz-relevante Proteine bestimmt und der Einfluss von verschiedenen Kompetenzproteinen auf die Ausbildung eines Pilus auf der bakteriellen Zelloberfläche nachgewiesen. Obwohl diese Struktur wichtig für eine effiziente DNA-Aufnahme ist, konnten wir auch seltene Transformationsereignisse beobachten, welche nicht von einem intakten Kompetenz-Pilus abhängig waren. Jedoch waren drei Proteine, die wahrscheinlich am Transportprozess beteiligt sind, essenziell für die natürliche Transformierbarkeit. Wie sich herausstellte, sind zwei dieser Proteine am Transport der DNA durch die innere Membran beteiligt, da sich DNA in Bakterien, die die entsprechenden Gene nicht besitzen, im Periplasma anreicherte. Ein Protein jedoch, ComEA, war unerlässlich für den Transport von DNA durch die äussere Membrane, unabhängig von der Präsenz von Kompetenz-Pili. Durch eine genauere Untersuchung dieses Proteins konnten wir aufzeigen, dass ComEA in das Periplasma von kompetenten *V. cholerae* Zellen transportiert wird, wo es an transformierende DNA bindet. Unsere Ergebnisse legen nahe, dass ComEA direkt zur Aufnahme von DNA beiträgt. Obwohl wir zeigen konnten, dass die Aufnahme von DNA durch die äussere Membran und deren Transport ins Zytoplasma funktionell nicht zusammenhängen, lässt sich aufgrund unserer Resultate darauf schliessen, dass sich diese beiden Ereignisse in unmittelbarer Nähe zueinander abspielen. Zusammenfas-

Zusammenfassung

send erlauben uns diese Erkenntnisse ein erstes mechanistisches Modell der DNA-Aufnahme in *V. cholerae* zu präsentieren. Zahlreiche Aspekte dieses Modells treffen mit einiger Wahrscheinlichkeit auch auf weitere natürlich kompetente Bakterien zu, weshalb diese Arbeit einen wichtigen Beitrag zum generellen Verständnis dieses grundlegenden biologischen Vorgangs darstellt.

Schlagwörter: Horizontaler Gentransfer, natürliche Kompetenz, Transformation, DNA-Aufnahme, Protein Lokalisation, Type IV Pilus, *Vibrio cholerae*, ComeEA

Contents

Abstract (English/Deutsch)	iii
List of figures	xi
List of tables	xiii
List of abbreviations	xv
1 Introduction	1
1.1 Horizontal gene transfer in bacteria	1
1.1.1 Horizontal gene transfer from a medical point of view	2
1.1.2 Conjugation and transduction	3
1.1.3 Natural transformation	4
1.2 The mechanism of DNA uptake during natural transformation	7
1.2.1 Type IV pili and type II secretion systems	8
1.2.2 DNA transport machineries in Gram-negative and Gram-positive bacteria	10
1.2.3 The need for new models	13
1.3 <i>Vibrio cholerae</i> , a naturally competent human pathogen	13
1.3.1 The dual role of <i>Vibrio cholerae</i> as human pathogen and member of aquatic ecosystems	14
1.3.2 The complex regulation of natural competence in <i>Vibrio cholerae</i> . . .	17
1.3.3 DNA uptake in naturally competent <i>Vibrio cholerae</i>	19
1.4 Aims and scope of the thesis	20
2 Components of the <i>Vibrio cholerae</i> DNA uptake machinery	21
2.1 Results	21
2.1.1 <i>In silico</i> prediction of DNA transport related competence genes	21
2.1.2 Transformability of mutants lacking individual competence genes . .	22
2.1.3 Detection of heterologous DNA uptake events in competent <i>Vibrio</i> <i>cholerae</i>	24
2.1.4 Natural transformability of competence gene mutants in a chitin-inde- pendent competence induction setup using TntfoX	26
2.1.5 Detection of rare transformation events on chitin flakes	29

Contents

2.1.6	DNA uptake across the outer membrane is not functionally coupled to inner membrane transport	29
2.2	Discussion	31
2.2.1	A first model of the <i>Vibrio cholerae</i> DNA uptake machinery	31
2.2.2	DNA uptake in <i>Vibrio cholerae</i> is a multi-step process	34
2.2.3	Uptake of heterologous DNA by naturally competent <i>Vibrio cholerae</i>	36
3	Visualization of competence pili	37
3.1	Results	37
3.1.1	Construction of a functional tagged version of PilA	37
3.1.2	Defining the <i>TntfoX</i> induced competence window	38
3.1.3	Visualization of PilA containing competence pili	39
3.1.4	Piliation of competence gene mutants	39
3.1.5	Localization of other pilus-related competence proteins	41
3.1.6	The ATPase activity of PilB is needed for protein function and its dynamic localization	43
3.2	Discussion	45
3.2.1	Localization of competence pili and outer membrane secretins	45
3.2.2	Pilus biogenesis in competence gene mutants	46
3.2.3	Distribution patterns of the cytoplasmic ATPases PilB and PilT	46
4	ComEA and the mechanism of DNA uptake	49
4.1	Results	49
4.1.1	ComEA forms a pool of mobile proteins within the periplasm	49
4.1.2	ComEA binds to DNA <i>in vivo</i>	51
4.1.3	tDNA induced ComEA foci are associated with PilQ clusters	54
4.1.4	Persistence of tDNA induced ComEA foci is heterogenous	55
4.1.5	ComEA contributes to DNA transport across the outer membrane	56
4.1.6	Dns is involved in the resolution of tDNA induced ComEA foci	56
4.1.7	Establishing a tool to visualize DNA transport across the inner membrane	57
4.1.8	DNA transport across the outer and inner membrane coincides spatially	61
4.2	Discussion	65
4.2.1	Periplasmic ComEA contributes to DNA uptake across the outer membrane	65
4.2.2	Specification of ComEA's DNA binding capacity	67
4.2.3	The role of the secreted nucleases Dns and Xds	68
4.2.4	Transport of DNA across the inner membrane	69
5	Conclusion and perspectives	73
5.1	Conclusion	73
5.2	Perspectives	74

6	Materials and methods	77
6.1	Culture media and growth conditions	77
6.2	Plasmid and strain construction	77
6.3	Homology search and sequence alignment	78
6.4	Natural transformation assays	79
6.5	Detection of DNA uptake by PCR	80
6.6	Fluorescence microscopy	82
6.7	Cell lysates, SDS-PAGE and western blot analysis	85
A	Appendix	87
A.1	Strain list	89
A.2	Plasmid list	95
	References	97
	Curriculum Vitae	111
	Acknowledgements	113

List of Figures

1.1	Modes of horizontal gene transfer	3
1.2	Homologous recombination during natural transformation	5
1.3	The type II secretion system and type IV pilus of Gram-negative bacteria	8
1.4	Putative composition of DNA uptake machineries	11
1.5	Scanning electron micrograph of <i>V. cholerae</i>	14
1.6	Serogroups and biotypes of <i>V. cholerae</i>	16
1.7	Regulation of natural competence in <i>V. cholerae</i>	17
2.1	Uptake of heterologous DNA by naturally competent <i>V. cholerae</i> cells	25
2.2	Chitin-independent natural transformation in strains lacking individual competence proteins	27
2.3	Detection of rare transformation events after chitin-mediated competence induction	29
2.4	Detection of internalized tDNA by whole-cell duplex PCR	30
2.5	Proposed model of the <i>V. cholerae</i> DNA uptake machinery	31
3.1	Chitin-independent transformation of <i>V. cholerae</i> tested throughout different growth phases	39
3.2	Visualization of the competence-induced pilus	40
3.3	Piliation of competence gene mutants	40
3.4	Cellular localization of specific competence proteins	42
3.5	Transient co-localization of the cytoplasmic ATPases PilB and PilT with the outer membrane secretin PilQ in time-lapse microscopy experiments	43
3.6	The atypical Walker B motif of PilB is essential for pilus formation and natural transformation	44
4.1	Localization of plasmid encoded ComEA-mCherry in competent <i>V. cholerae</i> cells	50
4.2	Fluorescence loss in photobleaching (FLIP) reveals ComEA mobility within the periplasm	50
4.3	Cytoplasmic ComEA binds to the chromosome of <i>E. coli</i>	51
4.4	Periplasmic ComEA-mCherry aggregates into fluorescent foci upon exposure of competence-induced cells to exogenous DNA	52
4.5	ComEA binds to DNA <i>in vivo</i>	53

List of Figures

4.6	Time-lapse microscopy series of competent bacteria exposed to exogenous DNA	54
4.7	The position of ComEA focus formation is associated with PilQ clusters	55
4.8	ComEA-mCherry focus persistence during DNA uptake	56
4.9	The absence of Dns and Xds does not rescue the $\Delta comEA$ phenotype	57
4.10	The absence of Dns correlates with a delay in the resolution of ComEA-mCherry foci	57
4.11	Localization and functionality of chromosomally encoded RecA-GFP	59
4.12	RecA-GFP accumulations are not part of misfolded protein aggregates	60
4.13	Co-localization of ComEA-mCherry and RecA-GFP in competence-induced live cells	62
4.14	Time-lapse microscopy imaging of RecA-GFP ComEA-mCherry expressing bacteria exposed to exogenous tDNA	63
4.15	Strains deficient in <i>dns</i> show an increased frequency of <i>de novo</i> RecA-GFP focus formation	64
4.16	Working model of how DNA translocation across the outer membrane might occur in <i>V. cholerae</i>	66
4.17	<i>In silico</i> -prediction of the ComEA-DNA complex	68
6.1	Replacement of chromosomal <i>pilA</i> through TransFLP	79

List of Tables

2.1	Competence gene homologs	22
2.2	Chitin-induced natural transformation assay of <i>V. cholerae</i> competence gene mutants	23
2.3	Natural transformability of <i>trans</i> complemented competence gene mutants	28
3.1	Functional validation of PilA-Strep constructs during natural transformation	38
3.2	Quantification of surface exposed pili in mutant strains of <i>V. cholerae</i>	41
3.3	Functional validation of fluorescent fusion constructs	41
4.1	Transformation frequencies of strains expressing translational fusion constructs	58
6.1	Primers used for the detection of DNA uptake by PCR	82
A.1	List of <i>V. cholerae</i> strains used in this work	89
A.2	List of plasmids used in this work	95

List of abbreviations

aa	Amino acid(s)
AI-2	Autoinducer-2
bp	Base pairs
CAI-1	Cholera autoinducer 1
cAMP	Cyclic adenosine monophosphate
CCR	Carbon catabolite repression
CFU	Colony forming units
CTX	Cholera toxin
DAPI	4',6-diamidino-2-phenylindole
DASW	Defined artificial seawater
DR	DNA receptor
dsDNA	Double stranded DNA
FOV	Field of view
FRT	Flippase recognition target
HGT	Horizontal gene transfer
HhH	Helix hairpin helix
kb	Kilo base pairs
kDa	Kilo dalton
L-ara	L-(+)-arabinose
LPS	Lipopolysaccharide
MCS	Multiple cloning site
OD ₆₀₀	Optical density measured at 600nm
PAI	Pathogenicity island
PBS	Phosphate buffered saline
PCR	Polymerase chain reaction
QS	Quorum sensing
ROI	Region of interest
SD	Standard deviation
ssDNA	Single stranded DNA
T2SS	Type II secretion system
T4P	Type IV pilus
T4SS	Type IV secretion system
TCP	Toxin coregulated pilus
tDNA	Transforming DNA
TF	Transformation frequency
VPI-1	<i>Vibrio</i> pathogenicity island 1
WT	Wildtype

1 Introduction

1.1 Horizontal gene transfer in bacteria

Bacterial genomes exhibit an enormous degree of plasticity. The ever-growing amount of whole genome sequence data available for different bacterial species, as well as for particular strains of one bacterial lineage, allows us to get a glimpse of the true genomic diversity in the bacterial kingdom. Important causes for the observed diversity are mutations in the bacterial chromosome that can cause modification, inactivation or altered expression of existing genes. However, the classical concept of mutations that cause variation, on the basis of which natural selection promotes the spread of beneficial traits within bacterial populations, falls short of explaining the entire extent of genomic diversity. Instead, the increased availability of whole genome sequences from various bacterial isolates clearly indicates that horizontal gene transfer (HGT) has played, and continues to play, a key role in evolution.

HGT, also referred to as lateral gene transfer, allows bacteria to acquire and exchange genetic information. This horizontal transfer of genetic material, as opposed to vertical transfer from parents to offspring, can occur between members of the same species, as well as across species boundaries and even between members of different kingdoms (reviewed recently by Julie C. Dunning Hotopp [1]). The constant flux of genetic information between and within taxonomic groups allows bacteria to rapidly adapt to new ecological niches or changing environmental conditions and has therefore had a tremendous impact on evolution (reviews covering the role of HGT during evolution include [2–6]).

Shortly after publication of the first genome sequence of an *Escherichia coli* strain in 1997 [7], the impact of HGT on the evolution of *E. coli* was assessed bioinformatically [8]. The authors of this study estimated that the *E. coli* chromosome has gained 755, or 17.6% of the 4,288 identified open reading frames through HGT. In fact, several important metabolic functions, such as lactose utilization or indole production, are encoded by genes that have been acquired horizontally. However, not only metabolic genes can readily be transferred by HGT. Early during the last century, it became evident that HGT plays an important role in transferring virulence factors. This process has the potential to render harmless commensal bacteria into lethal pathogens and is therefore of outstanding importance from a medical point of view, as outlined in the next paragraph.

1.1.1 Horizontal gene transfer from a medical point of view

In 1928, Fred Griffith performed experiments with different strains of *Streptococcus pneumoniae*, which demonstrated for the first time that virulence factors can be transferred laterally between these bacteria [9]. In his experiments, he mixed a heat inactivated mouse-pathogenic strain of *S. pneumoniae* with a viable, but non-pathogenic strain. This transformed the non-pathogenic viable strain into a lethal pathogen that quickly caused pneumonia and death in mice. At this time it was not clear, what agent was carrying the genetic information that was transferred from dead to viable bacteria. However, his work laid the foundation of the experimental proof that DNA, rather than proteins, is the universal carrier of genetic information. Several researchers, in particular Oswald Avery, Colin MacLeod and Maclyn McCarty continued to identify the “transforming principle” that was transferred between different strains of *S. pneumoniae*, and they finally suggested that genes are actually made of DNA [10].

Much later, with whole genome sequences of many human pathogens available, it became clear that transfer of virulence determinants from one strain to another, as observed for the first time by Griffith in 1928, was not an exception. HGT is responsible for the spread and exchange of many different virulence factors of diverse human pathogens. Such virulence factors are often arranged in so called pathogenicity islands (PAIs) [11, 12]. PAIs are distinct genetic elements on the chromosome of many bacterial pathogens and often harbor multiple virulence factors. They are acquired by HGT and therefore often show a distinct GC-content and codon usage pattern, which can differ dramatically from the remaining bacterial genome. Furthermore, PAIs are often absent in non-pathogenic strains of the same or closely related species. PAIs can mediate very different functions involved in pathogenicity, such as adherence (e.g. the *Vibrio cholerae* toxin co-regulated pilus), expression of toxins (e.g. α -hemolysin of uropathogenic *E. coli* strains), invasion into host cells (e.g. *inv* genes of *Salmonella spp.*), production of siderophores (e.g. yersiniabactin) or secretion of effectors (e.g. type III and IV secretion systems in *Yersinia* or *Shigella* species) [13, 14].

Additionally, there is another aspect of HGT that currently raises big concerns and poses even bigger challenges for the future. Since the 1950s, HGT has been directly associated with the spread of antibiotic resistances [15–17]. Today, it is widely accepted that HGT plays a key role in the spread of resistances, which renders many of the known antibiotics ineffective. Public-health officials around the globe are currently sounding an alarm, such as the chief medical officer of the United Kingdom, who recommends to add antibiotic resistances to the UK government’s list of threats to national security, like pandemic influenza and terrorism (see Editorial article in *Nature* 495:141; 2013). In the USA, the Centers for Disease Control and Prevention (CDC) published a report in autumn 2013, which presents the first snapshot of the burden and threats posed by antibiotic resistant human pathogens (Antibiotic Resistance Threats in the United States, 2013). They conclude that every year, at least 2 million people get infected with antibiotic resistant bacteria or fungi in the USA. As a consequence, 23,000 patients are estimated to die annually. Regarding the hazard level of different bacterial pathogens, the CDC introduced for the first time three distinct categories: urgent, serious and concerning. Three pathogens were classified as “urgent” threats, with a potentially devastating impact on human health and on economics: *Clostridium difficile*, carbapenem-resistant

1.1. Horizontal gene transfer in bacteria

Enterobacteriaecae and cephalosporin-resistant *Neisseria gonorrhoeae*. Not surprisingly, HGT is known to shape the genome of two of these pathogens (*C. difficile* and *N. gonorrhoeae*) and is implicated in the spread of carbapenem resistance among Enterobacteriaecae [18–22].

Given the huge impact of HGT on the evolution of pathogenic bacteria and the current spread of antibiotic resistances, it is of major interest to better understand the mechanisms that account for the constant flux of genetic information. Three general modes of HGT have been described so far (Figure 1.1): conjugation, transduction and natural transformation.

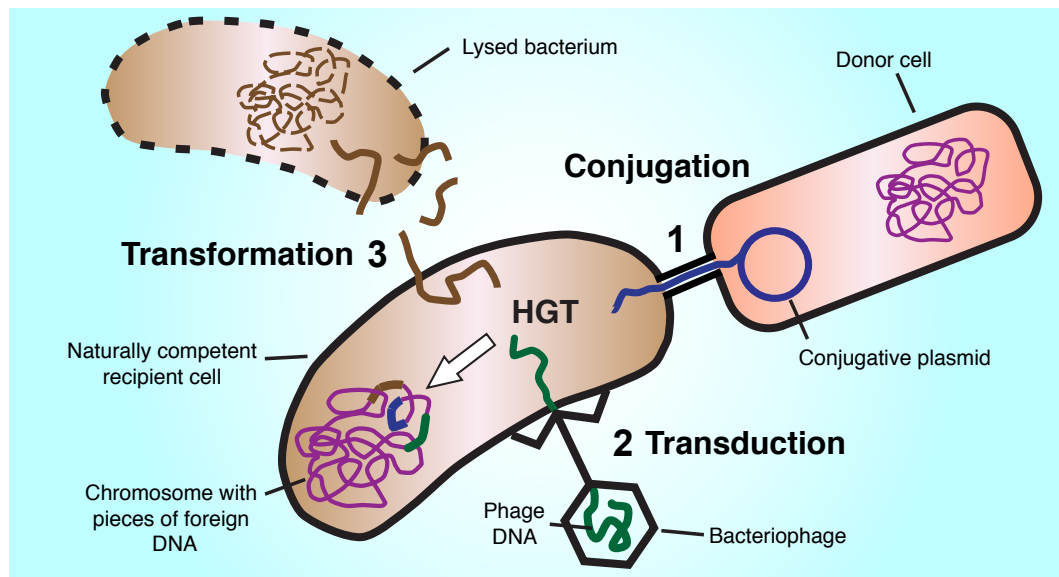


Figure 1.1: Modes of horizontal gene transfer. Foreign DNA can enter the bacterial cytoplasm through three general mechanisms; (1) Conjugation mediates transfer of conjugative plasmids (blue) from a donor to a recipient cell. Depending on the nature of the transferred DNA, it can either integrate into the recipient's chromosome (purple) or replicate autonomously as a plasmid (not shown). (2) Bacteriophages can inject DNA (green) directly into the cytoplasm, which is known as transduction. (3) Naturally competent cells are in a state in which they can take up free DNA (brown) from the environment and eventually integrate it into their genome. The latter process is called natural transformation. Transferred DNA can also be lost due to failure of chromosomal integration and subsequent degradation or cell lysis (not indicated). Scheme not drawn to scale.

1.1.2 Conjugation and transduction

Bacterial conjugation was discovered more than 65 years ago by Joshua Lederberg and Edward Tatum in *E. coli* [23]. Since then, our understanding of this process increased dramatically (see [24] for a review on the detailed mechanism of F conjugation). As a general rule, to which there are exceptions that are not further described in this introduction, conjugation is mediated by conjugative plasmids, which encode proteins that allow the establishment of cell-to-cell contacts between a donor and a recipient cell (Figure 1.1). In addition, these plasmids harbor genes that promote the actual transfer of DNA. In a first step, a complex molecular machine that belongs to the group of type IV secretion systems (T4SS) initiates the formation of a conjugative pilus. Conjugative pili are retractable cell appendages that can bind to recipient cells and bring them into close proximity to donor cells. A series of still not fully

understood steps then leads to the formation of a pore between the two cells, called the mating bridge (reviewed in [24]). Within the donor cell, transfer of DNA is initiated by nicking one strand of the DNA to be transferred - usually the conjugative plasmid itself - in a site-specific manner. The protein relaxase then binds covalently to the free 5' end of the nicked DNA and forms a nucleoprotein complex. Finally, the T4SS transfers the nucleoprotein complex into the recipient cell, where the complementary missing strand of the transferred single stranded DNA is synthesized. Upon re-circularization, the transferred DNA can replicate as plasmid, thereby converting the recipient cell into a potential donor cell.

Transduction on the other hand relies on bacteriophages that directly inject their genetic material into host cells for replication (see [25] for a general introduction). Upon receptor binding and DNA injection, lytic phages cause replication of their genome, followed by bacterial cell lysis to liberate new infective virions. During the packaging of viral DNA, prior to cell lysis, the enzymes responsible for this process can accidentally package parts of the host DNA instead of viral DNA. The resulting particles then have the potential to transfer host DNA to other bacteria (generalized transduction). Temperate phages in contrast can site-specifically integrate into the host chromosome and replicate as part of the bacterial genome (lysogenic cycle). After induction, viral DNA is excised and packaged into virions. When phage DNA is excised incorrectly, some of the host genes adjacent to the viral DNA can be co-transferred during this process. Such particles can then infect other cells and thereby spread the co-packaged host DNA (specialized transduction, [26]). In summary, both mechanisms, generalized as well as specialized transduction, have the potential to transfer bacterial DNA from one cell to another.

1.1.3 Natural transformation

Natural transformation is a process that allows bacteria to take up free DNA from the environment and subsequently recombine it into their genome. The physiological state in which bacteria can undergo natural transformation is called natural competence (for transformation).

Conceptually, natural transformation differs fundamentally from other modes of HGT. For both, conjugation and transduction, direct cell-to-cell contacts are required. Bacteriophages need to bind to specific receptors on the cell surface, in order to inject their genome into host cells. Similarly, conjugative plasmids have a defined host range to which they can be transferred. This limits the number of possible HGT events. In contrast, natural transformation does not require direct cell-to-cell contacts. It is solely initiated and controlled by the recipient cell. Competent bacteria therefore have access to an almost infinite genetic pool, which is present naturally in the environment. Amounts of free accessible DNA range from a few $\mu\text{g/l}$ in aquatic ecosystems [27] to 23-435 $\mu\text{g/g}$ within marine sediments [28]. Up to 12 $\mu\text{g/g}$ DNA can be isolated from soil samples [29] and even in human blood plasma, cell free DNA concentrations range from 1.6-29.1 $\mu\text{g/l}$ [30].

Nevertheless, as for conjugation and transduction, there are important limitations to natural transformation. Once DNA has entered the cytoplasm, it needs to replicate in order to persist in successive generations. While plasmids can replicate independently of chromo-

somal DNA, linear DNA fragments, which are much more efficiently transferred by natural transformation [31], need to recombine into the bacterial chromosome. Several mechanisms can account for that and have recently been reviewed by Thomas *et al.* [31].

DNA recombination during transformation

Homologous recombination can efficiently drive integration of horizontally transferred DNA into the bacterial chromosome, provided that there is a sufficient level of sequence similarity between incoming DNA and the recipient genome (Figure 1.2). Homologous recombination during natural transformation is initiated by the presence of single stranded DNA (ssDNA), which is thought to be the general product of the DNA transfer into the cytoplasm [32]. The events from entry of ssDNA into the cytoplasm to its recombination into the chromosome by homologous recombination have been investigated recently in an *in vitro* system, of *Streptococcus pneumoniae*, *B. subtilis* and *E. coli* proteins [33]. The authors propose a model, in which the single strand binding protein SsbB binds a large fraction of ssDNA, thereby protecting it from degradation. Another conserved competence protein, DprA (DNA processing A), then either binds to SsbB-bound DNA, thereby replacing SsbB or to free ssDNA. Either way, DprA facilitates loading of RecA on the nucleoprotein filament (Figure 1.2). RecA is a universally conserved DNA repair and maintenance protein, which can catalyze strand exchange and the formation of a heteroduplex between transforming DNA and the recipient chromosome during natural transformation (Figure 1.2). A high degree of sequence homology is needed during this step. In *Streptococcus pneumoniae*, for example, transformation frequencies drop exponentially with increasing sequence divergence [34]. Finally, the heteroduplex segregates during replication and cell division, yielding a transformed and a wildtype cell (Figure 1.2). Similar events likely take place in most other competent bacteria (reviewed in [35]).

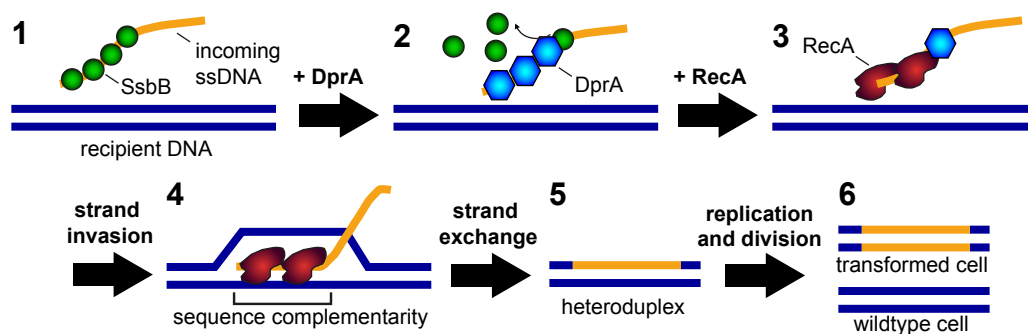


Figure 1.2: Homologous recombination during natural transformation. The events depicted are simplified and based on [33]. (1) Single stranded DNA (ssDNA, orange) enters the cytoplasm and is bound by the single strand binding protein SsbB, which protects ssDNA from immediate degradation. (2) DprA binds to SsbB-bound DNA and displaces SsbB. (3) DprA facilitates the loading of RecA onto the nucleoprotein filament. (4) RecA promotes alignment of homologous sequences and catalyzes strand invasion into the recipient chromosome (blue). (5) After strand exchange mediated by RecA, a heteroduplex of transforming DNA and recipient DNA is established. (6) Replication and cell division partitions the two strands of the heteroduplex, yielding a transformed and a wildtype cell.

Chapter 1. Introduction

While homologous recombination relies on extensive sequence similarities, there are also low-frequency recombination events that are less (or not at all) dependent on homology. In *S. pneumoniae*, as well as in *Acinetobacter* BD413 and *Pseudomonas stutzeri*, homology facilitated illegitimate recombination has been described to drive integration of foreign DNA of several thousand base pairs (bp) without the need of extensive sequence similarity. Homology facilitated illegitimate recombination is only dependent on a short region of homology (153-311bp) that serves as an anchor and initiates RecA-dependent strand exchange, which can then extend into regions of little or no sequence-similarity, thereby causing illegitimate recombination [36–38]. A mechanism of recombination that acts in the absence of any homology (double illegitimate recombination) has been described in *Acinetobacter baylyi* [39]. Moreover, Domingues and colleagues recently demonstrated that natural transformation efficiently promotes the transfer of mobile genetic elements, such as transposons, integrons or gene cassettes that confer antibiotic resistances [40]. These mobile genetic elements do not rely on classical homologous recombination for integration into the genome.

Natural competence is common in diverse bacterial species

Natural competence for transformation is widespread in the bacterial kingdom. More than 65 naturally competent bacterial species are described so far [41]. Amongst them, there are many important human pathogens, such as *Neisseria gonorrhoeae* and *Neisseria meningitidis*, *Haemophilus influenzae*, *Legionella pneumophila*, *Streptococcus pneumoniae* and *Vibrio cholerae*. Additionally, a plethora of environmental bacteria have been shown to be naturally transformable and due to the abundance of competence genes in various bacterial species, many more are expected to have the ability to enter the competence state, provided that proper competence-inducing conditions are encountered [42]. The reason for the evolutionary success and conservation of natural transformation in many unrelated bacterial species has been a matter of debate for many years. Three non-exclusive hypotheses are commonly discussed to explain the potential benefits of DNA uptake and transformation for bacteria (summarized in [43]): DNA uptake for food, DNA uptake for evolution and DNA uptake for repair.

Benefits of natural transformation

Probably the most controversial hypothesis suggests a direct benefit from DNA uptake as a source of nutrients. This could indeed provide a short-term fitness advantage, as put forward by Redfield [44]. Support comes from a recent study in *E. coli*, in which the authors demonstrate that DNA is sufficient as sole source of carbon and energy to sustain growth [45]. However, the exact mechanism through which DNA is taken up in this system and to what extent it is comparable to DNA uptake during natural transformation remains speculative. What raises most doubts against the “DNA for food” hypothesis is the fact that bacteria spend a lot of energy to actively import long stretches of DNA (see next section) and protect them from degradation within the cytoplasm by competence-specific proteins, such as DprA (Figure 1.2, [33]). One might wonder, why bacteria invest extra energy into the protection of DNA within the cytoplasm, if the main purpose of DNA uptake would be to gain energy and

1.2. The mechanism of DNA uptake during natural transformation

nucleotides. Furthermore, it is unclear whether the net balance of energy consumption for DNA transport through transformation machineries (see next section), and energy gain by acquisition of new nucleotides is indeed positive.

A second obvious benefit of natural transformation is its potential to promote genetic variation and diversity, thereby facilitating natural selection in bacterial populations. This hypothesis has been reviewed and supported strongly by Michiel Vos [46]. Vos suggests that natural transformation can be compared to eukaryotic sex, and that suggestions to explain the evolutionary benefits of sex could apply directly to homologous recombination in bacteria [46]. However, this is also true for some of the costs related to sex (reviewed in [47]), most importantly the risk of a fitness decline due to the breakup of beneficial gene combinations. One way of limiting the costs is to tightly regulate competence and to restrict it to situations, in which the potential evolutionary benefits exceed the risks of detrimental recombination effects. Indeed, many competent bacteria possess a complex regulatory network that controls competence induction [43].

Finally, DNA uptake might also provide templates for the repair of damaged chromosomal DNA. In this case, only DNA from the same or very closely related species would be beneficial. As a matter of fact, there is a strong bias towards uptake of such DNA in many competent bacteria. As an example, *N. gonorrhoeae* and *H. influenzae* both show preference for the uptake of DNA that contains certain sequence motifs, which are highly overrepresented in their genome [48–50]. *S. pneumoniae* in contrast can trigger the release of DNA from siblings by fratricide (reviewed in [51]). The “DNA uptake for repair” hypothesis is further supported by the finding that several bacterial species, namely *S. pneumoniae*, *H. pylori* and *L. pneumophila*, enhance or induce competence upon DNA damage caused by antibiotics or UV irradiation [52–54]. However, there are also contradictory results; no contribution of DNA uptake to repair could be detected in *H. pylori* or *L. pneumophila*, because bacterial strains lacking essential proteins for DNA uptake did not show an increased sensitivity to genotoxic agents under the tested laboratory conditions [53,54].

Understanding the molecular mechanism of transformation

Even though the importance of natural transformation for bacterial evolution and its impact on human health are undisputed, the precise molecular mechanisms governing this process are far from being understood. Many open questions, in particular regarding mechanistic aspects of DNA uptake, remain to be answered. Nevertheless, recent studies have advanced our understanding of this complex process considerably and helped to identify highly conserved features. The next section will give a brief overview on the current models used to describe DNA transport during natural transformation in Gram-negative and Gram-positive bacteria.

1.2 The mechanism of DNA uptake during natural transformation

The cellular architecture of both, Gram-negative and Gram-positive bacteria constitutes an impenetrable diffusion barrier for DNA molecules. Naturally competent bacteria therefore need a means to actively transport fragments of DNA from the extracellular environment into the cytoplasm. Many proteins implicated in this process have been identified in various

competent bacteria. Based on sequence homology of these proteins to components of other molecular machineries, models describing DNA uptake during natural transformation could be established (for recent reviews see [32, 35, 55–58]).

1.2.1 Type IV pili and type II secretion systems

All competent bacteria, with the exception of *H. pylori*, which will be discussed later, seem to use very similar proteins for the import of DNA. A large part of these proteins closely resembles components of type IV pili (T4P) and type II secretion systems (T2SSs) (Figure 1.3). T4P are filamentous cell appendages present on the surface of all Gram-negative (reviewed in [59]) and some Gram-positive (reviewed in [60]) bacteria that can mediate very diverse functions, such as cell adhesion, attachment to surfaces, cell aggregation, biofilm formation, phage attachment and a form of motility, termed “twitching motility” [59–61]. Components needed for biogenesis of T4P, in turn, are similar to proteins implicated in T2SSs (Figure 1.3). T2SSs are evolutionary related to T4P, as well as to archaeal flagella [62].

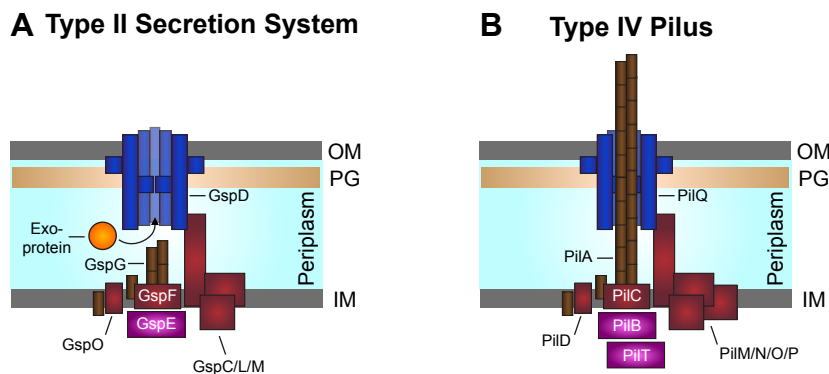


Figure 1.3: The type II secretion system and type IV pilus of Gram-negative bacteria. (A) The type II secretion system, consisting of an inner membrane (IM) subcomplex (GspC/L/M/F), and an outer membrane pore (GspD), is secreting protein substrates (exoprotein) through the outer membrane (OM) and peptidoglycan layer (PG) by assembly of a piston-like pseudopilus (GspG). Pseudopilus subunits are processed by GspO and assembled by the cytoplasmic ATPase GspE. The growing pseudopilus then pushes exoproteins through the OM pore. (B) The type IV pilus, exemplified by the *Pseudomonas aeruginosa* PAK pilus, consists of components very similar to proteins of the T2SS. Pilus subunits (PilA) are processed at the IM by PilD and integrated into the growing filament by the cytoplasmic ATPase PilB at an IM assembly complex (PilC, PilM/N/O/P). The pilus crosses the OM through a secretin pore made of PilQ. Another cytoplasmic ATPase, PilT, is powering disassembly and retraction of the pilus. Figure based on [59, 63, 64].

Type II secretion systems

T2SSs are found in many Gram-negative bacteria [65]. Also known as terminal branch of the general secretory pathway (GSP), the T2SS is used to translocate folded proteins from the periplasm across the outer membrane. The biogenesis, architecture and mechanism of this sophisticated multiprotein complex have recently been reviewed [63]. In summary, T2SS consist of four distinct subassemblies made of 12-15 different proteins that are usually encoded in a single operon [66]. For the sake of simplicity, not all proteins are discussed here. The four subassemblies include (Figure 1.3A): 1) a pseudopilus, consisting of multiple

1.2. The mechanism of DNA uptake during natural transformation

copies of minor and major pseudopilins (GspG), 2) an outer membrane complex with an outer membrane pore (GspD), 3) an inner-membrane complex containing GspF, GspC/L/M and a prepilin peptidase GspO, 4) a cytoplasmic ATPase (GspE).

The mechanistic understanding of the T2SS is still limited [63], but the current idea is that proteins destined for export across the outer membrane (exoproteins) by the T2SS are first transported to the periplasm through either of two inner membrane (IM) transport systems: the Sec translocon or the Tat complex. Exoproteins in the periplasm then interact with the pseudopilus (GspG), which acts as a piston and pushes protein substrates through the outer membrane pore (GspD). Elongation of the pseudopilus during the piston movement is catalyzed by the cytoplasmic ATPase GspE and is dependent on the prepilin peptidase GspO, which processes pre-pseudopilins during their incorporation into the growing pseudopilus at the inner membrane platform (GspF and others). This model is based on many biochemical and structural studies, as outlined in [63].

Type IV pili

While the T2SS is restricted to Gram-negative bacteria, T4P are truly universal in the bacterial kingdom. They have been observed in many bacterial genera, including Gram-negative as well as Gram-positive species [59, 60]. Morphologically, T4P are characterized as extremely thin (5-8 nm in width), long (up to several micrometers in length) and flexible filaments [59]. Many components of T4P have been identified [67]. Some key elements are presented in Figure 1.3 B. As for the T2SS, only a fraction of the 10-18 proteins that are thought to build these complex structures [67] are highlighted. Generally, T4P are polymers of single pilus subunits, termed type IV pilins. The major *P. aeruginosa* pilin, PilA, has been crystallized and its structure analyzed in detail [68, 69]. It consists of a globular C-terminal head domain, connected to a long, N-terminal α -helix [69]. Pilins are synthesized as precursors (prepilins), containing a hydrophilic leader peptide. This peptide is cleaved during pilus assembly by the prepilin peptidase (PilD) [70, 71]. Two distinct classes of pilins are distinguished, based on both, the length of the leader peptide and the mature protein: type IVa (T4a) and type IVb (T4b) pilins. T4a pilins are shorter, both in their leader peptide (less than 10 aa) and their overall size (150-160 aa) compared to T4b pilins (15-30 aa leader peptide, 190 aa average overall size [59]). While the latter are the main constituents of pili in rather few organisms (e.g. the toxin co-regulated pilus (TCP) of *V. cholerae* [69]), T4a pili are the predominant form identified in many bacteria, including the PAK pilus of *P. aeruginosa*, which is presented schematically in Figure 1.3 B [59, 67].

The exact mechanism of pilus biogenesis remains unclear, but nevertheless some key issues have been solved (reviewed in [67]). A cytoplasmic conserved traffic ATPase (PilB) is proposed to power pilus extension from a multiprotein inner membrane complex (PilC, PilM/N/O/P). The pilus crosses the outer membrane through a pore made of a secretin (PilQ). Secretins are a family of particularly stable, multimeric outer membrane proteins, which appear as ring-like cylindrical structures with a large gated central cavity [72–74]. Several findings support their role as a pore for T4P; Collins *et al.* showed that T4P interact with PilQ, inducing structural changes [75]. Furthermore, PilQ is dispensable for pilus assembly, but

not for surface exposure [76, 77]. In the absence of pilus retraction, T4P can be identified trapped in the periplasm of PilQ defective strains [76, 77], demonstrating the dispensability of PilQ for pilus biogenesis, but not surface exposure. In addition to the components that are responsible for biogenesis of T4P outlined so far, many bacteria contain a second cytoplasmic ATPase, PilT, which is responsible for pilus retraction by disassembly of subunits at the inner membrane [78–81]. This confers a dynamic quality, which allows T4P to mediate a form of surface movement termed twitching motility (see [64] for a recent review).

Twitching motility emerges through rounds of pilus extension, surface attachment at the pilus tip and pilus retraction. Strong forces exceeding 100 pN can be generated during pilus retraction events [78, 82, 83]. In fact, T4P are considered the strongest molecular motors identified so far [84]. Even though the exact mechanism driving pilus retraction is not clear, it most likely involves large domain movements within PilT upon nucleotide binding/release [80, 81].

Most importantly, dynamic T4P-like structures are not only implicated in motility, but also seem to play a central role in DNA uptake during natural transformation, since the presence of conserved proteins that are highly homologous to components of T4P are essential for transformability in virtually all competent bacteria [41].

1.2.2 DNA transport machineries in Gram-negative and Gram-positive bacteria

DNA uptake during natural transformation has mainly been studied in the Gram-positive bacteria *B. subtilis* and *S. pneumoniae* and in the Gram-negative bacteria *Thermus thermophilus*, *N. gonorrhoeae* and *H. pylori* [32, 35, 55–58]. Simplified models of the DNA uptake machineries of *N. gonorrhoeae*, *B. subtilis* and *H. pylori* are depicted in Figure 1.4 (based on [32, 57, 85]). *H. pylori* is a somewhat special case and will therefore be discussed separately.

Transport towards the cytoplasmic membrane

The first barrier that needs to be overcome during transport of DNA to the cytoplasmic membrane is the outer membrane of Gram-negative bacteria or the cell wall of Gram-positive bacteria. In *N. gonorrhoeae*, a putative type IV like competence pilus is involved in this first step (Figure 1.4 A). This pilus, mainly composed of the major subunit PilE, is assembled at the inner membrane and crosses the outer membrane through the secretin pore PilQ. Since the central cavity of type IV pili is rather hydrophobic and measures only approx. 1.6 nm at its narrowest point [59], double stranded DNA (dsDNA) of approx. 2 nm in diameter cannot pass through the lumen of pili. Instead, transport of DNA across the outer membrane is thought to occur through pilus retraction, which is powered by the cytoplasmic ATPase PilT. In *N. gonorrhoeae*, only DNA that contains certain sequence elements, called DNA uptake sequences (DUS), is efficiently transported [49, 50]. The molecular basis of this has recently been attributed to the minor (low abundance) pilin ComP, which preferentially binds to DNA uptake sequences [86].

DNA uptake during natural transformation is currently best characterized in the Gram-positive firmicute *B. subtilis* (Figure 1.4 B). Competence proteins localize to cell poles [87–89] and are organized in distinct layers [89]. Transport across the cell wall is dependent on a type

1.2. The mechanism of DNA uptake during natural transformation

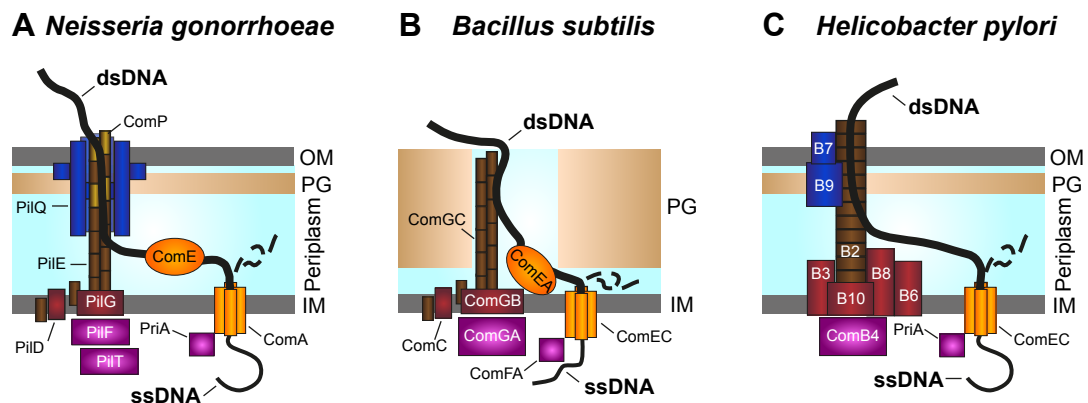


Figure 1.4: Putative composition of DNA uptake machineries in Gram-negative and Gram-positive bacteria. Only a selection of proteins implicated in pilus biogenesis is depicted. (A) In *N. gonorrhoeae*, a putative type IV competence pilus is assembled at an inner membrane (IM) complex containing PilG and the prepilin processing peptidase PilD. The cytoplasmic ATPase PilF is driving incorporation of pilus subunits (PilE) into the growing filament. The pilus crosses the peptidoglycan layer (PG) and passes the outer membrane (OM) through a secretin pore formed by PilQ. During retraction of pili, powered by the cytoplasmic ATPase PilT, DNA is transported to the periplasm. A minor pilin subunit of the pilus fiber, ComP, preferentially binds to DNA that contains certain sequence motifs [86]. The periplasmic protein ComE then binds to the incoming dsDNA, which is further transported to the cytoplasm through an inner membrane channel (ComA) with the help of the cytoplasmic protein PriA. During this process, dsDNA is degraded to ssDNA by a yet unknown mechanism. (B) In *B. subtilis*, a pseudopilus with its major subunit ComGC is assembled at the IM by the concerted action of ComC, ComGB and ComGA that mediate functions homologous to neisserial PilD, PilG and PilF. ComEA, ComEC and ComFA then mediate DNA transfer to the cytoplasm, similar to ComE, ComA and PriA in *N. gonorrhoeae*. (C) In *H. pylori*, a type IV secretion system (ComB system) mediates DNA transport to the periplasm. ComB7 and B9 most probably are part of the OM complex, while ComB3, B6, B8 and B10 are situated at the IM. The cytoplasmic ATPase ComB4 is driving assembly of a pseudopilus from ComB2 subunits at the IM. Once in the periplasm, DNA is transported to the cytoplasm through ComEC, as for *N. gonorrhoeae* and *B. subtilis*. Figure based on [57].

IV pseudopilus, made of ComGC subunits. The term “pseudopilus” is used to account for the striking similarities between ComGC and pseudopilins identified in T2SS (Figure 1.4 A, [90]). In the current model of DNA uptake in *B. subtilis* (Figure 1.4 B), pre-pseudopilins are processed by the ComC peptidase and, powered by the cytoplasmic ATPase ComGA, incorporated into the growing pseudopilus. Pseudopilus retraction then allows DNA to cross the cell wall and get in contact with inner membrane associated proteins that mediate subsequent steps. In contrast to *N. gonorrhoeae*, no specificity for DNA uptake motifs has been identified, thus no DNA receptor protein is postulated in the *B. subtilis* model. Whether competence pseudopili of *B. subtilis* directly interact with DNA remains controversial. Purified ComG proteins, including the major pseudopilin ComGC, do not bind to DNA [91]. On the other side, single cell force measurements for DNA uptake in *B. subtilis* were in the range of forces measured for T4P pilus retraction [92,93].

Once DNA has crossed the outer membrane/cell wall, it is bound by the highly conserved DNA binding protein ComE/ComEA (Figure 1.4 A, B). The membrane-anchored ComEA of *B. subtilis* is considered a DNA receptor [91] and is essential for DNA binding and transformation [94]. Also in *N. gonorrhoeae*, the presence of ComEA homologs (four identical copies of ComE) is correlating with levels of natural transformability [95]. Yet the exact role of this

protein remains speculative. ComEA might facilitate shuttling of DNA to the inner membrane transport protein ComEC, with which it has been suggested to interact [32, 96]. However, in a recent review Krueger *et al.* hypothesized on a more active role of ComEA in DNA transport [57] (without provision of experimental data). Binding and compaction of DNA by ComEA might *per se* generate a force and facilitate DNA transport [57]. Clearly, more experimental data is required to characterize the precise role of this protein.

Transport across the cytoplasmic membrane

The homologous polytopic membrane proteins ComA and ComEC of *N. gonorrhoeae* and *B. subtilis* respectively are needed for DNA transport into the cytosol (Figure 1.4 A, B) [97, 98]. ComEC of *B. subtilis* is currently best characterized. It is proposed to integrate into the cytoplasmic membrane as an oligomer and to form a channel that facilitates passage of DNA [97]. In addition, the ATP dependent DEAD-box helicase ComFA (Figure 1.4 B) is suggested to assist in and eventually power the transport process [99]. What drives translocation through ComEC in most other competent bacteria is less obvious. PriA, a ubiquitous DNA repair and recombination protein, which is also involved in restart of chromosomal replication in case of stalled replication forks (reviewed in [100]), is a close homolog of ComFA and has been shown to participate in natural transformation of *N. gonorrhoeae* [101]. However, whether this is indeed caused by a transport defect or rather due to downstream effects remains to be seen.

In both, *N. gonorrhoeae* and *B. subtilis*, DNA is transported to the cytoplasmic membrane as a double stranded (ds) molecule [98, 102]. However, only single stranded DNA (ssDNA) reaches the cytoplasm in both species [102, 103]. What causes degradation of one strand during transport across the cytoplasmic membrane is currently unknown. So far, no nuclease that could account for this observation has been identified in these two organisms. Since dsDNA is also converted to ssDNA in *H. pylori* [104], this might be a general feature of natural transformation and could be directly linked to transport through ComA/ComEC. Yet DNA degradation is not coupled to inner membrane transport in the Gram-positive bacterium *S. pneumoniae*, in which the membrane-anchored nuclease EndA degrades DNA even in the absence of ComEC [105]. Therefore it is currently unclear, to what extent the precise mechanism that converts dsDNA into ssDNA during natural transformation is conserved.

Helicobacter pylori, a special case

H. pylori is unique because it is not dependent on T4P for the transport of DNA to the cytoplasmic membrane. Instead, it uses a molecular machine that closely resembles type IV secretion systems (T4SS) [104, 106, 107] (Figure 1.4 C). T4SS are evolutionary related to conjugation machineries and usually implicated in transport of protein or DNA substrates across the cell envelope (reviewed in [108]). Despite the fact that *H. pylori* uses a T4SS rather than T4P for the first steps of DNA transport, subsequent steps seem to be conserved among all naturally competent bacteria. Once reaching the cytoplasmic membrane, ssDNA is transported into the cytoplasm through a close homolog of *B. subtilis* ComEC. ssDNA is then bound by cytoplasmic proteins, such as Ssb, DprA and RecA, which mediate protection and recombination (Figure 1.2). Consistent with this idea is the finding that DNA transport in *H. pylori*,

1.3. *Vibrio cholerae*, a naturally competent human pathogen

and potentially also in other competent bacteria, is a two-step process with a periplasmic intermediate [57, 104].

1.2.3 The need for new models

As outlined in the previous paragraphs, we are gaining a reasonable understanding of the conserved components that constitute DNA uptake machineries in competent bacteria. However, major knowledge gaps exist regarding the mechanistic aspects of the DNA transport process. Most features of current models (Figure 1.4) lack thorough experimental verification and rely to a large extent on functional predictions based on protein homologies and on indirect evidence. Furthermore, research on the mechanism of DNA uptake has focused on relatively few bacterial species, namely *B. subtilis*, *S. pneumoniae*, *H. pylori*, *N. gonorrhoeae*, *H. influenzae* and *T. thermophilus*.

Studying this process in the human pathogen *V. cholerae* has the potential to provide new, exciting insights, since this organism has some very attractive features: 1) Despite being an important human pathogen, it is relatively safe to work with, due to its high infective dose under laboratory growth conditions (approx. 10^8 bacteria in healthy volunteers, [109]). 2) *V. cholerae* is readily growing in standard culture media, such as LB medium, with extremely short generation times under aerated conditions. 3) Most importantly, there are excellent biochemical and genetic tools available to experimentally address biological questions. Finally, HGT, in particular natural transformation, is known to have shaped the genome of this bacterial species dramatically during evolution [110, 111]. Understanding the mechanism of natural transformation in this species will therefore also help to shed light on its evolution.

While *V. cholerae* has only been recognized to be naturally transformable in 2005 [112], its role as a human pathogen has been studied extensively for more than a century. The next section will give a very short overview on the biology of this organism and will highlight some important characteristics with respect to horizontal gene transfer.

1.3 *Vibrio cholerae*, a naturally competent human pathogen

V. cholerae, the causative agent of the diarrheal disease cholera, is a Gram-negative, comma-shaped, monotrichous bacterium (Figure 1.5). In 1884, the German physician and founder of modern bacteriology, Robert Koch, prepared and studied pure cultures of *V. cholerae* for the first time [113]. Since then, both the epidemiology, as well as the physiology of this bacterium have been studied extensively (see [114] for a recent review).

A first complete genome sequence of this organism was published in 2000 [115] and revealed some interesting characteristics. *V. cholerae* contains two circular chromosomes of 2.96 mega base pairs (Mbp) (large chromosome) and 1.07 Mbp (small chromosome). Most of the genes essential for basic cell functions and pathogenicity are located on the large chromosome, while the small chromosome carries some additional, though essential, metabolic genes. Furthermore, some genes for DNA repair, signal transduction, and a large gene capturing system (the integron island), are present on the small chromosome [115].

Since 2000, a variety of additional genome sequences from clinical and environmental *V. cholerae* strains became available. The genome of 23 of these strains has recently been

analyzed and compared in detail [110]. The results of this study highlight the tremendous impact of HGT on the evolution of this bacterial species. Chun *et al.* identified 73 individual genomic islands, each containing five or more open reading frames, for which lateral transfer was obvious [110]. Several of these genomic islands are associated with virulence factors, linking once again HGT and pathogenicity.

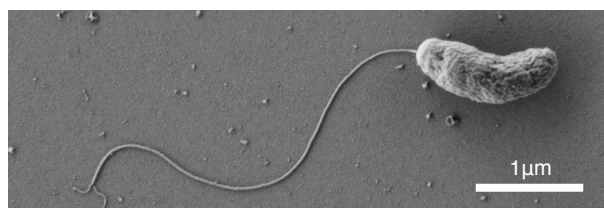


Figure 1.5: Scanning electron micrograph of *V. cholerae*. *V. cholerae* is a Gram-negative, curved, monotrichous bacterium of approx. 1-2 μm (cell body only) (Sample preparation by M. Blokesch; image taken by Graham Knott, EPFL Bio-EM facility, 2011).

1.3.1 The dual role of *Vibrio cholerae* as human pathogen and member of aquatic ecosystems

Vibrio cholerae, a human pathogen

Infection with *V. cholerae* causes severe watery diarrhea, commonly accompanied by vomiting. Fluid loss of up to one liter per hour can lead to rapid dehydration, hypotensive shock and death within hours of the first symptoms. During early stages of cholera epidemics, with little resources for treatment and disease control available, mortality can reach 10% [116]. In contrast, appropriate treatment lowers the case/fatality rate to less than 1% [117, 118]. Rehydration and compensation of electrolyte imbalances is the mainstay of therapy. Up to 80% of all patients can be treated successfully with oral rehydration solutions. The use of antibiotics is only recommended in cases of very severely dehydrated patients, in order to shorten the duration of diarrhea and *V. cholerae* excretion and to reduce the volume of rehydration fluids needed [118]. Only few health organizations, such as the “International Centre for Diarrhoeal Disease Research, Bangladesh”, recommend antibiotics also for treatment of less severe cases and under endemic settings [119]. However, considering the role that HGT has played in the evolution of *V. cholerae*, mass administration of antibiotics is highly questionable, since it will most certainly lead to the rapid spread of resistances, as has already been observed in large parts of Africa (reviewed in [120]).

The clinical signs and symptoms of cholera are mainly caused by the major virulence factor of pathogenic *V. cholerae*, cholera toxin (CTX). After ingestion of large numbers of bacteria, some organisms occasionally survive the passage through the gastric tract and start colonizing the small intestine. There, CTX is secreted as an exotoxin and translocates into eukaryotic cells of the small intestine. Within its target cells, CTX then enzymatically stimulates adenylate cyclase, which dramatically raises intracellular cyclic AMP (cAMP) levels. This ultimately leads to the elevated secretion of Cl^- ions and H_2O to the intestinal lumen

1.3. *Vibrio cholerae*, a naturally competent human pathogen

(see [121, 122] for reviews on cholera toxin).

Successful colonization of the small intestine requires a second essential virulence factor, the toxin co-regulated pilus (TCP) [123, 124]. TCP is a bundle forming type IVb pilus and mediates attachment to epithelial cells [123, 125], as well as playing an additional role in mediating bacterium-bacterium interactions [126]. As its name suggests, TCP expression is co-regulated with CTX. Moreover there is a second connection between CTX and TCP: the genes encoding both virulence factors were acquired horizontally [127].

Genes encoding the TCP are part of a genomic island referred to as *Vibrio* Pathogenicity Island 1 (VPI-1) [128]. The mechanism by which VPI-1 is exchanged between strains remains controversial [127]. In contrast, there is general agreement on the fact that CTX genes are part of the genome of a filamentous phage (CTX ϕ), which can reside as prophage within the chromosome of *V. cholerae* [129]. Interestingly, TCP serves as surface receptor for CTX ϕ [129], which suggests sequential acquisition of TCP and CTX ϕ in pathogenic *V. cholerae*.

Current situation, strains and pandemics

Cholera outbreaks are primarily associated with poor sanitation and contaminated drinking water, as suggested by the London physician John Snow during a cholera epidemic in London between 1849 and 1854. Today the disease is rare in developed countries and restricted to a few imported cases per year [130]. In contrast, cholera still causes an estimated 3-5 million cases, with more than 100,000 deaths per year in areas with poor housing conditions and a breakdown or lack of proper sanitation [118]. In 2012, cholera was reported to be endemic in 51 countries, mainly affecting the African and Asian continents and an estimated 1.4 billion people remain at risk of cholera outbreaks [131]. In order to lower the high global disease burden, WHO seeks to implement a multidisciplinary approach, based on efficient surveillance and preparedness to react rapidly to epidemic outbreaks, and prevention, with a special focus on provision of safe potable water, adequate sanitation and hygiene education. In addition, two internationally marketed vaccines that have proven to be safe and effective are now considered a short-term option for the treatment of populations living in high-risk areas [130].

Even though hundreds of *V. cholerae* strains have been identified, only a few are responsible for most of the global disease burden. *V. cholerae* strains are classified primarily according to their surface antigens (O-antigens), which are part of the outer membrane lipopolysaccharide (LPS) (Figure 1.6). Based on this classification, more than 200 serogroups are described [132]. Only strains of serogroups O1 and O139 are currently associated with large-scale epidemic or pandemic cholera outbreaks [118].

The origins of cholera are likely within the Bay of Bengal, where the disease has been endemic for centuries. From there, cholera spread around the globe in seven pandemics, starting in 1817. Between 1817 and 1923, six pandemics caused cholera cases all over the world, including outbreaks in South East Asia, China, Russia, the Middle East, Europe, Africa and both, North and South America [117]. A 7th ongoing pandemic started in 1961 in Indonesia [133]. Persisting for more than half a century, the 7th pandemic is by far the longest on record [134]. While isolates from the 6th pandemic represent almost exclusively O1 classical strains, the

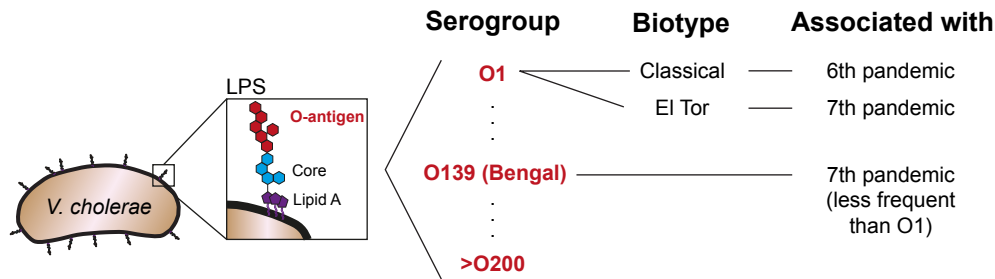


Figure 1.6: Serogroups and biotypes of *V. cholerae*. *V. cholerae* strains are classified into more than 200 serogroups according to their O-antigens within the surface exposed lipopolysaccharide (LPS). Only strains of serogroups O1 and O139 are causing large-scale cholera epidemics. Serogroup O1 is further divided into two biotypes: Classical and El Tor. While the O1 classical strain was causative for the 6th (and probably also earlier) cholera pandemic, O1 El Tor is mainly responsible for the currently ongoing 7th pandemic.

7th pandemic is dominated by *V. cholerae* O1 El Tor (Figure 1.6), which has replaced the classical biotype [114]. Only in 1992 a new serogroup, O139, was identified to cause epidemic cholera outbreaks in India and Bangladesh [135] (Figure 1.6). As it turned out, this strain likely resulted from one or several horizontal gene transfer events, during which the O1 serogroup determinants of the O1 El Tor strain have been replaced with genes coding for the O139 antigen [136]. Experimental proof that such an O1 to O139 serogroup conversion can indeed take place in the natural aquatic environment of *V. cholerae* was presented in 2007 [137]. Blokesch and Schoolnik demonstrated that O1 El Tor recipient bacteria could undergo serogroup conversion to O139 by natural transformation in a microcosm experiment [137]. This represents another prime example of the evolutionary power of horizontal gene transfer, in particular natural transformation, and the global impact that such events can have.

***Vibrio cholerae* in the aquatic environment**

Beside its role as a human pathogen, *V. cholerae* is also ubiquitous in the aquatic environment, where it can be isolated from rivers, coastal waters and estuaries [138–140]. Within these aquatic ecosystems, *V. cholerae* is often associated with the exoskeleton of zooplankton, their molts or egg cases, which provides the bacteria with nutrients, increases stress tolerance and mediates protection from predators [140–145]. This is not only important from an ecological point of view, but has direct epidemiological implications. On these biotic surfaces, bacteria can grow to high numbers [140, 142], which increases the risk of ingesting an infective dose of *V. cholerae* from contaminated water. Indeed, filtration of water through sari cloth, which removes zooplankton, most phytoplankton and particulates >20 µm, but which is permeable to free swimming bacteria, reduced cholera cases by almost 50% [146]. Through the association with zooplankton, there is also a link between *V. cholerae* numbers in the environment and climate [143, 144]. Interesting examples in this context are the seasonal cholera outbreaks in Bangladesh, where the number of cholera cases peak twice a year; once in spring, before the summer monsoon and once in autumn, after the monsoon period [147–150]. This pattern closely follows the seasonal changes in sea surface water temperatures, as has been shown by the evaluation of satellite data [149]. Additionally, other abiotic conditions, such as water

1.3. *Vibrio cholerae*, a naturally competent human pathogen

salinity and pH are influencing the appearance of *V. cholerae* in the environment [144, 151]. Finally, if environmental conditions are unfavorable, *V. cholerae* can enter a viable but non-culturable state [152, 153].

Association of *V. cholerae* with other aquatic organisms, ranging from aquatic birds to protozoa, has also been reported, but their ecological and epidemiological role remains not well understood [154].

Environmental *V. cholerae* bacteria are not only important as an infective reservoir. In fact, most environmental isolates are non-pathogenic strains of diverse serogroups that lack important virulence factors, such as CTX [155]. Instead, *V. cholerae* mediates important ecosystem functions, in particular with respect to chitin cycling. Chitin is a polymer of N-acetylglucosamine (GlcNAc) and represents the most abundant polysaccharide in the aquatic environment, comparable to cellulose on land [156]. Aquatic organisms, especially zooplankton, are estimated to produce more than 10^{11} metric tons of chitin annually [156]. Keyhani *et al.* stated: “If this enormous quantity of insoluble carbon and nitrogen was not converted to biologically useful material, the oceans would be depleted of these elements in a matter of decades.” [156]. *V. cholerae* is able to readily grow on chitin surfaces, such as the chitinous exoskeleton of zooplankton and degrade the complex polymer into soluble nutrients by secreting extracellular chitinases [157, 158]. As a result, *V. cholerae* may contribute substantially to global chitin cycling (reviewed in [145]).

Most importantly, it is also the association with chitin that triggers induction of the natural competence program in *V. cholerae* [112], as described below.

1.3.2 The complex regulation of natural competence in *Vibrio cholerae*

The induction of natural competence is tightly regulated in *V. cholerae* (for recent reviews see [43, 159]). Chitin sensing, as well as limitations of preferred carbon sources and high cell densities are all required to activate the regulatory cascades that control competence induction (Figure 1.7).

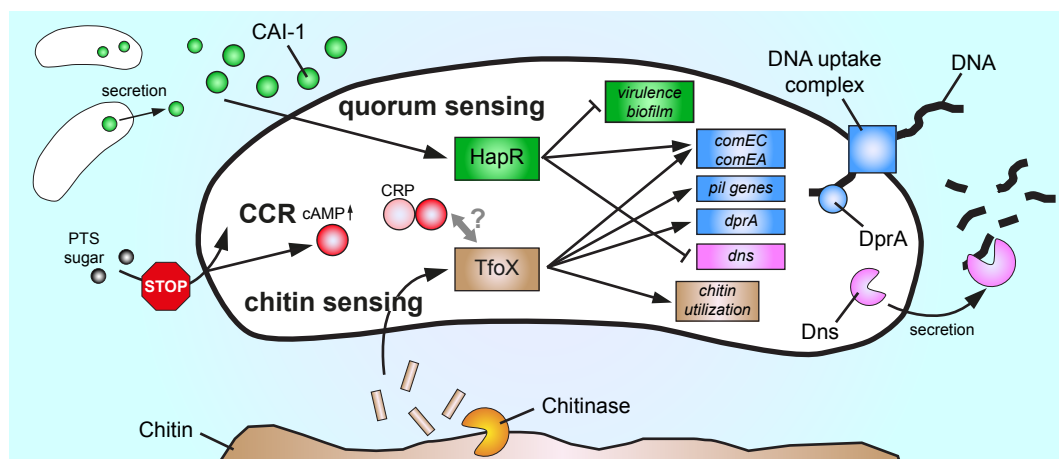


Figure 1.7: Regulation of natural competence in *V. cholerae*. A complex regulatory network, involving chitin sensing, carbon catabolite repression (CCR) and quorum sensing, controls competence induction in *V. cholerae*. Depicted is a simplified scheme, based on [160]. Details are provided in the text.

Chapter 1. Introduction

To access extracellular, insoluble chitin as a source of carbon and nitrogen, chitinolytic bacteria, including *V. cholerae*, secrete chitinases that cleave the polymer into smaller (GlcNAc)_n oligosaccharide fragments. These fragments are then transported into the cell, thereby initiating a complex chitin sensing cascade that controls expression of many genes that are needed for efficient colonization, degradation and metabolism of chitin (chitin utilization) [158]. In addition, chitin sensing also activates the master regulator of competence, TfoX. In fact, natural competence in *V. cholerae* has been discovered due to chitin dependent upregulation of genes that are reminiscent of T4P-encoding genes from other organisms [112, 158]. Control of TfoX expression is complex and occurs on the transcriptional, as well as translational level [160–164]. Its production is needed for activation of several genes involved in chitin degradation, as well as competence-specific genes [112, 160]. Constitutive expression of *tfoX* *in trans* or *in cis* allows chitin-independent competence induction [112, 160]. Though essential for competence induction, TfoX alone is not sufficient.

In addition to TfoX, elevated intracellular levels of cyclic adenosine monophosphate (cAMP) in combination with the transcriptional regulator cAMP receptor protein (CRP) are strictly required to activate natural competence [160, 165]. cAMP is a secondary messenger and mediates alternative carbon source utilization through carbon catabolite repression (CCR) (see [166] for a review on CCR). CCR allows bacteria to adapt their gene expression profile in response to the availability of preferred carbon sources. When the availability of preferred sugars, which are transported through phosphoenolpyruvate:carbohydrate phosphotransferase systems (referred to as PTS), becomes limiting, cAMP accumulates within the cell. cAMP then activates, in combination with CRP, genes for alternative sugar uptake and metabolism, as well as many other genes. In addition, cAMP and CRP are also involved in activation of competence genes [160, 165], though the exact molecular mechanisms underlying this process remain unclear. One hypothesis, based on observations in *H. influenzae*, which contains a close homolog of TfoX, is that cAMP-CRP acts in concert with TfoX to promote competence gene expression [160, 165]. Consistent with the need of elevated cAMP levels and the role of CCR is the finding that glucose, a PTS sugar, is efficiently inhibiting competence induction [112, 165].

In addition to chitin sensing and CCR, high cell densities are a prerequisite for natural transformation in *V. cholerae*. High cell densities are detected through a system of cell-to-cell communication termed quorum sensing (QS). QS allows bacteria to co-ordinate gene expression according to the population density by producing and sensing chemical signals termed autoinducers [167]. *V. cholerae* produces two autoinducers: Cholera Autoinducer 1 (CAI-1), which is restricted to certain Vibrionaceae members and Autoinducer 2 (AI-2), which is produced and sensed by various bacterial species [168–170]. Low cell density causes a low concentration of extracellular autoinducers, which leads to post-transcriptional repression of synthesis of the master regulator of quorum sensing, HapR [171, 172]. In contrast, high cell density results in a high concentration of autoinducers, which causes production of HapR. HapR then controls expression and repression of many quorum sensing regulated genes that are involved in various processes, including virulence [173] and biofilm formation [174, 175]. Additionally, HapR regulates a subset of the identified competence genes, namely ComEC and ComEA [160, 164]. Deletion of *hapR* completely inhibits natural transformation [112]. Also

1.3. *Vibrio cholerae*, a naturally competent human pathogen

deletion of *cqsA*, which abolishes production of CAI-1, has a major effect on transformability [176, 177]. AI-2 in contrast plays only a minor role in natural transformation [176, 177] and is therefore not indicated in Figure 1.7.

It is important to note that HapR is not only promoting the expression of competence genes, but also represses production of the secreted nuclease Dns, which counteracts natural transformation by degrading extracellular, surrounding DNA. Indeed, a *dns* deficient strain is hypertransformable [178]. Recently, Lo Scudato and Blokesch demonstrated that HapR directly interacts with the promoter region of *dns*, but not with promoters of the competence genes [164]. Instead, an intermediate QS and TfoX dependent regulator (QstR), is mediating regulation of *comEC* and *comEA* [164] (not indicated in Figure 1.7 for the sake of clarity).

While we are approaching a reasonable understanding of the processes that govern the regulation of natural competence in *V. cholerae*, close to nothing is known about the mechanism of DNA uptake during natural transformation.

1.3.3 DNA uptake in naturally competent *Vibrio cholerae*

Gene expression profiling of *V. cholerae* growing on a natural chitin surface or in the presence of soluble chitin oligosaccharides revealed significantly increased expression of a set of twelve genes, which are predicted to encode proteins involved in biogenesis of a type IV pilus of unknown function [158, 179]. Since type IV pili have long been associated with natural transformation in other organisms, Meibom *et al.* tested whether chitin might also induce natural competence in *V. cholerae* [112]. Indeed, the authors showed that chitin induces natural competence in *V. cholerae* and that transformability correlates with the presence of three predicted components of the chitin regulated pilus, namely VC2423 (PilA), VC2424 (PilB) and VC2630 (PilQ) [112]. The respective genes were named according to their homology to genes that encode components of classical type IV pili, as outlined in Figure 1.3 B. Even though growth on chitin surfaces is therefore likely to induce production and assembly of a surface exposed type IV pilus, no such structure could be identified in transmission and scanning electron microscopy experiments [112]. The authors hence concluded that “[...] this assembly complex likely directs the synthesis of a competence pseudopilus” [112].

In addition to the three pilus-related genes, a homolog of *B. subtilis comEA* (Figure 1.4 B), *VC1917*, was identified in *V. cholerae* and subsequently shown to be required for natural transformation [112]. Apart from these four genes, no other putative components of the DNA uptake machinery were experimentally analyzed when this study was initiated. Moreover, no experimental data on the function of PilA, PilB, PilQ or ComEA was available. Their role in DNA uptake was solely inferred from their strict requirement for successful natural transformation. The genome of *V. cholerae* does however contain additional annotated competence genes [115] and many more chitin-upregulated genes are likely involved in biogenesis of a competence (pseudo)pilus and therefore in DNA uptake during natural transformation. Their unambiguous identification and systematic experimental analysis was one of the core goals of this work.

1.4 Aims and scope of the thesis

Given the impact of natural transformation on the evolution of *V. cholerae* and its consequences on human health, a better understanding of the molecular mechanisms underlying this process is of major interest. Due to the likely conserved mechanistic aspects of DNA uptake during natural transformation, insights gained from studying this process in *V. cholerae* will most likely also be applicable to a wide range of other bacterial species of medical importance.

In this sense, the main aim of this thesis was to establish a first working model of the mechanism of DNA uptake in naturally competent *V. cholerae*. The thesis is divided into three parts, of which each highlights different aspects of the DNA uptake process.

First, we aimed to identify and verify the main components needed to build the molecular machinery that mediates DNA transport. Furthermore, we developed an assay to quantify internalization of DNA, which we derived from different bacterial species. This assay also allowed us to distinguish between two distinct steps during DNA transport: crossing of the outer membrane and shuffling of DNA across the inner membrane. We therefore analyzed the contribution of individual components of the DNA uptake machinery to transport across either of the two membranes.

Second, we visualized the predicted competence pilus of *V. cholerae* and investigated, which components of the DNA uptake complex were involved in or dispensable for pilus biogenesis. Using fluorescence microscopy, we also visualized three additional components of the pilus biogenesis machinery and showed their relative positions to each other. This is especially important, since the vast majority of competence related localization studies were so far performed in one single Gram-positive bacterium, i.e. *B. subtilis*.

Third, we investigated in detail the role of one particular, tightly regulated, and highly conserved competence protein (ComEA). We analyzed its dynamic distribution upon exposure of competent bacteria to exogenous DNA and proposed a model for the mechanism of DNA transport across the outer membrane. In addition, we clarified, whether DNA uptake across the outer membrane and inner membrane coincides or whether these events are spatially uncoupled.

Results presented and discussed in these three parts give insights into the processes that mediate DNA transport during natural transformation of *V. cholerae*. Our findings enabled us to present a first mechanistic model of DNA uptake in this organism, and to better understand conserved aspects of this process in nature.

2 Components of the *Vibrio cholerae* DNA uptake machinery

2.1 Results

2.1.1 *In silico* prediction of DNA transport related competence genes

A first step towards understanding the complex mechanism of DNA uptake in naturally competent *V. cholerae* was to identify genes that are likely implicated in this process. For this purpose, we started to look for genes, whose expression was significantly increased during growth under competence inducing conditions, i.e. growing on a chitin surface or in the presence of GlcNAc-oligosaccharides [112]. Furthermore, we included genes whose expression was enhanced during chitin-independent competence induction through expression of the competence regulator *tfoX* [112]. Genes that are likely implicated in chitin colonization, degradation, transport or metabolism were excluded. The same applies to genes that mediate functions in the general stress response. Furthermore, genes within the same gene cluster as competence-induced genes were included in the analysis, even in cases in which their expression was not significantly enhanced during chitin exposure or *tfoX* overexpression.

Next, we looked for homologs of these genes in other competent bacteria and *vice versa* (e.g. we checked for the presence of identified competence-specific genes from other bacterial species in *V. cholerae*). In this way, we identified a set of 26 potential components of the *V. cholerae* DNA uptake complex, including proteins, which might be essential for steps immediately downstream of DNA uptake, such as protection of single stranded DNA (ssDNA) or homologous recombination of transforming DNA (tDNA). The genes encoding these components (referred to as competence genes from now on) and their homologs in *Neisseria gonorrhoeae*, *Haemophilus influenzae*, *Bacillus subtilis* and in three related *Vibrio* species are listed in Table 2.1.

Predicted competence genes were strictly conserved between *V. cholerae*, *Vibrio parahaemolyticus*, *Vibrio vulnificus* and *Vibrio fischeri*. Conservation of competence genes was also striking between *V. cholerae* and *N. gonorrhoeae*, in which only one gene cluster, *VC0857-0861*, was absent. The high degree of conservation confirms the current notion that the DNA uptake process during natural transformation might be close to universal.

Chapter 2. Components of the *Vibrio cholerae* DNA uptake machinery

Table 2.1: Competence gene homologs with potential contribution to DNA uptake, protection or recombination in *V. cholerae*

Locus Tag ¹	Gene name	Homolog(s) ²					
		N.g.	H.i.	B.s.	V.p.	V.v.	V.f.
↓VC0032	<i>comM</i>	NGO1550	<i>comM</i>	-	<i>comM</i>	<i>comM</i>	VF2555
↓VC0048	<i>dprA</i>	<i>dprA</i>	<i>dprA</i>	<i>dprA</i>	<i>dprA</i>	<i>dprA</i>	<i>dprA</i>
↓VC0217	<i>radC</i>	<i>radC</i>	<i>radC</i>	<i>radC</i>	<i>radC</i>	<i>radC</i>	<i>radC</i>
↓VC0397	<i>ssb</i>	<i>ssb</i>	<i>ssb</i>	<i>ssbA</i>	<i>ssb</i>	<i>ssb</i>	<i>ssb</i>
↓VC0462	<i>pilT</i>	<i>pilT</i>	-	-	<i>pilT</i>	<i>pilT</i>	<i>pilT</i>
↓VC0463	<i>pilU</i>	<i>pilU</i>	-	-	VP2614	<i>pilU</i>	<i>pilU</i>
↓VC0543	<i>recA</i>	<i>recA</i>	<i>recA</i>	<i>recA</i>	<i>recA</i>	<i>recA</i>	<i>recA</i>
↑VC0857	VC0857	-	-	-	<i>pilE</i>	<i>pilE</i>	<i>pilA1</i>
↓VC0858	VC0858	-	-	-	VP0657	<i>fimT</i>	VF0571
↓VC0859	VC0859	-	-	-	VP0658	<i>pilW</i>	VF0570
↓VC0860	VC0860	-	-	-	VP0659	VV1_0350	VF0569
↓VC0861	VC0861	-	-	-	VP0660	VV1_0349	VF0568
↓VC1612	<i>pilF</i>	<i>pilW</i>	<i>pilF2</i>	-	<i>pilF</i>	<i>pilF</i>	<i>pilF</i>
↓VC1879	<i>comEC</i>	<i>comA</i>	<i>rec2</i>	<i>comEC</i>	<i>rec2</i>	<i>rec2</i>	<i>comA</i>
↑VC1917	<i>comEA</i>	<i>comE</i>	<i>comE1</i>	<i>comEA</i>	<i>comE</i>	VV_0017	<i>comE1</i>
↓VC2423	<i>pilA</i>	<i>pilE</i>	<i>pilA</i>	<i>comGC</i> ³	<i>pilA</i>	<i>pilA</i>	<i>pilA</i>
↓VC2424	<i>pilB</i>	<i>pilF</i>	<i>pilB</i>	<i>comGA</i>	<i>pilB</i>	<i>pilB</i>	<i>pilB</i>
↓VC2425	<i>pilC</i>	<i>pilG</i>	<i>pilC</i>	<i>comGB</i>	<i>pilC</i>	<i>vvpC</i>	<i>pilC</i>
↓VC2426	<i>pilD</i>	<i>pilD</i>	<i>pilD</i>	<i>comC</i>	<i>pilD</i>	<i>vvpD</i>	VF2188
↑VC2630	<i>pilQ</i>	<i>pilQ</i>	<i>comE</i>	-	<i>pilQ</i>	<i>pilQ</i>	<i>pilQ</i>
↓VC2631	<i>pilP</i>	<i>pilP</i>	<i>comD</i> ³	-	<i>pilP</i>	<i>pilP</i>	VF2294
↓VC2632	<i>pilO</i>	<i>pilO</i>	<i>comC</i> ³	-	<i>pilO</i>	<i>pilO</i>	<i>pilO</i>
↓VC2633	<i>pilN</i>	<i>pilN</i>	<i>comB</i>	-	<i>pilN</i>	<i>pilN</i>	<i>pilN</i>
↓VC2634	<i>pilM</i>	<i>pilM</i>	<i>comA</i> ³	-	<i>pilM</i>	<i>pilM</i>	<i>pilM</i>
↑VC2678	<i>priA</i>	<i>priA</i>	<i>priA</i>	<i>priA</i>	<i>priA</i>	<i>priA</i>	<i>priA</i>
↓VC2719	<i>comF</i>	<i>comF</i>	<i>comF</i>	<i>comFC</i>	<i>comF</i>	VV_0863	<i>comF</i>

¹ The genetic organization of competence genes is indicated. VC numbers according to [115].

² Homologs are based on protein-sequence similarities, the position of genes in operons, and their predicted functions. N.g. *Neisseria gonorrhoeae*; H.i. *Haemophilus influenzae*; B.s. *Bacillus subtilis*; V.p. *Vibrio parahaemolyticus*; V.v. *Vibrio vulnificus*; V.f. *Vibrio fischeri*

³ No significant BLAST hits. The indicated homology is based on the predicted function or on the organization of the operon.

2.1.2 Transformability of mutants lacking individual competence genes

Only four of the 26 *V. cholerae* genes listed in Table 2.1 have already been studied experimentally in the context of natural transformation (*pilA*, *pilB*, *pilQ*, *comEA*) [112]. All four have been shown to be required for chitin-mediated natural transformation of *V. cholerae* [112]. To test for the involvement of the other 22 predicted competence genes (Table 2.1), we attempted to establish single gene deletion strains (referred to as competence gene mutants; Table A.1). In addition to the published four competence gene mutants (strains Δ *pilA*, Δ *pilB*, Δ *pilQ*, Δ *comEA*), we were able to create twenty strains deficient in a single competence gene. There was no obvious effect on growth in liquid medium for 18 of the twenty newly created knock-out strains. Deletion of *recA* had a slightly negative effect on growth in liquid medium, which was more pronounced for growth on solid LB-agar plates. In contrast, one of the twenty newly

established deletion mutants, $\Delta pilD$, had a strong growth phenotype. Therefore, this strain was excluded from further experiments. All attempts to knock out *ssb* and *priA* failed, which is in accordance with recent studies showing their essentiality in *V. cholerae* [180, 181].

We then continued to assess transformability of all competence gene deletion strains that were not severely impaired in growth (19 of our newly established strains, plus the four published deletion mutants). To this end, we used a previously established natural transformation assay, which is based on growth of bacteria on a chitin surface (chitin flakes) and subsequent exposure to genomic DNA (gDNA) of a *V. cholerae* strain that contains a kanamycin resistance cassette inserted into the *lacZ* gene as selection marker [182, 183]. Results are summarized in Table 2.2.

Table 2.2: Chitin-induced natural transformation assay of *V. cholerae* competence gene mutants

Strain	Transformation frequency ¹	Relative to WT ²	Detection limit
wildtype	$3.4 \pm 2.1 \times 10^{-4}$	1	-
$\Delta comM$	$3.3 \pm 1.2 \times 10^{-5}$	0.1	-
$\Delta dprA$	< d.l.	-	$1.4 \pm 0.6 \times 10^{-7}$
$\Delta radC$	$1.7 \pm 1.8 \times 10^{-4}$	0.5	-
$\Delta pilT$	< d.l.	-	$7.0 \pm 5.5 \times 10^{-8}$
$\Delta pilU$	$2.3 \pm 0.7 \times 10^{-4}$	0.7	-
$\Delta recA$	< d.l.	-	$7.4 \pm 2.0 \times 10^{-8}$
$\Delta VC0857$	$8.9 \pm 2.0 \times 10^{-6}$	0.03	-
$\Delta VC0858$	< d.l.	-	$7.6 \pm 5.9 \times 10^{-8}$
$\Delta VC0859$	$1.8 \pm 1.7 \times 10^{-8}$ ⁽³⁾	0.0001	-
$\Delta VC0860$	$7.0 \pm 1.7 \times 10^{-7}$	0.002	-
$\Delta VC0861$	< d.l.	-	$4.8 \pm 0.9 \times 10^{-8}$
$\Delta pilF$	< d.l.	-	$1.3 \pm 0.6 \times 10^{-7}$
$\Delta comEC$	< d.l.	-	$9.0 \pm 5.1 \times 10^{-8}$
$\Delta comEA$	< d.l.	-	$1.3 \pm 0.6 \times 10^{-7}$
$\Delta pilA$	< d.l.	-	$9.8 \pm 2.0 \times 10^{-8}$
$\Delta pilB$	< d.l.	-	$6.7 \pm 2.2 \times 10^{-8}$
$\Delta pilC$	< d.l.	-	$3.6 \pm 3.0 \times 10^{-7}$
$\Delta pilQ$	< d.l.	-	$1.3 \pm 0.8 \times 10^{-7}$
$\Delta pilP$	< d.l.	-	$7.6 \pm 7.0 \times 10^{-7}$
$\Delta pilO$	< d.l.	-	$2.8 \pm 1.2 \times 10^{-7}$
$\Delta pilN$	< d.l.	-	$4.9 \pm 3.4 \times 10^{-7}$
$\Delta pilM$	< d.l.	-	$7.0 \pm 2.3 \times 10^{-8}$
$\Delta comF$	< d.l.	-	$1.0 \pm 0.8 \times 10^{-7}$

¹ Transformation frequencies were determined as in [182]. Shown are average transformation frequencies/detection limits (d.l.) \pm SD of at least three independent experiments.

² Average transformation frequency relative to wildtype (WT).

³ The transformation frequency was below the detection limit in one of three experiments.

17 of the tested 23 competence genes were required for natural transformation (Table 2.2). *comM*, *radC* and *pilU* were dispensable to reach transformation frequencies that were less than ~ 10 -fold reduced compared to a wildtype strain (Table 2.2). Strains deficient in one of these three genes were therefore not considered further. Deletion of *VC0857* had an intermediate, but significant effect on transformability. Transformation frequencies of the remaining 19

mutants were all at least ~500-fold decreased or under the limit of detection. We concluded that the respective competence genes, which are affected in those twenty mutants, are part of the minimal, but likely not complete, core set of components that constitutes the DNA uptake complex.

2.1.3 Detection of heterologous DNA uptake events in competent *Vibrio cholerae*

Some Gram-negative bacteria, e.g. *N. gonorrhoeae* and *H. influenzae*, preferentially take up DNA that contains specific sequence motifs (DNA uptake sequences, DUS) [48–50]. As no such sequence motifs have been described for *V. cholerae*, we developed a PCR based assay to experimentally verify whether DNA uptake in *V. cholerae* can occur across species boundaries. To this end, we designed primers that specifically anneal to the chromosome of *V. cholerae* acceptor bacteria, and primers that were specific for DNA isolated from either *V. cholerae* A1552-LacZ-kan (annealing to the kanamycin resistance marker, which is absent in wildtype *V. cholerae*), or specific for DNA isolated from *E. coli* or *B. subtilis* (Figure 2.1 A). We then tested cross-reactivity of combinations of these primer pairs in a duplex PCR (i.e. using two primer pairs per PCR) (Figure 2.1 B). Primers were indeed specific for the detection of gDNA derived from acceptor bacteria (wildtype *V. cholerae* A1552) or gDNA from donor strains (A1552-LacZ-kan, *E. coli* BL21(DE3) and *B. subtilis* 168).

Next, we tested whether different competence gene mutants of *V. cholerae* could take up DNA. Briefly, we induced competence in *V. cholerae* acceptor strains (deficient in *pilQ*, *dprA*, or *recA*) by growth on chitin surfaces, and exposed them to gDNA derived from different donor bacteria (*V. cholerae*, *E. coli* or *B. subtilis*). DNA, which was not transported across the outer membrane, was removed by a DNase treatment. Finally, successful DNA uptake was detected in a whole-cell duplex PCR reaction, using primer pair combinations as outlined in Figure 2.1 A. Intact acceptor bacteria with potentially internalized donor DNA served as template (hence the name *whole-cell* duplex PCR).

As stated in [176], we detected donor gDNA in the wildtype strain (lane 1) and the strain lacking ComEC (annotated inner membrane transporter, lane 3) (Figure 2.1 C). Whereas the PCR fragment derived from the wildtype sample (lane 1) could be the results of the three different locations of the template (donor gDNA), namely, in the periplasm, in the cytoplasm, or recombined into the chromosome, a *comEC*-negative strain (lane 3) is nontransformable (Table 2.2), as it is blocked for periplasm-to-cytoplasm transport of the incoming DNA. Thus, the donor gDNA exclusively accumulates in the periplasmic space. In contrast, no donor DNA was taken up in a strain devoid of the putative outer membrane secretin PilQ (lane 2) (Figure 2.1 C). This also represents an important control for whole-cell duplex PCR, confirming that the DNase treatment removed all traces of extracellular donor gDNA.

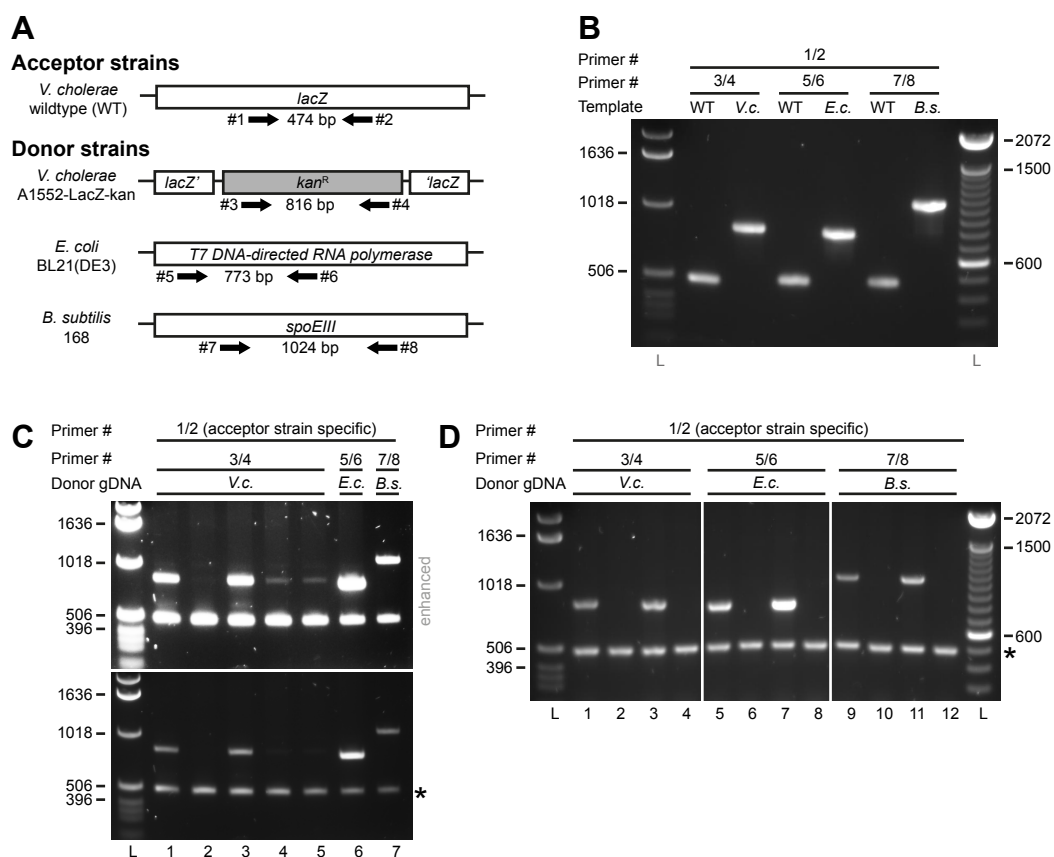


Figure 2.1: Uptake of heterologous DNA by naturally competent *V. cholerae* cells. (A) Scheme of acceptor and donor strain-specific genomic DNA (gDNA) regions. Acceptor strains were *lacZ*-positive and detectable with primers #1/#2. Donor gDNA of the *V. cholerae* strain A1552-LacZ-kan [182] lacks the respective part of the *lacZ* gene due to the replacement with a kanamycin resistance cassette (*aph*), which is detectable with primers #3/#4. A chromosomal region specific to *E. coli* BL21 (DE3) gDNA encodes the T7 DNA-directed RNA polymerase (CP001509 [184]), to which primers #5/#6 anneal. For *B. subtilis* 168, primers annealing specifically to the *spoEIII* gene were designed (#7/#8). The expected PCR fragment sizes are indicated (not to scale). (B) Control experiment to validate primers in the duplex PCR (i.e. using two primer pairs per reaction). Primer combinations are indicated above the figure. The different templates included gDNA derived from *V. cholerae* acceptor strain A1552 (WT), and donor gDNA derived from *V. cholerae* strain A1552-LacZ-kan (*V.c.*), *E. coli* strain BL21(DE3) (*E.c.*) or *B. subtilis* strain 168 (*B.s.*). (C) Detection of DNase I resistant donor gDNA after induction of natural competence on chitin surfaces. *V. cholerae* strains A1552 (wildtype, lane 1), Δ pilQ (lane 2), Δ comEC (lanes 3, 6, 7), Δ dprA (lane 4), and Δ recA (lane 5) were induced for natural competence by growth on chitin flakes. After incubation in presence of donor gDNA derived from *V. cholerae* A1552-LacZ-kan (*V.c.*), *E. coli* BL21(DE3) (*E.c.*), and *B. subtilis* 168 (*B.s.*), the cells were analyzed for internalization of donor DNA by whole-cell duplex PCR. The asterisk indicates the quantification of acceptor strains using primer pair 1/2. Both images depict the same agarose gel, but the upper image has been uniformly enhanced for contrast and brightness. Primer combinations are indicated above the figure and refer to primer numbers as indicated panel (A). (D) Semiquantitative DNA uptake assay following artificial competence induction in liquid medium. Chitin- and surface-independent DNA uptake was performed in liquid medium by overexpression of *tfoX* from a plasmid. This method allowed for the quantification of bacterial cells by optical density measurements. *V. cholerae* strains tested were Δ dns (lanes 1, 5, 9), Δ dns Δ pilQ (lanes 2, 6, 10), Δ dns Δ comEC (lanes 3, 7, 11). All strains contained the plasmid pBAD-*tfoX*-stop for the induction of competence. As negative control, strain Δ dns Δ comEC/pBAD-*tfoX*-stop was tested in the absence of *tfoX* inducer (lanes 4, 8, 12). Donor gDNA and primer combinations are indicated above the figure as in panel (C). Shown are the results of one representative experiment of at least three independent replicates. L, ladder (left, 1-kb ladder; right 100-bp ladder [Invitrogen]).

We detected minimal amounts of donor gDNA in the two strains lacking DprA and RecA, respectively (Figure 2.1 C, upper image [after enhancement of brightness and contrast]). Based on the knowledge of other naturally competent bacteria, the donor gDNA is not impaired in transport across the cytoplasmic DNA in these strains and thus can enter the cytoplasm [105, 185–187]. However, as the incoming ssDNA is not protected from degradation and/or is unable to homologously recombine into the chromosome, it is prone to quick degradation in this compartment. Indeed, both strains were nontransformable based on the lack of detection of transformants on selective agar plates (Table 2.2). Therefore, we hypothesize that the faint donor gDNA-specific PCR band shown in Figure 2.1 C is derived from leftover gDNA that has not yet been transported from the periplasmic space into the cytoplasm. We also demonstrated that the DprA strain is not impaired in the first step of the DNA uptake process, namely, the transport across the outer membrane, as a *dprA comEC* double mutant resulted in the same intense donor gDNA-specific PCR band as observed for the *comEC* single mutant (data not shown).

After establishing this assay, we were able to test for non-species-specific DNA uptake. We used donor gDNA from a representative sampling of both Gram-negative (*E. coli*) and Gram-positive (*B. subtilis*) bacteria (Figure 2.1 C, lanes 6 and 7). In both cases, the donor gDNA successfully accumulated in the periplasm of a *comEC*-deficient acceptor strain, proving that the DNA uptake machinery of *V. cholerae* does not differentiate between species-specific and non-species-specific DNA.

To obtain more quantitative results, we switched from the chitin surface experimental setup to artificial *tfoX* overexpression in chitin- and surface-independent natural transformation conditions (Figure 2.1 D). Furthermore, we deleted the extracellular nuclease gene *dns* in these strains to exclude uneven donor gDNA degradation outside the cells. Apart from the *dns* deletion, the genotypes of the *V. cholerae* strains were unchanged (Figure 2.1 D, lanes 1, 5, and 9), deleted in *pilQ* (lanes 2, 6, and 10), or devoid of the *comEC* gene (lanes 3, 4, 7, 8, 11, and 12). For the last strain, two cultures were tested: one culture contained the *tfoX* inducer arabinose (Figure 2.1 D, lanes 3, 7, and 11), and one control culture was not induced for competence (lanes 4, 8, and 12). As illustrated in Figure 2.1 D, no difference was observed with respect to the uptake process between species-specific (lanes 1 to 4) and non-species-specific (lanes 5 to 12) DNA in this semiquantitative assay. Furthermore, no DNA uptake occurred in the absence of the outer membrane secretin PilQ or in the absence of artificial *tfoX* induction (Figure 2.1 D, even lanes). These data indicate that DNA uptake by *V. cholerae* requires the induction of the competence genes, including *pilQ*, and that the DNA uptake process itself does not depend on species-specific donor DNA.

2.1.4 Natural transformability of competence gene mutants in a chitin-independent competence induction setup using *TntfoX*

When growing on chitin surfaces, only a subpopulation of bacteria expresses the competence genes, as demonstrated recently [160]. This is likely due to the heterogenous environment surrounding the chitin surface [160]. As a consequence, we might have overestimated the detection limit of our chitin-dependent natural transformation assay (Table 2.2), because

the detection limit was calculated based on the assumption that all cells of the culture enter the competence state. To increase our detection power and to induce competence genes more homogeneously, we used a recently developed system that allows inducible low-level production of the master regulator of competence, TfoX, in a chitin-independent manner [160]. In this system, Lo Scrudato and Blokesch put *tfoX* under control of an arabinose-inducible promoter, which is repressed in the absence of arabinose and cloned the construct into a mini-Tn7 transposon [188], which site-specifically integrates into the large chromosome of *V. cholerae*. This construct was named TntfoX and allowed efficient chitin-independent competence induction [160].

To assess transformability of competence genes mutants independent of chitin, we introduced the TntfoX transposon in all strains listed in Table 2.2 that were severely impaired in natural transformability in the chitin-dependent setting.

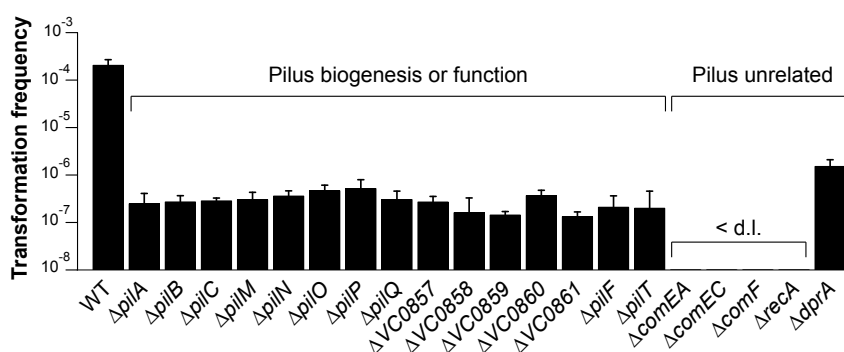


Figure 2.2: Chitin-independent natural transformation in strains lacking individual competence proteins. The natural transformability of a wildtype (WT) strain and derivatives thereof lacking individual competence genes was tested in a chitin-independent assay [160]. All strains contain TntfoX for competence induction. Shown are average transformation frequencies of at least three independent biological replicates. Error bars indicate standard deviations. All mutants were significantly impaired in natural transformability ($P < 0.02$). < d.l., below detection limit. The average d.l. of non-transformable strains was $7.1 \pm 3.3 \times 10^{-8}$.

As for chitin-mediated competence induction (Table 2.2), we observed a dramatic decrease of transformability in all strains (Figure 2.2). Also, transformation frequencies of a wildtype strain were in the range of previous experiments on chitin flakes (Figure 2.2, Table 2.2).

To exclude polar effects as the cause of the observed phenotypes, we complemented all strains *in trans* by providing a wildtype copy of the respective gene on a plasmid. Expression of the constructs was driven by the arabinose inducible P_{BAD} promoter. This restored transformability to significant levels (Table 2.3), even though the stoichiometry of DNA uptake components is likely disturbed under these commonly used *trans*-complementation conditions. Interestingly, we observed severe toxicity for two genes (*pilP* and *pilQ*), when their expression was induced in *E. coli* (data not shown). This is in line with the reduced complementation efficacy of the respective *V. cholerae* deletion strains (Table 2.3).

In contrast to chitin-mediated competence induction, 16 genes were dispensable for transformability, though significantly reduced with respect to the frequency with which trans-

Chapter 2. Components of the *Vibrio cholerae* DNA uptake machinery

formants were observed (Figure 2.2). Most importantly, there was a strong correlation between the putative function of competence genes and their dispensability for natural transformation. Based on their genome annotation, twelve of the identified *V. cholerae* competence genes that were needed for efficient transformation (Figure 2.2) (*pilA/B/C*, *pilM/N/O/P/Q*, *VC0857-0858*, *VC0861*, *pilF*) have been previously suggested to encode proteins involved in the biogenesis of a type IV pilus (Figure 1.3), [112, 158], although the presence of this pilus has only been inferred from protein homologies. PilT, annotated as “twitching motility protein” (<http://genodb.pasteur.fr/cgi-bin/WebObjects/GenoList>), might contribute to pilus retraction, as has been shown for PilT homologs in other organisms [78–81]. Finally, due to their operon organization (Table 2.1), *VC0859-0860*, might be involved in similar processes as *VC0858* and *VC0861*. While all genes encoding proteins that are potentially responsible for pilus biogenesis/function were dispensable to still acquire transformants at low frequencies, four proteins required for pilus-independent functions during natural transformation (*ComEA*, *ComEC*, *ComF*, *RecA*) were essential (Figure 2.2).

Table 2.3: Natural transformability of *trans* complemented competence gene mutants

Strain ¹	Transformation frequency ²		Significance ³
	Vector control	Complemented	
$\Delta pilA$	$1.4 \pm 1.2 \times 10^{-6}$	$1.2 \pm 0.3 \times 10^{-5}$	**
$\Delta pilB$	$1.1 \pm 0.7 \times 10^{-6}$	$5.9 \pm 3.6 \times 10^{-5}$	**
$\Delta pilC$	$9.6 \pm 7.9 \times 10^{-7}$	$6.8 \pm 4.8 \times 10^{-6}$	*
$\Delta pilT$	$8.8 \pm 3.2 \times 10^{-8}$	$1.5 \pm 0.4 \times 10^{-5}$	**
$\Delta pilF$	$1.0 \pm 0.7 \times 10^{-6}$	$4.3 \pm 2.6 \times 10^{-5}$	**
$\Delta pilM$	$1.2 \pm 0.7 \times 10^{-6}$	$1.3 \pm 0.5 \times 10^{-4}$	*
$\Delta pilN$	$2.3 \pm 0.6 \times 10^{-6}$	$5.9 \pm 5.1 \times 10^{-5}$	**
$\Delta pilO$	$4.6 \pm 2.1 \times 10^{-7}$	$1.5 \pm 0.9 \times 10^{-4}$	**
$\Delta pilP$	$1.5 \pm 0.3 \times 10^{-6}$	$7.2 \pm 2.9 \times 10^{-6}$	*
$\Delta pilQ$	$1.2 \pm 0.9 \times 10^{-6}$	$6.6 \pm 3.2 \times 10^{-6}$	*
$\Delta VC0857$	$6.2 \pm 2.2 \times 10^{-7}$	$6.7 \pm 4.6 \times 10^{-5}$	*
$\Delta VC0858$	$9.7 \pm 5.7 \times 10^{-7}$	$3.7 \pm 0.9 \times 10^{-6}$	*
$\Delta VC0859$	$1.4 \pm 0.2 \times 10^{-6}$	$1.7 \pm 0.9 \times 10^{-5}$	*
$\Delta VC0860$	$1.0 \pm 0.2 \times 10^{-6}$	$5.8 \pm 3.6 \times 10^{-6}$	*
$\Delta VC0861$	$1.1 \pm 0.6 \times 10^{-6}$	$1.1 \pm 0.9 \times 10^{-5}$	**
$\Delta comEA$	< d.l. ⁴	$1.7 \pm 0.8 \times 10^{-4}$	**5
$\Delta comEC$	< d.l. ⁴	$1.2 \pm 0.1 \times 10^{-4}$	**5
$\Delta comF$	< d.l. ⁴	$4.3 \pm 2.0 \times 10^{-5}$	**5
$\Delta recA$	< d.l. ⁴	$5.9 \pm 4.2 \times 10^{-6}$	**5
$\Delta dprA$	$9.1 \pm 7.3 \times 10^{-7}$	$1.3 \pm 0.1 \times 10^{-5}$	*

¹ Strains are deficient in the genes indicated and harbor the *Tn_{foX}* transposon for competence induction.

² Shown are average transformation frequencies \pm SD of at least three independent biological experiments.

³ Statistical significance was tested with Welch’s t-test on log-transformed values.

* $P < 0.05$; ** $P < 0.01$.

⁴ Detection limits (d.l.) were $8.4 \pm 2.1 \times 10^{-8}$, $9.4 \pm 1.5 \times 10^{-8}$, $5.9 \pm 1.2 \times 10^{-8}$, and $1.2 \pm 0.4 \times 10^{-7}$ for $\Delta comEA$, $\Delta comEC$, $\Delta comF$, and $\Delta recA$, respectively.

⁵ Detection limits were used for statistical analysis.

2.1.5 Detection of rare transformation events on chitin flakes

The differences in transformation frequencies for chitin-mediated and *Tn_{tfoX}*-mediated competence induction was unexpected. To test whether we could also detect rare transformation events under chitin-inducing conditions (Table 2.2), we slightly adjusted the procedure. After detachment of bacteria from chitin flakes, we enriched the culture for several hours in rich medium (without selection pressure), before selecting for transformants on antibiotic containing plates. This significantly improved the detection limit compared to the standard chitin-mediated transformation assay (Figure 2.3).

Indeed, we detected rare transformation events for strains deficient in *pilA*, *pilB* or *pilQ*, but not for strains lacking *comEA*, *comEC* or *comF* (Figure 2.3), which is in line with our observation in the chitin-independent transformation assay (Figure 2.2).

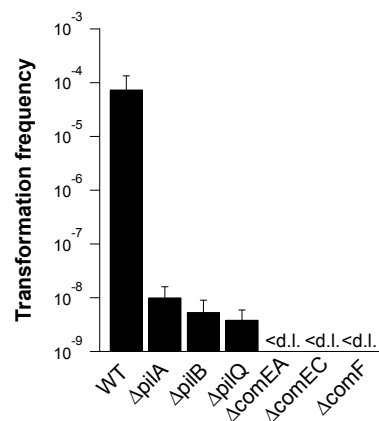


Figure 2.3: Detection of rare transformation events after chitin-mediated competence induction. Chitin-induced natural transformation was performed as described [182, 183], with minor modifications. Briefly, after detachment of bacteria from the chitin surfaces, the cells were enriched in 2-YT (2 × Yeast extract and tryptone) broth for 8 h before being plated and enumerated for antibiotic resistant and total CFU. Shown are average transformation frequencies (\pm SD) of at least three independent experiments. <d.l., below detection limit, which was on average $2.9 \pm 1.2 \times 10^{-9}$.

2.1.6 DNA uptake across the outer membrane is not functionally coupled to inner membrane transport

Transport defects across either of the two cell membranes of *V. cholerae* could account for the observed reduction in transformation frequencies of competence genes mutants (Figure 2.2). To better characterize the putative role of individual competence proteins in DNA uptake with respect to transport across the outer membrane (OM) or DNA transport into the cytoplasm, we slightly modified our DNA uptake assay (section 2.1.3). Briefly, we used *Tn_{tfoX}* for competence induction instead of chitin flakes. Furthermore, we unified the number of bacteria used in the whole-cell duplex PCR reactions and used primers specific to *E. coli* BL21 (DE3) gDNA, which was used as transforming DNA (tDNA). This allowed us to distinguish between DNA uptake beyond the OM and DNA uptake across the inner membrane (IM) (Figure 2.4).

Strains lacking components important for efficient DNA transport across the OM are not able to protect tDNA from extracellular digestion by DNase I and therefore would not result in a tDNA-derived PCR band. This was obvious for all components predicted to be involved in pilus biogenesis or function (Figure 2.4A). Concomitant deletion of *comEC* in these strains did not result in detection of tDNA by PCR (Figure 2.4A). This confirmed that ComEC

Chapter 2. Components of the *Vibrio cholerae* DNA uptake machinery

acts downstream of DNA transport across the OM. In contrast, a strain lacking only *comEC* accumulated tDNA in the periplasm and depicted a stronger PCR band derived from tDNA than a wildtype (WT) strain (Figure 2.4 A, B). Most interestingly, a strain lacking *comF*, a gene of unknown function, accumulated periplasmic tDNA to similar levels as a *comEC* deficient strain, independent of the concomitant presence or absence of *comEC* (Figure 2.4 A, B). This strongly suggests that ComF mediates a function in IM DNA transport, along with or in concert with ComEC. Finally, co-deletion of *comEC* and *recA* or *dprA* increased tDNA accumulation compared to a *recA*-negative and a *dprA*-negative strain (Figure 2.4 A, B). This verified that RecA and DprA act downstream of ComEC and are not implicated in the transport process.

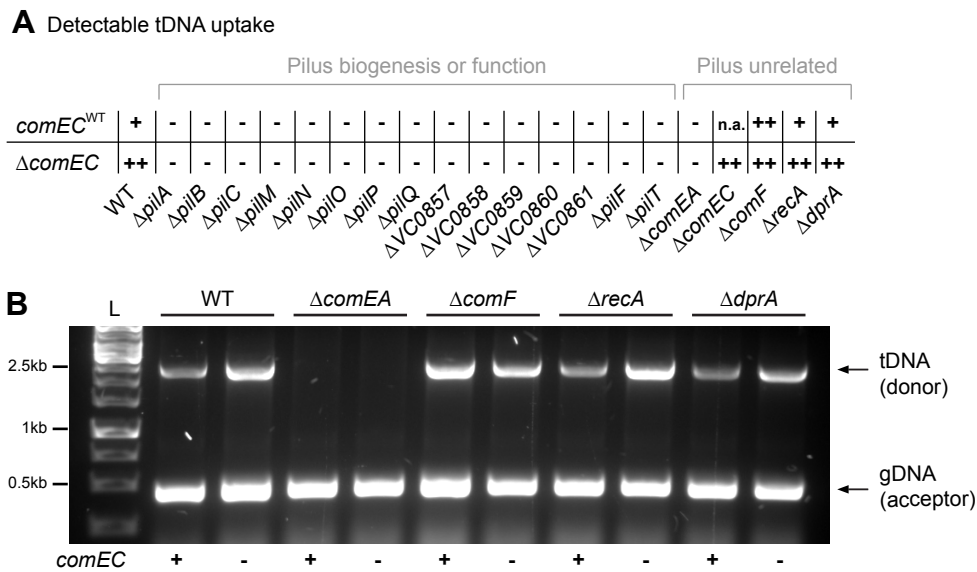


Figure 2.4: Detection of internalized tDNA by whole-cell duplex PCR. DNA uptake was tested by whole-cell duplex PCR (section 2.1.3) in a chitin-independent setting. All strains contained the *TntfoX* transposon for competence induction. (A) Detection of tDNA uptake in competence mutant strains (upper row, *comEC*^{WT}) and in double-knock-out strains from which *comEC* was concomitantly absent (lower row, Δ *comEC*). Labels: -, no tDNA detectable, +/++, tDNA detected by PCR; n.a. not applicable. Band intensities of PCR products were judged relative to that of the wildtype strain. (B) DNA uptake in wildtype and representative mutant strains (Δ *comEA*, Δ *comF*, Δ *recA*) of *V. cholerae*. All strains were either wildtype for *comEC* (+) or *comEC*-deficient (-), as indicated below the image. The PCR reactions contained primers specific to the transforming DNA (tDNA, 2,652 bp) and to the genomic DNA (gDNA) of the acceptor bacteria (474 bp). Shown is a representative example of two independent biological replicates. L, ladder (1-kb GeneRuler).

2.2 Discussion

2.2.1 A first model of the *Vibrio cholerae* DNA uptake machinery

We identified a set of 20 genes that is needed for efficient natural transformation of *V. cholerae* on chitin surfaces (Table 2.2) or in a chitin-independent transformation assay (Figure 2.2). Based on these genes, we propose a first model for DNA uptake in naturally competent *V. cholerae* (Figure 2.5).

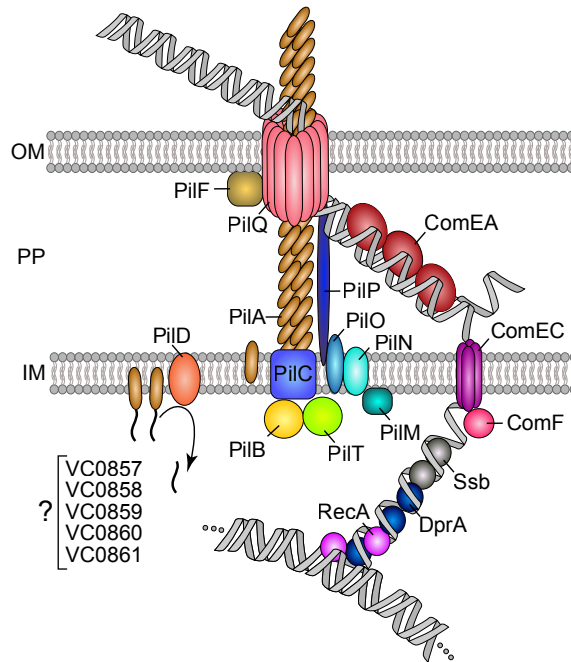


Figure 2.5: Proposed model of the DNA uptake machinery of naturally competent *V. cholerae*. The proposed model is composed of components that are needed for efficient natural transformation (Table 2.2 and Figure 2.2) of *V. cholerae*. The architecture is based on homologies to (predicted) competence proteins from other competent bacteria or other type IV pili-containing organisms. OM, outer membrane; PP, periplasm; IM, inner membrane. Details are described in the text.

In the center of our model is a type IV pilus with PilA as the major pilin. The pilus is assembled at the inner membrane, where prepilins are processed by the prepilin peptidase PilD. This protein has already been shown to be involved in cholera toxin secretion through the eps type II secretion system and to mediate processing of prepilins of another, yet competence unrelated, type IV pilus in *V. cholerae* (the mannose-sensitive hemagglutination pilus (MSHA)) [71, 179]. The involvement of PilD in different protein export systems might explain the growth defect, which we observed by generating a *pilD* knock-out strain, and which has been reported previously [71, 179]. Processed PilA is subsequently incorporated into the growing filament by the well conserved traffic ATPase PilB (Table 2.1). The pilus then crosses the outer membrane through a pore composed of PilQ subunits. VC1612, which we proposed to name PilF due to its high level of sequence identity with homologs in other *Vibrio* species (e.g. PilF of *V. vulnificus*, *V. fischeri* and *V. parahaemolyticus*; for some strains also annotated as PilW), might be responsible for PilQ stability and formation of the outer membrane pore, as suggested

for the *Neisseria meningitidis* homolog PilW [77]. Similarly, Koo *et al.* have shown that PilF of *Pseudomonas aeruginosa* is needed for the multimerization and localization of the outer membrane secretin in this species [189, 190].

PilC, as well as PilM/N/O form an inner membrane platform for pilus biogenesis. Homologs of these proteins have been recently studied in *Neisseria meningitidis*, *Thermus thermophilus* and *Myxococcus xanthus*, which revealed many structural details on the composition of the inner membrane platform [191, 192] and the sequential order, in which these proteins are assembled [193]. Based on these studies, we propose PilC and PilN/O to be integral membrane proteins in our model, while PilM is associated with this complex within the cytoplasm. *pilP*, the fourth gene within the *pilM/N/O/P* cluster, likely encodes a protein that bridges the periplasm and contacts PilN/O, as well as the outer membrane secretin PilQ [194, 195]. The cytoplasmic ATPase PilT likely drives pilus retraction. All proteins of our model (Figure 2.5) discussed so far finally mediate biogenesis and retraction of a type IV pilus, which is involved, be it either directly or indirectly, in transport of DNA across the outer membrane. Our data are fully consistent with this model, since strains lacking pilus-related genes were unable to accumulate periplasmic DNA, as deduced from a whole-cell duplex PCR assay (Figure 2.4), and were consequently severely impaired in natural transformability (Table 2.2, Figure 2.2).

The role of the *VC0857-VC0861* gene cluster is less clear. These genes have not been analyzed previously in *V. cholerae* and they do not possess close homologs in better studied competent bacteria, such as *N. gonorrhoeae*, *H. influenzae* or *B. subtilis* (Table 2.1). We hypothesize that *VC0857-0861*, of which some genes are annotated to encode minor pilins, might assist initiation of PilA polymerization, as it has been shown for unrelated minor pseudopilins of the *Klebsiella oxytoca* type II secretion system [196]. This would fit our observations that strains deficient in individual genes of this cluster were not able to efficiently transport DNA across the outer membrane, as all other pilus-related deletion strains (Figure 2.4).

In addition to the pilus-related components, we identified five proteins that are thought to mediate pilus-unrelated functions during DNA uptake (ComEA, ComEC, ComF, DprA and RecA). ComEA has been shown to be important for transformability of *V. cholerae* earlier [112]. We confirmed these data and showed that ComEA acts upstream of ComEC (Figure 2.4). No DNA uptake was detectable in a *comEA* or a *comEA comEC* double mutant, suggesting that ComEA is implicated in DNA transport across the outer membrane (section 4 will follow up on this idea). However, its precise role remains vague. We suggest that PilT driven pilus retraction allows short stretches of DNA to enter the periplasm, where it is bound by ComEA and further shuttled to an inner membrane channel made of ComEC. Indeed, a ComEC mutant strongly accumulated DNA (Figure 2.4) within the periplasm, where it is protected from degradation by extracellular nucleases. The same was true for a *comF* deletion strain. This is especially interesting since no putative function could be attributed to ComF.

ComFC, which constitutes the ComF homolog in *B. subtilis* (Table 2.1), has been shown to be implicated in DNA uptake, although the authors of this study only observed a five-fold decrease in transformation frequencies [197]. It is important to note, however, that *comFC* was not completely deleted in this study, but rather disrupted by integration of an erythromycin resistance cassette at the 3' end of the gene. This could still allow production of a truncated

protein with residual activity and therefore explain the weak transformation phenotype in the study by Londoño-Vallejo and Dubnau [197]. Instead of creating insertional mutants, we deleted all genes of interest, which resulted in complete inhibition of natural transformation in a *comF*-negative strain (Table 2.2, Figure 2.2). Deletion of *comF* also resulted in strong accumulation of periplasmic DNA, independent of *comEC* (Figure 2.4). We therefore conclude that ComF participates in transport of DNA across the inner membrane along with or in concert with ComEC.

In addition to *B. subtilis comFC*, *comFA*, another gene within the same operon, has been shown to participate in DNA uptake by this species [197]. However, we could not identify a close homolog of this gene in *V. cholerae*. VC1886, annotated as “transcription-repair coupling factor”, shares some sequence similarity with *B. subtilis* ComFA, but the average transformation frequency (TF) of a VC1886 deletion strain was not significantly affected (WT, $TF = 2.4 \pm 0.5 \times 10^{-4}$; $\Delta VC1886$, $TF = 3.3 \pm 1.3 \times 10^{-4}$; average $TF \pm SD$ of at least three independent experiments on chitin flakes). PriA also shares some sequence similarity with *B. subtilis* ComFA. Its homolog in *N. gonorrhoeae* has been suggested to participate in transport of DNA across the inner membrane [101]. Additionally, PriA has been shown to mediate non-competence related functions, such as restart of chromosomal replication in case of stalled replication forks in *E. coli* (reviewed in [100]). Provided that PriA mediates similar housekeeping functions in *V. cholerae*, this might explain why we could not establish a *priA* deletion in *V. cholerae*. This is in line with previous transposon mutagenesis experiments or their evaluation in *V. cholerae* that classified *priA* as “potentially essential” [198] or essential [180, 181].

Similarly, we could not create a deletion in the single strand binding protein gene, *ssb*. The Ssb homolog of *E. coli* is known to be important for the stabilization of single stranded DNA (ssDNA), and it is implicated in many basic cellular functions, such as DNA recombination, replication, or repair (reviewed in [199]). As in *E. coli*, *ssb* of *V. cholerae* has been proposed to be essential for cell survival [180, 181, 200]. We could therefore not assess whether Ssb is involved in natural transformation or not. In contrast, we showed that a second ssDNA binding protein, DprA, is indeed needed for high levels of transformability (Table 2.2, Figure 2.2). We also showed that DprA mediates functions downstream of ComEC, i.e. transport across the inner membrane, since a *dprA*-negative strain only contained small amounts of tDNA, while accumulation of tDNA increased in a *dprA comEC* double mutant (Figure 2.4). DprA likely protects incoming ssDNA and facilitates loading of RecA, as it has been shown in *in vitro* systems of *S. pneumoniae*, *B. subtilis* and *E. coli* proteins [33, 201]. Finally, RecA catalyzes homologous recombination of transforming DNA with the chromosome (Figure 1.2).

Interestingly, DprA was the only pilus-independent competence gene, which was not essential for natural transformation (Figure 2.2). Although transformation frequencies were ~100-fold lower compared to wildtype, a *dprA*-negative strain was still able to be naturally transformed in rare cases. This is in contrast to what has been shown for *S. pneumoniae*, in which DprA is strictly required for transformation [187]. In the absence of DprA, transforming DNA is in fact taken up efficiently, but it is degraded rapidly upon entry into the cytoplasm of streptococci [187]. In addition, DprA has been shown to confer regulatory functions in competence shut-off in this organism [202]. A *dprA* deficient strain showed decreased growth

upon competence induction, which might explain the strict dependence on DprA for transformation in *S. pneumoniae* [202]. In contrast, we did not observe any growth defect in *dprA* deficient strains after competence induction, and so far, no regulatory functions have been described for this protein in *V. cholerae*. Apart from *S. pneumoniae*, DprA is required for efficient transformation with chromosomal DNA in *H. influenzae*. Transformants were detectable in a $\Delta dprA$ strain, but at a roughly 10,000-fold reduced frequency compared to wildtype [186]. Yet there are competent bacteria, in which DprA seems to be more dispensable, similar to our observations in *V. cholerae*. In *H. pylori*, for example, transformation frequencies of a *dprA*-deficient strain were only 100-1,000-fold reduced [203, 204]. In *B. subtilis*, transformability with chromosomal DNA was even less affected, with a roughly ten- to fifty-fold reduction in transformation frequencies [205, 206]. It therefore seems likely that the highly conserved DprA protein is indeed important for natural transformation in all competent bacteria, including *V. cholerae*, but that its precise role differs between individual organisms, possibly depending on the presence of other ssDNA binding proteins and/or its implication in competence regulation.

2.2.2 DNA uptake in *Vibrio cholerae* is a multi-step process

While this work was ongoing, Sinha *et al.* published their results on the DNA uptake complex of *H. influenzae* [207]. They identified 17 genes, which were absolutely required for transformation. Of these 17 genes, 14 were presumably involved in the assembly and function of a type IV competence pilus. Concerning these findings, we stated previously [208] that although the chitin-dependent transformation assays of the competence gene mutants investigated in our study supported these results for *V. cholerae* (Table 2.2), we observed a slight but meaningful difference after chitin-independent transformation. Under the latter conditions, rare transformants were reproducibly detected for all mutants lacking competence proteins involved in pilus synthesis and function, whereas we never observed rare transformants for mutants lacking pilus-independent competence genes (with the exception of DprA, Figure 2.2). These diverging results between chitin-dependent and chitin-independent transformation first appeared contradictory; however, upon closer inspection of the data, we hypothesized that the rare transformants reproducibly observed under chitin-independent conditions might have been under the limit of detection of the chitin-dependent approach (Table 2.2). Notably, the detection limit of this assay was calculated on the basis of the total number of colony forming units (CFU) and was therefore based on the assumption that each cell entered the competence state when grown on a chitin surface. However, Lo Scudato and Blokesch have previously shown that due to the heterogenous environment around the chitin surface, only a part of the population enters the competence state [160]. The “real” detection limit based on the number of competent cells is therefore most likely higher, rendering rare transformants undetectable. To test this assumption, we repeated the chitin-dependent transformation assay with slight modifications, in order to increase the detection limit of the assay. Interestingly, we reproducibly detected rare transformants for the pilus-related mutants with this assay, but we never observed transformants for the pilus-unrelated mutants tested (i.e. *comEC*, *comEA* and *comF*, Figure 2.3). This strongly supports the data from the chitin-independent assay.

Although those rare transformants might be negligible in a global picture of the DNA uptake machinery, the difference between the appearance of rare transformants in the pilus-related mutants and their absence in the pilus-unrelated mutants is still meaningful, as it provides insight into the mechanistic aspects of the DNA uptake. Indeed, on the basis of these data, we conclude that DNA uptake must occur in at least two independent steps, whereby the second step (mediated by ComEA, ComEC, and ComF) cannot be circumvented. Our data therefore present a unique experimental indication of a two-step (at least) DNA uptake process in an organism containing a competence-induced type IV pilus, thereby confirming earlier hypotheses [57, 209].

A distinction into two groups of competence genes is also reflected by their regulation. While expression of most of the tested competence genes is under control of the competence regulator TfoX and subject to carbon catabolite repression, only *comEC* and *comEA* are co-regulated by quorum sensing [112, 160, 164, 165]. In contrast, pilus-related genes, such as *pilA* or *pilM*, are not dependent on quorum sensing [160] (Figure 1.7).

We suggest that the pilus part of the DNA uptake machinery is primarily involved in transport of tDNA across the outer membrane and that tDNA can occasionally enter the periplasm in a different way. To test whether the mannose-sensitive hemagglutination pilus (MSHA), another *V. cholerae* type IV pilus, which promotes adherence to zooplankton [210], could compensate for the lack of PilA competence pili, we constructed a strain, which was concomitantly deficient in *pilA* and in the outer membrane secretin of the MSHA pilus (*mshL*). However, this strain did not show a significant decrease in transformability compared to a *pilA* mutant ($\Delta pilA$ -TntfoX, TF = $1.8 \pm 0.4 \times 10^{-7}$; $\Delta mshL \Delta pilA$ -TntfoX, TF = $1.2 \pm 0.2 \times 10^{-7}$; average TF \pm SD of at least three independent experiments). Additionally, we created a deletion in *epsD*, the gene encoding the outer membrane secretin of the *V. cholerae* eps secretion system (a type II secretion system). Transformation frequencies were significantly reduced in the $\Delta epsD$ -TntfoX strain (average transformation frequency of three independent experiments \pm SD was $8.7 \pm 7.0 \times 10^{-7}$). Since growth was also affected in this strain, we could not draw conclusions on the involvement of the eps system in natural transformation. Finally, Melanie Blokesch established double- and triple-knock-out strains lacking combinations of *pilA*, *tcpA* (encoding the major pilin of the toxin co-regulated pilus), *mshA* (encoding the major pilin of the MSHA pilus) and the whole *Vibrio* pathogenicity island 1. However, transformation frequencies of these strains did not differ significantly [208]. Therefore, we can currently not explain how tDNA enters the periplasm in the absence of the type IV pilus part of the DNA uptake machinery.

Our observations also strengthen the longstanding hypothesis that the competence type IV pilus might fulfill a secondary function. Indeed, Meibom *et al.* reported on a fitness disadvantage of *pilA*-negative strains growing on a chitin surface [158]. Importantly, this strain was concomitantly deficient in quorum sensing, hence not naturally transformable. Bakkali even went one step further, when suggesting that DNA uptake during natural transformation could be a side effect of bacterial adhesion and twitching motility [211]. Our results support this idea to some point, since PilA-pili are not strictly required for low frequency transformation and might therefore have been hitchhiked evolutionary for transport of DNA across the outer

membrane. However, such a scenario is highly speculative and we currently do not have further data to strengthen this hypothesis.

2.2.3 Uptake of heterologous DNA by naturally competent *Vibrio cholerae*

N. gonorrhoeae and *H. influenzae* have been shown to discriminate between foreign and self DNA by the recognition of sequence motifs named DUS (DNA uptake sequence) and USS (uptake signal sequence), respectively [48–50]. Only DUS-containing DNA is efficiently transported across the outer membrane of *N. gonorrhoeae* [49, 50], although the extent of DUS-enhanced transformation varies significantly between different strains [212]. Frye and colleagues recently identified distinct DUS “dialects” that differ in their nucleotide sequences and in their impact on natural transformation of another neisserial species, *N. meningitidis* [213].

DUS and USS are highly overrepresented within the genomes of the respective bacteria. For example, 1,471 USS copies have been detected in the *H. influenzae* genome, which results in roughly 1 USS per 1.2kb [214]. In contrast, no such highly overrepresented sequence motifs have been identified in *V. cholerae*. We therefore speculated that DNA uptake is non-species-specific in this organism. To test our hypothesis, we developed a whole-cell duplex PCR assay that allowed us to detect DNA uptake across the outer membrane. Indeed, we observed similar levels of DNA uptake of donor DNA derived either from another Gram-negative bacterium, *E. coli*, or from an unrelated, Gram-positive bacterium, *B. subtilis* (Figure 2.1). We therefore concluded that *V. cholerae* does not discriminate between species-specific and non-specific DNA during DNA transport across the outer membrane. At the same time, we cannot exclude that some specificity might still occur, when naturally competent *V. cholerae* is exposed to DNA with an extreme GC content. However, preliminary results indicated that even GC rich DNA from *Mycobacterium smegmatis* (GC content 67.4% [NCBI sequence reference: NC008596.1]) is readily taken up (data not shown).

From an evolutionary perspective, taking up DNA from close relatives and siblings appears more beneficial, since it provides bacteria with templates for the repair of damaged chromosomal DNA (see section 1.1.3). Our finding that *V. cholerae* also takes up DNA from distantly related bacterial species, such as *B. subtilis*, seems to be contradictory in this context. However, instead of discriminating between self and foreign DNA at the level of DNA uptake, *V. cholerae* limits its competence state to occasions when it is surrounded by high numbers of other *Vibrios* [176]. This is achieved through coupling the regulation of natural competence to the sensing of the species-specific cholera autoinducer-1 (CAI-1), as has been shown by Suckow *et al.* [176] (Figure 1.7). Competence induction requires sufficiently high concentrations of secreted CAI-1, which is only produced by certain *Vibrio spp.* [215] and therefore maximizes chances of DNA uptake from close relatives or siblings, despite the fact that the DNA uptake process itself is not species-specific (Figure 2.1).

3 Visualization of competence pili

3.1 Results

3.1.1 Construction of a functional tagged version of PilA

As described in the last chapter, 15 of the identified competence genes encode proteins that are presumably catalyzing the biogenesis/function of a type IV competence pilus. Although it has been suggested earlier that PilA is the main component of such a type IV pilus [112, 179], no corresponding surface structure has been observed in an earlier study [112]. The authors of this study therefore suggested that the identified competence genes direct the synthesis of a competence “pseudo” pilus, which would not reach far beyond the outer membrane. To test this hypothesis, we created a tagged version of PilA, by fusing the 8 aa *Strep-tag*[®] II (IBA) to the C-terminus of the protein.

The PilA-Strep construct was cloned into the pBAD/Myc-HisA protein expression vector and transferred into *V. cholerae* cells by electroporation. We then tested whether PilA-Strep was still functional, i.e. whether it can complement a *pilA* knock-out in chitin-mediated natural transformation assays. Indeed, we detected transformants in this strain, although transformation frequencies were 100- to 1,000-fold reduced (data not shown). Since the correct stoichiometry of competence proteins might be important for correct assembly and consequently functionality of competence pili, we decided to switch from expression of PilA-Strep *in trans*, to replacement of the wildtype copy of *pilA* on the bacterial chromosome by the strep-tagged allele. To achieve this goal, we used the recently developed TransFLP method [182, 183] (Figure 6.1). In this way, we created the strain A1552-PilA-Strep::FRT, which carries the *pilA-strep* allele, followed by a short FRT scar, at the native *pilA* locus. In order to verify that the residual FRT scar in the chromosome does not confer any polar effects, thereby lowering transformation frequencies by disturbing the operon organization, we also constructed a strain carrying only the FRT scar between *pilA* and *pilB* (A1552-PilA::FRT).

Next, we tested whether these strains were transformable in chitin-mediated and chitin-independent transformation assays (Table 3.1). While we detected transformants for all strains, there were significant differences between the two assays (Table 3.1). On chitin surfaces, we observed only minor, not significant ($P = 0.56$, one-way ANOVA on log-transformed values) differences between the three strains. In contrast, chitin-independent transformation of strains carrying *TntfoX* revealed a different picture. While we observed a slight, though

Chapter 3. Visualization of competence pili

significant decrease in transformability of A1552-PilA::FRT, A1552-PilA-Strep::FRT was even more impaired in natural transformation. The average transformation frequency was ~36-fold lower compared to the wildtype strain and ~9-fold compared to the A1552-PilA::FRT strain. Nevertheless, even in chitin-independent transformation assays, we could consistently show that PilA-Strep is at least partially functional, since transformation frequencies were significantly higher for A1552-PilA-Strep::FRT, compared to A1552- $\Delta pilA$ (Table 3.1, Figure 2.2).

Table 3.1: Functional validation of PilA-Strep constructs during natural transformation

Strain	TntfoX on chromosome	Transformation frequency ¹	
		Chitin-dependent	Chitin-independent
WT	-	$4.1 \pm 2.7 \times 10^{-4}$	-
PilA::FRT	-	$2.8 \pm 1.0 \times 10^{-4}$	-
PilA-Strep::FRT	-	$1.6 \pm 1.3 \times 10^{-4}$	-
WT	+	-	$1.9 \pm 0.7 \times 10^{-4}$
PilA::FRT	+	-	$4.9 \pm 1.7 \times 10^{-5}$
PilA-Strep::FRT	+	-	$5.3 \pm 6.4 \times 10^{-6}$

¹ The average transformation frequency of at least three independent experiments \pm SD is shown.

3.1.2 Defining the TntfoX induced competence window

The use of chitin as competence inducer is problematic for the visualization of competence pili in *V. cholerae*. Chitin surfaces are irregular in shape and highly autofluorescent. Furthermore, competence induction has been shown to be heterogenous surrounding chitin surfaces [160], which creates major problems for epifluorescence microscopy experiments. Therefore, we decided to use the chitin-independent TntfoX system, to perform all microscopy experiments presented in this work.

First we aimed to determine the optimal growth phase for microscopy experiments (Figure 3.1). To this end we grew *V. cholerae* strain A1552-TntfoX in LB medium, containing low concentrations of L-arabinose (which induces *tfoX* expression from the transposon (see section 2.1.4)) and determined the optical density at 600 nm (OD_{600}) of the culture at hourly intervals. Along with the OD_{600} , we tested the level of transformability at bihourly intervals by exposing bacteria to transforming DNA (tDNA) for 30 min and subsequently digesting all external DNA by a DNase I treatment. Transformants and the total number of CFU were then scored on selective and plain LB plates, as in the standard transformation assay.

Although *tfoX* expression was induced artificially throughout the experiment, transformants were only detected after four hours of growth (Figure 3.1). This is in agreement with the proposed regulation of natural competence in *V. cholerae*, in particular with the requirement of elevated levels of cAMP and high cell densities (see Figure 1.7). Transformation frequencies peaked in the late exponential growth phase after six to eight hours of incubation (Figure 3.1). Interestingly, we still detected transformants after prolonged incubation for a total of 24 h (data not shown). Since transformation frequencies were highest after six to eight hours of growth, we decided to perform all subsequent microscopy experiments within this timeframe (Figure 3.1).

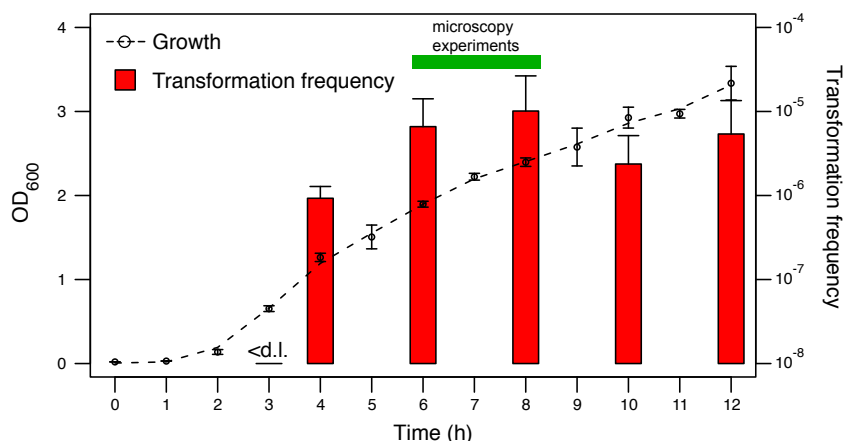


Figure 3.1: Chitin-independent transformation of *V. cholerae* tested throughout different growth phases. *V. cholerae* strain A1552-TntfoX was grown in LB medium containing 0.02% L-arabinose (open circles). OD₆₀₀ values and natural transformability were determined at hourly (OD₆₀₀) or at bihourly (transformation) intervals. Smoothing splines were fitted to the experimental OD₆₀₀ values (dashed line). Average OD₆₀₀ values and transformation frequencies of three independent experiments ± SD are shown in the graph. The timeframe for microscopy experiments presented in this work is indicated by the green bar. <d.l., below detection limit which was on average $3.5 \pm 3.0 \times 10^{-7}$.

3.1.3 Visualization of PilA containing competence pili

To visualize the PilA containing type IV pilus in living *V. cholerae*, we induced competence in the PilA-Strep::FRT-TntfoX strain as described above. We then used fluorescently labeled antibodies against the Strep-tag to detect surface exposed competence pili. Indeed, we observed filaments of variable length in a fraction (6.8%) of the bacteria (Figure 3.2 A). At the same time, we observed many free floating pili suggesting that shearing occurs easily. Most of the piliated bacteria (94.5%) contained only one pilus per cell, which was not associated with a distinct cellular localization (Figure 3.2 B). Irrespective of size, pili were observed at cell poles (~40% of cells), as well as at 1/4 or 3/4 and at central positions (Figure 3.2 B). Finally, we demonstrated that piliated cells retain their polar flagellum, as demonstrated by co-staining of both appendages (Figure 3.2 C). While flagella are known to associate with the old cell pole [216], we observed pili at both, the new and the old cell pole (Figure 3.2 C).

3.1.4 Piliation of competence gene mutants

From our previous observations on DNA uptake across the outer membrane, we concluded that all pilus-related components were needed for this step, while pilus-independent proteins, with the exception of ComEA, were dispensable (Figure 2.4). Since Strep-tagged PilA allowed us to visualize competence pili directly, we decided to study the role of individual components of the DNA uptake machinery in biogenesis or stabilization of this structure. To this end, we transferred the *pilA-strep::kan* construct into all knock-out strains, in which we previously studied DNA uptake and transformability (Figure 2.4, Figure 2.2). We then tested the respective strains for surface exposed pili, as described above.

Chapter 3. Visualization of competence pili

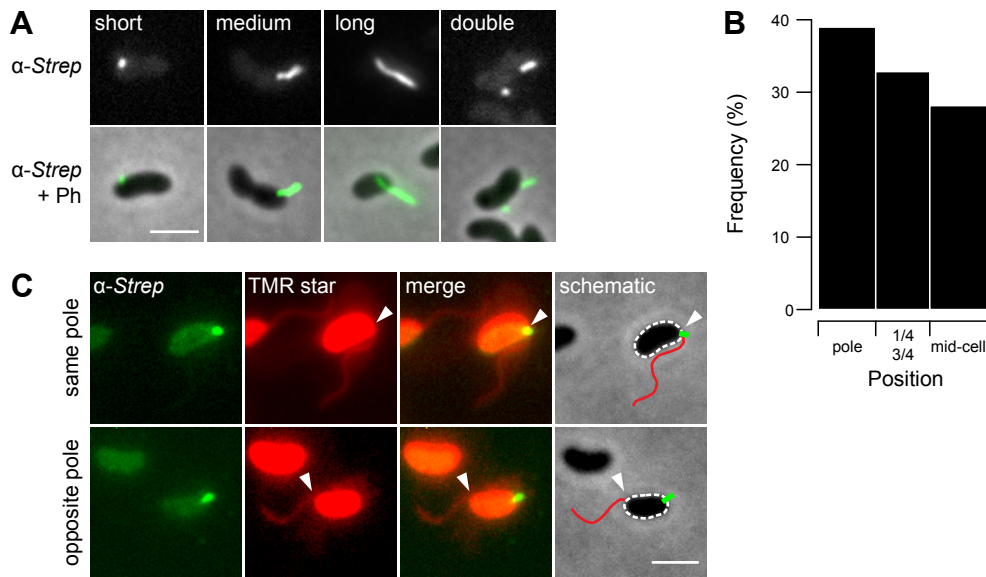


Figure 3.2: Visualization of the competence-induced pilus. The major pilus subunit PilA was fused to an affinity tag, and the construct (*pilA-strep*) was brought onto the chromosome, replacing the wildtype copy of *pilA*. Pili were visualized by immunofluorescence microscopy using an Oyster488 conjugated anti-*Strep*-tag antibody. The strain contained the *TnfoX* transposon for competence induction. (A) Diverse polar and nonpolar pilus structures were observed. Depicted are fluorescence images (upper row) and overlays with the phase contrast (Ph) images (lower row). (B) A total of 5,863 bacteria were analyzed for pilus positioning in random fields of view. The relative distance of the pilus origin along the length of the cell was evaluated (polar position, 1/4 or 3/4 position, mid-cell position). (C) Polar pilus localization is not biased towards the old or the new pole. Fixed cells were stained for pili and flagella using Oyster488-labeled anti-*Strep* antibodies and the SNAP-cell TMR star substrate, respectively. The origins of flagella are highlighted with white arrowheads. Both fluorescence channels were imaged (PilA-Strep in green, TMR star in red) and superimposed (merge). A schematic representation indicating the position of the flagellum and the pilus was projected onto the phase-contrast image (schematic). Scale bars, 2 μ m.

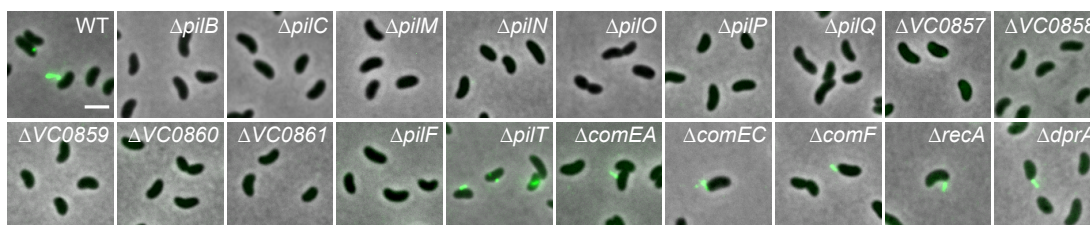


Figure 3.3: Piliation of competence gene mutants. Visualization of competence-induced pili in knock-out strains. Wildtype *pilA* was replaced with *pilA-strep::kan* in a wildtype strain (WT) and competence gene mutants. Pili were visualized by immunofluorescence staining as in Figure 3.2. Shown are overlays of fluorescence (green) and phase contrast images. All strains contained *TnfoX* for competence induction. Scale bar, 2 μ m.

Mutants lacking pilus-related genes, including the newly identified gene cluster *VC0857-0861*, which does not have close homologs in non-*Vibrio* species (Table 2.1), were non-piliated (Figure 3.3). In contrast, mutants deficient in *comEA*, *comEC*, *comF*, *recA* and *dprA*, which were all either severely impaired in natural transformation ($\Delta dprA$, Figure 2.2) or non-transformable ($\Delta comEA$, $\Delta comEC$, $\Delta comF$, $\Delta recA$, Figure 2.2), still displayed pili. A mutant carrying a deletion in *pilT*, which potentially encodes a retraction ATPase (Figure 2.5), still possessed surface exposed pili as well. In fact, this strain showed an overpiliation phenotype in agreement with

its proposed function. We quantified the number of pili per cell for this strain and a strain, which, in addition to the indigenous copy of *pilB* (presumably encoding a cytoplasmic ATPase, which is responsible for pilus elongation, Figure 2.5), carried an inducible copy of *pilB* on a plasmid (Table 3.2). Both strains, displayed >two-fold more surface exposed pili (Table 3.2). Additionally, cells with more than one pilus per cell were observed more frequently, which was especially obvious for the $\Delta pilT$ strain (Table 3.2).

Table 3.2: Quantification of surface exposed pili in mutant strains of *V. cholerae*

Strain ¹	<i>N</i> ²	Piliated (%)	1 pilus (%) ³	2 pili (%) ³	> 2 pili (%) ³
PilA-Strep::FRT	5,863	6.8	94.5	5.0	0.5
PilA-Strep::kan	3,212	5.3	96.4	3.6	0
PilA-Strep::kan $\Delta pilT$	3,787	14.0	81.3	15.7	3.0
PilA-Strep::kan/pBAD-pilB	2,958	11.0	90.8	8.0	1.2

¹ All strains carry the *Tn_{tfoX}* transposon for competence induction.

² Number of cells analyzed.

³ Percentage of piliated cells with one, two, or more than two pili per cell.

3.1.5 Localization of other pilus-related competence proteins

After visualizing the competence pilus itself, we aimed to localize other components of the DNA uptake machinery. First, we created a translational fusion between the potential outer membrane secretin PilQ and the fluorescent protein mCherry (using the same methodology as for *pilA-strep* (Figure 6.1)). Since the C-terminus of the protein might be critical for correct multimerization, as has been shown for its homolog in *N. meningitidis* [73], we decided to place mCherry right downstream of the predicted N-terminal signal sequence cleavage site of PilQ. We hypothesized that this would result in a N-terminal fusion of mCherry to the mature PilQ protein, with little disturbance of protein multimerization and/or function. Indeed, a strain in which we replaced the chromosomal wildtype copy of *pilQ* with the *mCherry-pilQ* allele was fully transformable (Table 3.3).

Table 3.3: Functional validation of fluorescent fusion constructs

Strain ¹	Transformation frequency ²
WT	$1.9 \pm 0.7 \times 10^{-4}$
mCherry-PilQ	$1.6 \pm 0.5 \times 10^{-4}$
PilB-GFP	$3.2 \pm 1.4 \times 10^{-5}$
PilT-GFP	$6.2 \pm 1.0 \times 10^{-6}$

¹ All strains carry the *Tn_{tfoX}* transposon for competence induction.

² The average transformation frequency of at least three independent experiments \pm SD is shown.

Using epifluorescence microscopy, we observed several mCherry-PilQ clusters in competence-induced cells (Figure 3.4 A). Fluorescence signals were weak, most likely as a consequence of expression of the fusion construct under control of its native promoter. In order to determine the relative distribution of competence pili and PilQ clusters, we transferred

Chapter 3. Visualization of competence pili

the *pilA-strep* construct into the strain carrying *mCherry-pilQ*. Interestingly, co-localization experiments with this strain indicated that for the majority ($\geq 76\%$) of piliated cells ($n = 80$ cells), the base of their pili was located close to one of the PilQ secretin clusters, thus suggesting that both components are indeed part of a larger DNA uptake complex (Figure 3.4 B).

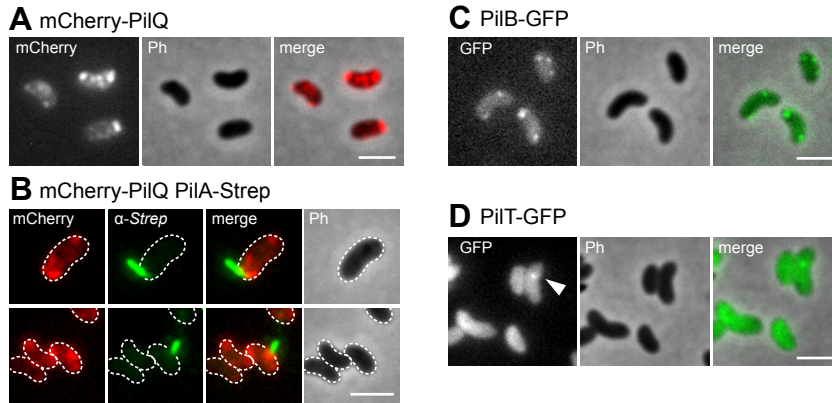


Figure 3.4: Cellular localization of specific competence proteins. Wildtype versions of the competence genes *pilQ*, *pilB* and *pilT* were replaced by functional translational fusion constructs to visualize their localization. All strains contained the *TntfoX* transposon for competence induction. Shown are representative fluorescence images (mCherry, α -Strep and GFP), phase contrast (Ph) images, and overlays of fluorescent channels and Ph channels (merge). Cells are outlined with dashed lines for panel B. *V. cholerae* strains carrying *mCherry-pilQ* (A), *mCherry-pilQ* and *pilA-strep* (B), *pilB-gfp* (C) and *pilT-gfp* (D) were subject to epifluorescence microscopy (after immunostaining for panel B). Co-localization of mCherry-PilQ and the pilus base was observed in a majority of piliated cells (B). Rarely observed minor foci of PilT-GFP are indicated by the white arrowhead (D). Scale bars, 2 μ m.

Next, we fused the predicted pilus-elongation ATPase PilB and its putative counterpart PilT, which is thought to promote pilus retraction, to the green fluorescent protein (GFP). Again, the fusion proteins, which replaced wildtype copies of PilB and PilT, retained their ability to mediate natural transformation (Table 3.3) and showed very weak fluorescence signals. Like PilQ, PilB did not form a single focus at a distinct subcellular localization, but instead distributed to several distinctive foci throughout the cell (Figure 3.4 C). In contrast, its putative opponent, the traffic ATPase PilT, showed a uniform localization throughout the cytoplasm. PilT-GFP foci, which we observed rarely, were restricted to one single spot per cell (Figure 3.4 D).

To test whether foci of PilB overlap with those of the PilQ secretin, we created a strain containing both translational fusions by replacing their wildtype alleles, and performed two-color time-lapse microscopy. We observed that PilB foci were often mobile and seemingly traveled from one PilQ focus to the next, resulting in temporary co-localization of both proteins (Figure 3.5 A).

Similarly, we created a strain producing concomitantly PilT-GFP and mCherry-PilQ, both encoded chromosomally on their native loci. Although PilT-GFP foci appeared only rarely and were limited to one spot per cell, we consistently observed a dynamic behavior of the construct (Figure 3.5 B). Single PilT foci occasionally showed a temporary co-localization with PilQ (Figure 3.5 B).

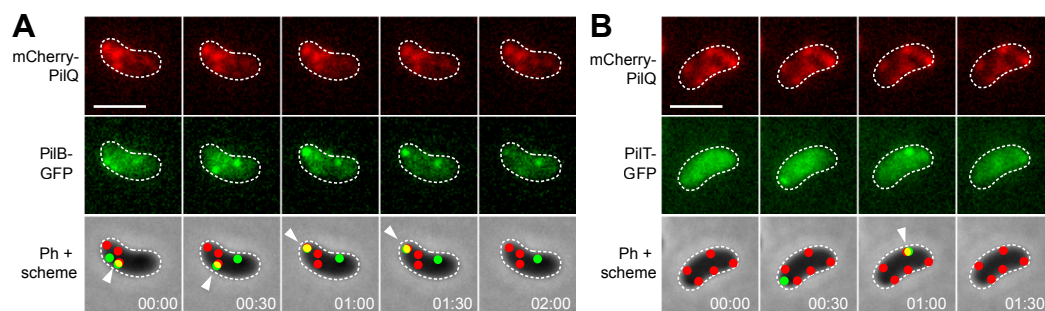


Figure 3.5: Transient co-localization of the cytoplasmic ATPases PilB and PilT with the outer membrane secretin PilQ in time-lapse microscopy experiments. Representative examples of two-color time-lapse microscopy experiments, showing transient co-localization of PilB-GFP (green) (A) or PilT-GFP (green) (B) with mCherry-PilQ (red). Observed spots/clusters for all fluorescent proteins are schematically depicted and projected on the phase-contrast (Ph) images (bottom row). Co-localization events are indicated by a white arrowhead. The time is given in minutes. Scale bars, 2 μm .

3.1.6 The ATPase activity of PilB is needed for protein function and its dynamic localization

The cytoplasmic traffic ATPase PilB, which we showed to be needed for piliation (Figure 3.3) and DNA uptake (Figure 2.4), and which is mobile within the cytoplasm (Figure 3.5 A), contains several conserved sequence motifs, such as the P-loop containing Walker A box and an atypical Walker B box (DhhhhGE; h, hydrophobic amino acid) [217]. Indeed, the Walker B motif is conserved between PilB of *V. cholerae* and other bacterial homologs (Figure 3.6 A). As stated in [208], we therefore decided to test whether ATP hydrolysis is important to PilB's role in DNA uptake/natural transformation, as for a very different phenotype, the type IV pilus dependent gliding motility of *Myxococcus xanthus* [218]. We first cloned a plasmid carrying *pilB* with a site-directed mutation (E394A) and tested the variant in a complementation assay with natural transformation as the readout. The single amino acid exchange of the conserved glutamate completely abolished PilB's functionality (Figure 3.6 B). Moreover, the PilB^{E394A} variant was unable to restore pilus formation, unlike complementation with wildtype *pilB in trans* (Figure 3.6 C).

Next, we generated a *pilB*^{E394A} variant as a translational fusion with GFP, which was used to replace the wildtype copy of *pilB* on the chromosome. By imaging this strain under competence-inducing conditions, we observed that the PilB^{E394A}-GFP protein was not degraded and that its localization pattern was comparable to that of PilB-GFP (Figure 3.6 D); however, in contrast to that in the wildtype counterpart (Figure 3.4 C), we never observed any dynamic behavior. The *V. cholerae* strain carrying the *pilB*^{E394A}-*gfp* allele at the native *pilB* locus was also impaired in natural transformation (to the same level as the *pilB* knock-out strain, Figure 3.6 B).

3.2 Discussion

3.2.1 Localization of competence pili and outer membrane secretins

We visualized the competence-related type IV pilus of *V. cholerae* for the first time, by fusing a C-terminal *Strep*-tag to the major pilin PilA. We have chosen to target the C-terminus of PilA, because structural models of type IV pili and homologies between *V. cholerae* PilA and crystallized PilA of the *P. aeruginosa* PAK pilus suggested that the protein's N-terminus might rather be facing the inside of pilus fibers [59]. The C-terminus, in contrast, is possibly sticking out of assembled pili [59], and might therefore be accessible to antibodies.

This construct was fully functional for natural transformation on chitin surfaces and also yielded significant levels of transformation in the chitin-independent setup (Table 3.1). The marked difference in transformability between the chitin-dependent and the chitin-independent transformation assays is most likely a consequence of the different incubation conditions. For the chitin-mediated transformation assay, bacteria were incubated statically on chitin surfaces for up to 24 h in the presence of transforming DNA, while for the chitin-independent assay competence was induced in aerated/agitated liquid cultures and exposure to transforming DNA was limited to five hours. Therefore, assuming that the C-terminal *Strep*-tag of PilA could slightly interfere with pilus stability, the transformability of the cells would be more affected in the chitin-independent assay, due to potential shearing of pili caused by culture agitation. Furthermore, a much shorter exposure time to transforming DNA occurs in this assay. However, it is important to note that also in the *TntfoX* setup, transformation frequencies of the PilA-*Strep*::FRT strain (Table 3.1) were significantly higher compared to the *pilA* knock-out strain (Figure 2.2).

Using immunofluorescence microscopy, we showed that *V. cholerae* does indeed produce a filamentous cell appendage that could extend for up to two μm from the cell surface (Figure 3.2). The term “pseudo”pilus, as suggested by Meibom *et al.* [112] therefore does not seem appropriate. In addition, we showed that the localization of competence pili is not biased towards the cell pole, as it is the case for *B. subtilis* [89]. In this organism, Kaufenstein *et al.* quantified the number, as well as the position, of ComGC (major pilin of the *B. subtilis* competence pilus) foci and concluded that 95% of cells with a ComGC signal contained at least one polar ComGC focus [89]. This is in agreement with previous findings on the localization of other *B. subtilis* competence proteins that preferentially localize to cell poles [87, 88]. Furthermore, most (71%) of the *B. subtilis* cells with ComGC signals contained more than one focus per cell [89]. In contrast, we generally observed only one single competence pilus at various cellular positions (Figure 3.2).

Also other competence proteins, such as the predicted outer membrane secretin PilQ, fused to the fluorescent protein mCherry, were not restricted to cell poles. mCherry-PilQ localized to several, non-polar clusters, reminiscent of what has been observed for components of the *V. cholerae* type II secretion system (T2SS) [219]. The authors of this study have shown that at least two proteins of the type II secretion apparatus formed discrete foci along the length of the cell. This was in contrast to previous findings, which suggested polar localization of the T2SS [216]. However, polar accumulation of type II complex proteins, studied by Scott *et al.* [216], most likely resulted from an overexpression artifact, as suggested by Lybarger

et al. [219]. These two studies highlight the importance of expressing fluorescent protein fusions “in stoichiometric ratios with their partner proteins at levels as close to wild type as possible” [219], in order to gain an accurate representation of intracellular protein distributions. We accounted for this fact by replacing wildtype genes on the bacterial chromosome by translational fusion constructs (e.g. *pilA-strep* [Figure 6.1], *mCherry-pilQ*, *pilB-GFP* and *pilT-GFP*), rather than using plasmids for expression *in trans*.

3.2.2 Pilus biogenesis in competence gene mutants

The presence of detectable, surface exposed pili in competence gene mutants (Figure 3.3) correlated well with our observations on DNA uptake across the outer membrane (Figure 2.4). On the one hand, all strains with detectable DNA transport across the outer membrane (wildtype, $\Delta comEC$, $\Delta comF$, $\Delta recA$, $\Delta dprA$) still produced competence pili (Figure 3.3). On the other hand, we could not detect surface exposed competence pili for almost all strains deficient in outer membrane DNA transport. The only two exceptions to this rule were strains lacking the predicted cytoplasmic pilus retraction ATPase PilT and the putative periplasmic DNA binding protein ComEA. Both strains were piliated (Figure 3.3), although barely or not at all transformable (Figure 2.2) and not able to take up DNA into a DNase I resistant state (Figure 2.4).

For the *pilT* deficient strain, we even observed overpiliation, i.e. an increased percentage of piliated cells (14% compared to 5.3% in WT, Table 3.2). Moreover, the percentage of piliated cells with two or more pili per cell increased from 3.6% in the wildtype strain to 18.7% in the *pilT* deficient strain (Table 3.2). At the same time we did not detect any difference in the pilus length. These findings strongly support the hypothesis that PilT indeed plays a role in pilus retraction. A similar increase of piliated cells was observed upon overexpression of *pilB* from a plasmid (Table 3.2), which is in line with PilB's putative role as pilus extension ATPase.

The second strain deficient in DNA uptake, but still producing competence pili, was the *comEA* mutant. The fact that ComEA is dispensable for pilus biogenesis is in agreement with its differential regulation compared to other pilus components (expression of *comEA*, but not of pilus-related genes, is quorum sensing dependent [112, 160, 164]; Figure 1.7).

Finally, it is important to note that deletion of any gene within the *VC0857-0861* cluster completely blocked the appearance of surface exposed pili (Figure 3.3). This strengthens our hypothesis that proteins encoded in this cluster might assist initiation of PilA polymerization (see section 2.2.1, page 32).

3.2.3 Distribution patterns of the cytoplasmic ATPases PilB and PilT

Similar to mCherry-PilQ clusters, we also observed discrete spots of the cytoplasmic ATPase PilB (Figure 3.4). Furthermore, PilB and PilQ clusters often co-localized temporarily, as observed by time-lapse microscopy (Figure 3.5 A). Although foci of the second cytoplasmic ATPase PilT were rare, weak, and generally restricted to one focus per cell (Figure 3.4), we also observed transient co-localization with PilQ clusters in time-lapse microscopy experiments for this construct (Figure 3.5 B). In contrast, we never observed any mobility or dynamics of PilQ foci within the tested time-lapse intervals.

On the basis of these observations, it is tempting to speculate that the membrane-bound components of the competence-induced pili, apart from the pilins, are preassembled at different locations around the cell periphery or the pole (as observed for PilQ), and that the temporary interaction with the ATP-hydrolyzing PilB and PilT proteins initiates pilin polymerization or pilus retraction, respectively.

Such a model has been previously proposed for *Myxococcus xanthus*, which uses elongation and retraction of type IV pili for gliding motility on surfaces [220]. Bulyha *et al.* demonstrated that the outer membrane secretin PilQ, as well as the inner membrane protein PilC and the cytoplasmic protein PilM, localized to cell poles in a symmetric, bipolar manner, where they remained stationary [220]. The cytoplasmic ATPases PilB and PilT, in contrast, predominantly localized to opposite cell poles, with large accumulations of PilB at the leading and a big cluster of PilT at the lagging cell pole. Interestingly, the two ATPases were not stationary (as PilQ, PilC and PilM), but oscillated between the cell poles during cellular reversals. Furthermore, PilT showed burst of accumulation at the leading pole, which has been hypothesized to cause pilus retraction between reversals [220]. Given the parallels in *V. cholerae* and *M. xanthus* type IV pilus protein-mobility, it therefore seems possible that stationary pilus assembly platforms and dynamic localization of cytoplasmic ATPases are a more general phenomenon, which play important roles for the function of retractable type IV pili in competence, as well as in motility.

Bulyha *et al.* also tested whether ATPase activity was important for correct localization of PilB/PilT in *M. xanthus*. Indeed, they showed that mutations affecting ATP hydrolysis also affected the subcellular distribution of these two proteins. Both ATPases lost their polar localization and distributed either into discrete foci over the entire cell body (PilB), or did not show focal accumulations anymore (PilT) when ATP hydrolysis was impaired [220]. We therefore introduced a point mutation into *V. cholerae* PilB (E394A) that mimicked the situation studied by Bulyha *et al.*. Although we did not observe an obvious difference in the localization of PilB^{E394A}-GFP, its mobility was completely inhibited (Figure 3.6 D). Concomitantly, we did not observe competence-induced pili in a strain carrying this mutation, and transformation frequencies dropped to the level of a *pilB* knock-out strain (Figure 3.6 B, C). Therefore, even though the result of dynamic pilus elongation and retraction is very different in *M. xanthus* and *V. cholerae* (motility in *M. xanthus* and DNA uptake in *V. cholerae*), our results suggest that the underlying molecular mechanisms, in particular the roles of mobile cytoplasmic traffic ATPases, might be strikingly similar. Although these findings are by no means direct proof, they nevertheless support Bakkali's suggestion that DNA uptake might have developed as a by-product of twitching motility [211].

4 ComEA and the mechanism of DNA uptake

4.1 Results

4.1.1 ComEA forms a pool of mobile proteins within the periplasm

Given the complex regulation of *comEA* in *V. cholerae* (section 1.3.2), and its indispensability even for unfrequent transformation events (Figure 2.2) and PCR-detectable DNA transport across the outer membrane (Figure 2.4), this protein likely plays a key role in DNA uptake. We therefore decided to investigate the function of ComEA in more detail and started by determining its subcellular localization.

In a previous study on *N. gonorrhoeae* ComE (the ComEA homolog in this species), a putative N-terminal signal peptide was identified, which presumably targets the protein to the periplasm by sec-dependent protein export [95]. Since cleavage of this signal peptide was detected in whole-cell lysates of *N. gonorrhoeae*, the authors concluded that “[...] the mature protein should be released into the periplasm” [95]. However, no further evidence supporting this hypothesis has been presented.

Such a N-terminal sec-dependent signal peptide is also predictable for ComEA of *V. cholerae* (amino acids 1-25). Based on this, we speculated that ComEA is targeted to the periplasm of *V. cholerae* and we decided to experimentally address the localization of this protein *in vivo* through epifluorescence microscopy. For this purpose, we constructed a translational fusion between ComEA and mCherry. Additionally, Melanie Blokesch engineered a second translational fusion between the predicted sec-signal peptide of ComEA and mCherry (termed ss[ComEA]-mCherry) as control. For both constructs, we observed a uniform localization pattern at the cell periphery of naturally competent *V. cholerae* cells (Figure 4.1), which is in agreement with a periplasmic localization of ComEA.

Next, we aimed to investigate whether ComEA is motile within the periplasm by using a fluorescence loss in photobleaching (FLIP, Figure 4.2) approach. In [221] we stated that in contrast to fluorescence recovery after photobleaching (FRAP), where fluorescent proteins within a small area of the cell are bleached and the back-diffusion of the surrounding non-bleached proteins into this region is recorded, FLIP consists of repetitive bleaching of the same region (e.g. region of interest 1 in Figure 4.2), thereby preventing fluorescence recovery

Chapter 4. ComEA and the mechanism of DNA uptake

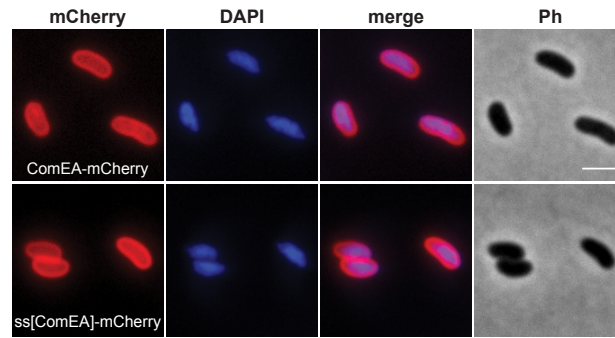


Figure 4.1: Localization of plasmid encoded ComEA-mCherry in competent *V. cholerae* cells. Expression and distribution of ComEA-mCherry (upper row) or ss[ComEA]-mCherry (amino acids 1-25 of ComEA fused to mCherry) (lower row) within competent *V. cholerae* cells. Fluorescence signals of mCherry or DAPI-stained genomic DNA were visualized and compared to each other (merge) and the corresponding phase contrast (Ph) image. Scale bar, 2 μ m.

in that region. Moreover, any mobile protein from elsewhere in the same compartment (e.g. region of interest 2 in Figure 4.2) will also enter this continuously photo-bleached area, eventually resulting in a complete loss of fluorescence in the compartment. In contrast, any not connected compartment will be spared from bleaching (e.g. region of interest 3 in Figure 4.2). Therefore, FLIP is often used to reveal the mobility of proteins within certain compartments of the cell [222], which is what we were aiming for.

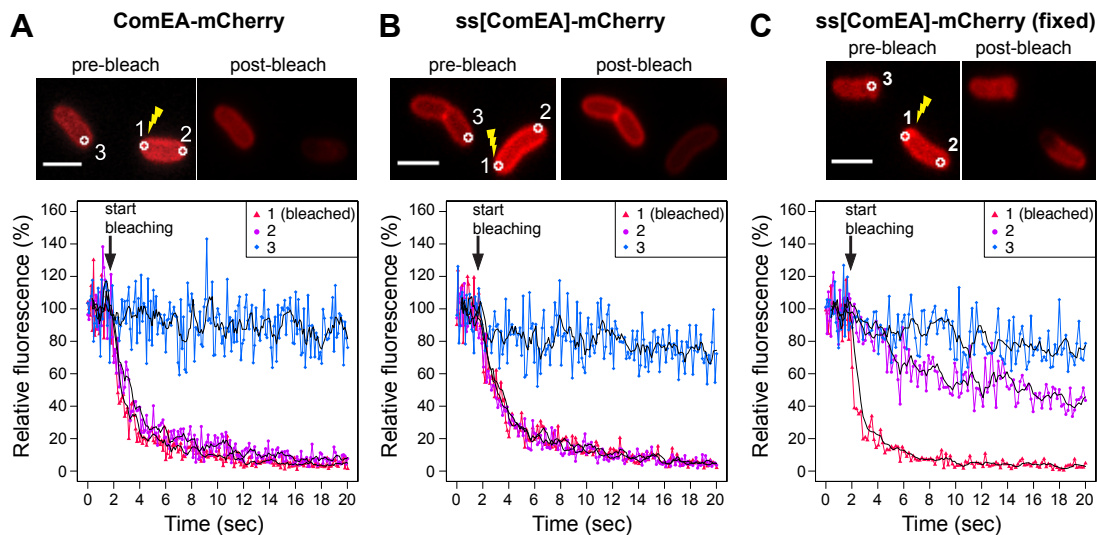


Figure 4.2: Fluorescence loss in photobleaching (FLIP) reveals ComEA mobility within the periplasm. Live *V. cholerae* cells (A-B) and paraformaldehyde fixed bacteria (C), expressing ComEA-mCherry (A) or ss[ComEA]-mCherry (B-C) were tested for mCherry mobility by FLIP. Bleaching of the region of interest (ROI) 1 (indicated as 1 in the images above fluorescence intensity plots) was initiated after acquisition of 20 frames and repeated after every frame. The fluorescence intensities of ROIs 1-3 were measured for a total of 20 sec and normalized to the average fluorescence intensity of the first 10 frames (fluorescence intensity plots). Trendlines (moving averages, period $n = 5$) are indicated with black lines. The average fluorescence intensity projections before (pre-bleach) and after bleaching (post-bleach) are shown above the fluorescence intensity plots. Scale bars, 2 μ m.

Indeed, our FLIP experiments indicated that ComEA was highly mobile within the periplasm (Figure 4.2 A). Likewise, a translational fusion between the signal sequence of ComEA alone and mCherry (ss[ComEA]-mCherry) resulted in a similar mobility pattern (Figure 4.2 B). In contrast, when proteins were cross-linked by a paraformaldehyde treatment prior to photo-bleaching, little mobility was detected (Figure 4.2 C).

4.1.2 ComEA binds to DNA *in vivo*

Studies on ComEA homologs from various naturally competent bacteria, such as *B. subtilis*, *N. gonorrhoeae* or *Campylobacter jejuni*, have demonstrated that the protein binds to DNA *in vitro* [91, 95, 223]. However, *in vivo* binding of ComEA to DNA, i.e. binding of ComEA to DNA in living bacteria, has never been shown. Interestingly, this is exactly what we observed, by generating a ComEA-GFP protein fusion, in which we replaced the sec-signal peptide of ComEA by a tat-signal peptide. This construct was engineered to be transported to the periplasm in a folded state (as GFP is improperly folded when translocated to the periplasm in a sec-pathway dependent manner [224]). We observed fluorescence signals predominantly at the cell periphery of *E. coli* cells, when we induced expression of a control construct that contained only the tat-signal peptide fused to GFP (tat-GFP, Figure 4.3). The tat-ComEA-GFP fusion in contrast failed to translocate correctly. Instead, ComEA was tightly bound to the bacterial chromosome, which appeared as a highly compacted structure (Figure 4.3). This was paralleled by serious toxicity and cell death at high protein expression levels, indicating that *in vivo* binding of ComEA to the DNA interfered with cellular processes (data not shown).

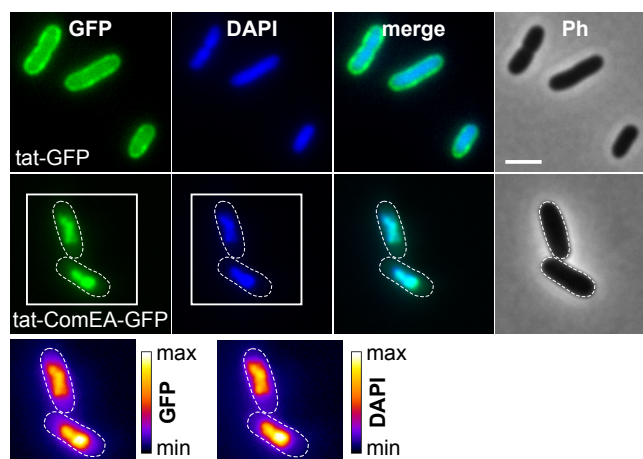


Figure 4.3: Cytoplasmic ComEA binds to the chromosome of *E. coli*. Plasmid-encoded *gfp* (tat-GFP) or *comEA-gfp* (tat-ComEA-GFP), both preceded by a tat-signal sequence, were expressed in *E. coli*. The images correspond to the GFP channel, DAPI channel (to visualize DAPI-stained DNA), merged fluorescence images (merge), and phase contrast (Ph) images. The cells are outlined with dashed lines for tat-ComEA-GFP. Heat-maps showing the fluorescence intensities of the GFP and DAPI signals are depicted for the *tat-comEA-gfp* expressing cells below the images. Scale bar, 2 μ m.

Based on these findings, we decided to conduct further experiments using the ComEA-mCherry fusion, despite the lower signal intensity of mCherry compared with GFP. To exclude

Chapter 4. ComEA and the mechanism of DNA uptake

artifacts caused by artificial (over-)expression, we substituted chromosomal *comEA* with *comEA-mCherry*. As in the previous part, this guaranteed co-regulation of the fluorescent fusion construct with other competence genes and an expression level of *comEA-mCherry* comparable to the level of *comEA* in a wildtype strain. For competence induction, we again used the *TntfoX* transposon (section 3.1.2). The functionality of the ComEA-mCherry construct was verified in chitin-independent transformation assays. Transformation frequencies (TFs) were not significantly affected compared to the parental wildtype strain (WT, $TF = 1.9 \pm 0.3 \times 10^{-4}$; ComEA-mCherry, $TF = 1.2 \pm 1.1 \times 10^{-4}$; average $TF \pm SD$ of at least three independent experiments). Although fluorescence signals were weak, chromosomally encoded ComEA-mCherry depicted the same uniform periplasmic distribution pattern in competence-induced cells, as observed for the plasmid encoded construct (Figure 4.4 A).

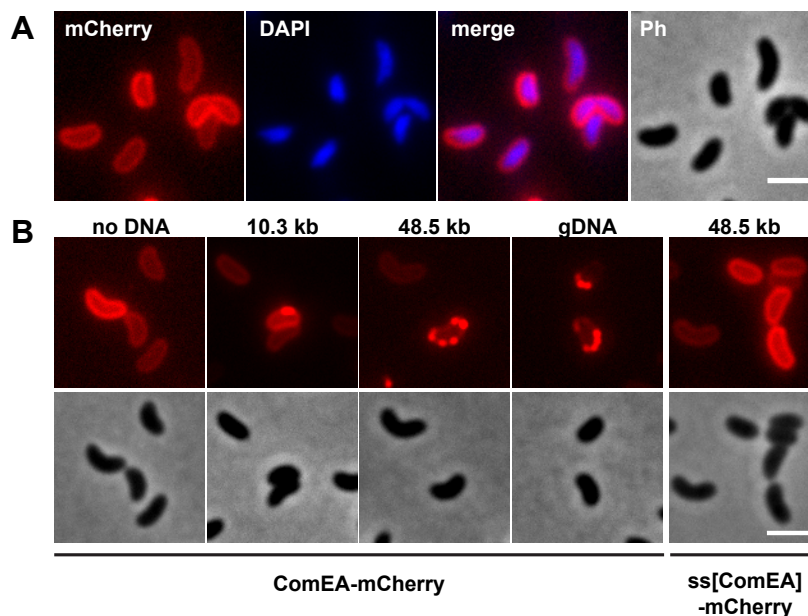


Figure 4.4: Periplasmic ComEA-mCherry aggregates into fluorescent foci upon exposure of competence-induced cells to exogenous DNA. The *comEA* gene of *V. cholerae* was replaced by the *comEA-mCherry* or *ss[ComEA]-mCherry* allele using bacterial genetics (TransFLP analogous to *pilA-strep*, Figure 6.1). (A) Representative microscopy images of competence-induced bacteria carrying the *comEA-mCherry* allele. The chromosome was stained with DAPI. Shown are fluorescence signals for mCherry (red), DAPI (blue), an overlay of the two channels (merge), and the corresponding phase contrast (Ph) image. (B) ComEA-mCherry aggregation and focus formation after the addition of exogenous DNA. Competence-induced cells without (no DNA) or with exogenous DNA were imaged in the red (mCherry, upper row) or the phase contrast channel (lower row). The DNA fragments differed in lengths (PCR fragment, 10.3 kb; phage- λ DNA, 48.5kb; genomic DNA (gDNA), various lengths). Exogenous DNA did not lead to focus formation of periplasmic mCherry alone (preceded by the ComEA signal sequence; *ss[ComEA]-mCherry*). Scale bars, 2 μ m.

Interestingly, the addition of external DNA to competence-induced cells caused the formation of distinctive ComEA-mCherry foci (Figure 4.4 B). The size and number of these protein accumulations were dependent on the length of DNA fragments to which the bacteria were exposed. Short PCR products (10.3 kb) mostly caused only single distinct foci, while bacteria exposed to longer stretches of DNA (phage- λ DNA, 48.5 kb or genomic DNA of *V. cholerae*,

various sizes) often depicted more than one focus per cell. Periplasmic mCherry alone did not show any aggregation (Figure 4.4, ss[ComEA]-mCherry). To verify that our observations are consistent with DNA uptake in a chitin-induced competence state, we incubated bacteria on chitin beads and exposed the cells to an excess of exogenous transforming DNA (tDNA). Indeed, bacteria depicted a uniform distribution pattern of ComEA-mCherry in the absence of external DNA, but they showed fluorescence foci upon provision of exogenous tDNA [221].

Our observations suggest that ComEA binds DNA in the periplasm of competent *V. cholerae*. To further test this hypothesis, we exposed competence-induced cells carrying the *comEA-mCherry* construct to YoYo-1 labeled DNA. YoYo-1 is a dsDNA intercalating dye, which is virtually nonfluorescent in aqueous solution [225] and has been previously used to visualize periplasmic DNA in naturally competent *H. pylori* [104]. As stated in [221], we observed a perfect co-localization pattern when the fluorescence signals of ComEA-mCherry and YoYo-1 were compared (Figure 4.5). ComEA focus formation and co-localization with YoYo-1 labeled DNA were absent in a strain lacking the outer membrane pore PilQ, whereas the absence of the inner membrane transporter ComEC did not interfere with ComEA-DNA co-localization (Figure 4.5). Similar focus formation of YoYo-1-labeled DNA was also observed in a strain carrying wildtype ComEA, excluding an artifact resulting from the translational mCherry-fusion (Figure 4.5). Notably, YoYo-1 foci were absent in a *comEA*-negative strain, which was also the case for a strain lacking the major type IV pilus subunit Pila [221].

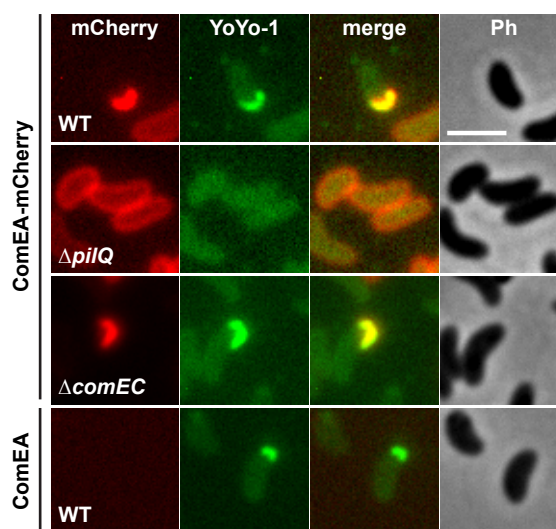


Figure 4.5: ComEA binds to DNA *in vivo*. Competence-induced bacteria carrying the *comEA-mCherry* (rows 1-3) or the wildtype *comEA* (row 4) alleles were exposed to external YoYo-1 stained DNA and imaged in the red (mCherry), green (YoYo-1) and phase contrast (Ph) channels. Overlays of the two fluorescence channels are shown (merge). Scale bar, 2 μ m.

Competence-induced cells that were exposed to long stretches of DNA (e.g. 48.5 kb phage- λ DNA) depicted either a uniform distribution pattern, single isolated foci, or multiple clusters of ComEA-mCherry per cell (Figure 4.4 B). This raised the question whether aggregation of ComEA during DNA uptake always starts at a single point, followed by subclustering of foci, or

Chapter 4. ComEA and the mechanism of DNA uptake

whether in some cells, multiple ComEA-mCherry aggregates develop simultaneously. To solve this issue, we performed time-lapse microscopy experiments in competence-induced cells carrying the *comEA-mCherry* construct, shortly after they have been exposed to long stretches (48.5 kb) of DNA (Figure 4.6).

We consistently observed rapid (within seconds) accumulation of ComEA-mCherry fluorescence in a single spot during DNA uptake (Figure 4.6 A). When cells were imaged at longer time intervals (2 min), we often observed the formation of single foci, followed by subclustering and a reversal to the initial uniform distribution pattern (Figure 4.6 B). Interestingly, this observation was independent of the presence of the inner membrane channel protein ComEC (Figure 4.6 C), suggesting that the transport across the inner membrane is not functionally coupled to the resolution of ComEA foci. Furthermore, cells could undergo multiple rounds of ComEA focus formation and resolution, as shown in Figure 4.6 C.

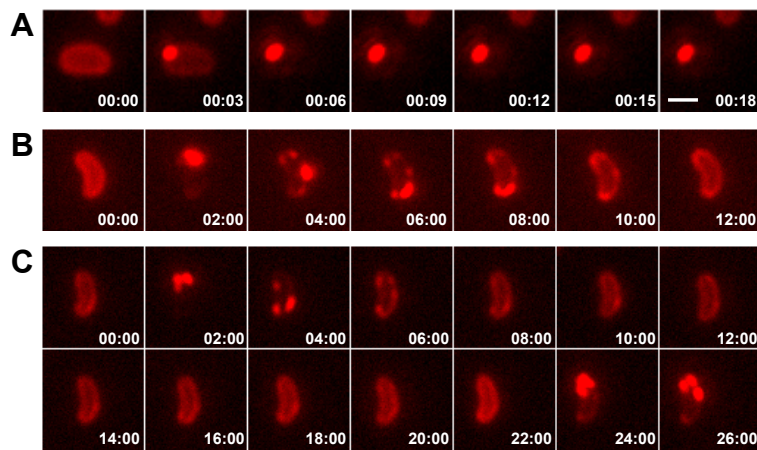


Figure 4.6: Time-lapse microscopy series of competent bacteria exposed to exogenous DNA. Competence-induced *V. cholerae* cells carrying *comEA-mCherry* at the native *comEA* locus were exposed to exogenous phage- λ DNA (48.5 kb) and imaged at 3 sec (A) or 2 min (B-C) intervals. (C) Time-lapse microscopy series as in (B), but in a $\Delta comEC$ background. Scale bar, 1 μ m.

4.1.3 tDNA induced ComEA foci are associated with PilQ clusters

In our model of DNA uptake, DNA is thought to cross the outer membrane through the PilQ secretin pore (Figure 2.5). Since ComEA accumulates around periplasmic DNA (Figure 4.4), we hypothesized that ComEA foci would assemble in close proximity to PilQ clusters. To test this hypothesis, we created a translational fusion between the gene encoding superfolder-GFP (sfGFP) and *pilQ* and replaced the wildtype *pilQ* allele on the chromosome of *V. cholerae* by this construct (*sfGFP-pilQ*). In contrast to classical GFP, sfGFP can fold in the periplasm [226]. We then tested the functionality of this new construct to promote natural transformation. Indeed, transformation frequencies were not significantly different from a wildtype strain, which indicates that the sfGFP-PilQ fusion is fully functional (WT, TF = $9.2 \pm 1.5 \times 10^{-5}$; sfGFP-PilQ, TF = $1.1 \pm 0.2 \times 10^{-4}$; average TF \pm SD of at least three independent experiments). Next, we created a strain that concomitantly expressed ComEA-mCherry and sfGFP-PilQ and analyzed

the relative position of each of the two protein fusions within competence-induced bacteria by time-lapse microscopy (Figure 4.7). Cells were exposed to external tDNA to induce ComEA-mCherry focus formation. In a majority of the cells with newly forming mCherry foci and detectable sfGFP clusters (70%; 69 events evaluated), we observed co-localizing foci of the two fluorescent proteins (Figure 4.7).

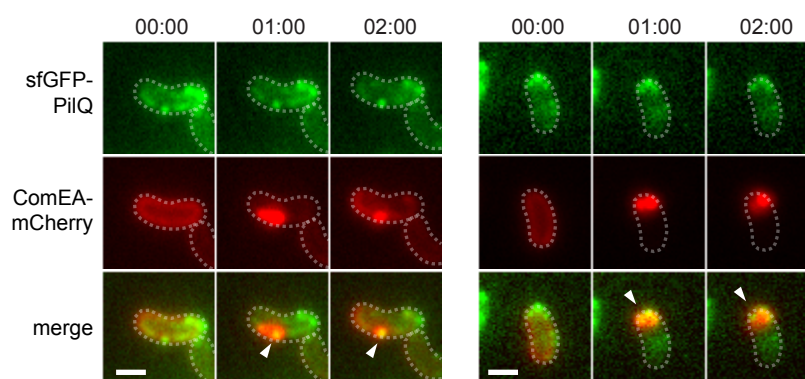


Figure 4.7: The position of ComEA focus formation is associated with PilQ clusters. Chromosomal *comEA* and *pilQ* were exchanged by fluorescent fusion constructs (*comEA-mCherry* and *sfGFP-pilQ*). Competence-induced bacteria were exposed to external tDNA and imaged in the green (sfGFP) and red (mCherry) channels. Co-localization was assessed in overlays of fluorescence channels (merge). The cells are outlined with dashed lines. Two representative examples of time-lapse microscopy experiments are shown. Co-localization of ComEA-mCherry foci and sfGFP-PilQ clusters is highlighted with an arrowhead. The time is given in minutes above the images. Scale bars, 1 μm .

4.1.4 Persistence of tDNA induced ComEA foci is heterogenous

While ComEA focus formation always started at a single point, mostly co-localizing with clusters of PilQ (Figure 4.7), resolution of ComEA foci was much more heterogenous. This heterogeneity comprised two different aspects: 1) subclustering of foci, as observed frequently for long stretches of DNA, but rarely for short DNA fragments (Figure 4.6), and 2) the duration of focus persistence, i.e. the timespan between formation of ComEA foci and the reversal to a uniform distribution pattern. We quantified this latter aspect in individual cells exposed to either a short 10.3 kb PCR fragment or 48.5 kb phage- λ DNA. To this end, we recorded time-lapse microscopy images at 2 min intervals for a total of 40 min (yielding 21 frames) shortly after exposure of competent bacteria to exogenous DNA. We then analyzed individual bacteria that showed ComEA-mCherry focus formation from a previously uniform distribution pattern early on in the time-lapse experiment (between frames 2 and 10). Within these cells, we counted the number of frames (\cong time) in which a fluorescence focus was present (Figure 4.8).

We observed a high degree of heterogeneity with respect to the duration of focus persistence for both, cells exposed to 10.3 kb PCR fragments (Figure 4.8 A, C) or to 48.5 kb phage- λ DNA (Figure 4.8 B). However, there was a clear correlation between the duration of focus persistence and the length of DNA fragments, which were added to the bacteria. In the presence of 10.3 kb PCR fragments, ComEA clusters disappeared within ten frames (\cong 20 min) in 82% of the cases (Figure 4.8 A). In contrast, foci persisting for more than ten frames were observed in

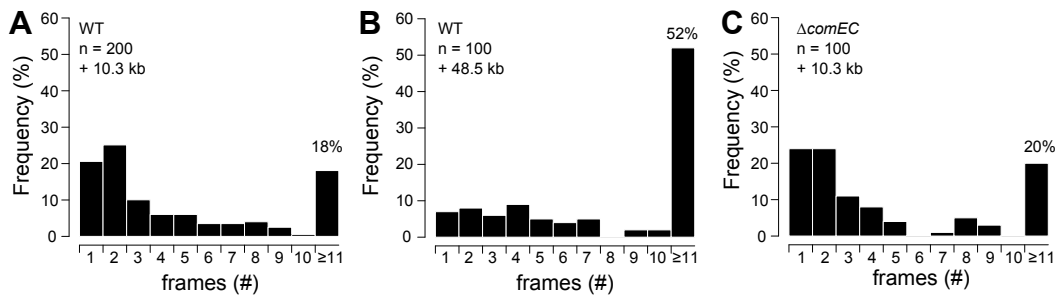


Figure 4.8: ComEA-mCherry focus persistence during DNA uptake Competence-induced strains carrying chromosomally encoded *comEA-mCherry* were exposed to 10.3 kb PCR fragments (A, C) or phage- λ DNA (48.5 kb) (B) and imaged at 2 min intervals for 21 frames. 100-200 cells depicting early mCherry focus formation were analyzed for the duration of focus persistence (number (#) of frames). Frequencies (%) of observed phenotypes are shown as barplots. ComEA-mCherry focus persistence was quantified in a wildtype (WT) (A, B) or $\Delta comEC$ background (C).

52% of the cases, when cells were exposed to 48.5 kb DNA (Figure 4.8 B).

Additionally, we also quantified the duration of focus persistence in a *comEC* deficient strain (Figure 4.8 C). A lack of *comEC* did not have any obvious effect on the resolution of ComEA clusters. This confirmed our previous hypothesis that ComEA focus resolution is not dependent on the presence of ComEC (Figure 4.6).

4.1.5 ComEA contributes to DNA transport across the outer membrane

Based on our previous finding that *comEA* is needed for PCR-detectable DNA accumulation within the periplasm (Figure 2.4), we hypothesized that ComEA contributes directly to the transport of DNA across the outer membrane. However, ComEA might also protect and stabilize incoming tDNA against potential nucleases within the periplasm, which would also explain the lack of PCR-detectable DNA uptake in a *comEA* deficient strain. Indeed, two exported nucleases, Dns and Xds, have been described for *V. cholerae* [227]. Interestingly, Focareta and Manning demonstrated that even though Dns can be recovered from culture supernatants, it was also detectable in the periplasmic space of *V. cholerae* [228].

Therefore, to rule out the possibility that ComEA might protect incoming tDNA against Dns or Xds, we tested *dns*, *xds*, and *comEA* single, double and triple mutants for natural transformation and PCR-detectable DNA uptake (Figure 4.9). As described in [221], the absence of *dns* resulted in higher transformability (Figure 4.9 A), which is consistent with a previous study by Blokesch and Schoolnik [178]. A lack of *dns* and *xds* also resulted in the increased detection of DNase-resistant tDNA within the bacteria (Figure 4.9 B). However, no transformants or translocated tDNA were detectable if *comEA* was concomitantly absent (Figure 4.9). We therefore concluded that ComEA's main role is not to protect incoming tDNA against degradation by the nucleases Xds or Dns, though we can not exclude the presence of any other hitherto unidentified nuclease in the periplasm of *V. cholerae*.

4.1.6 Dns is involved in the resolution of tDNA induced ComEA foci

Our results have shown that no DNA is taken up into a DNase-resistant state in a *comEA* deficient strain, even in the concomitant absence of the two nucleases Dns and Xds (Figure 4.9 B).

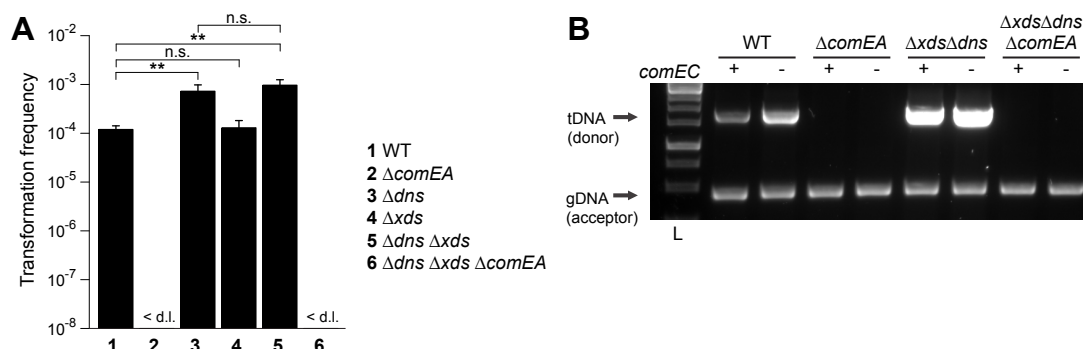


Figure 4.9: The absence of Dns and Xds does not rescue the $\Delta comEA$ phenotype. (A) Natural transformation of the indicated strains was scored using the *TnfoX* based chitin-independent transformation assay. The transformation frequencies shown on the Y-axis are averaged from at least three independent replicates (\pm SD). <d.l., below detection limit. Statistically significant differences are indicated (** $P < 0.01$); n.s. not statistically different. (B) DNA uptake assay as described for Figure 2.4. The genotypes of the tested strains are indicated above the figure. L, ladder.

However, this does not exclude the possibility that Dns and Xds play a role downstream of DNA transport across the outer membrane. In fact, in *B. subtilis*, as well as in *S. pneumoniae*, nucleases have been shown to be involved in cleavage of DNA during DNA transport [102, 105].

To test whether Dns or Xds might play a similar role within the periplasm of naturally competent *V. cholerae* cells, we quantified the duration of ComEA-mCherry focus persistence in different knock-out strains (Figure 4.10). As for transformation frequencies, a deletion in *xds* did not have an effect on ComEA focus persistence (Figure 4.10 B). In contrast, deletion of *dns* or *dns* and *xds* resulted in a striking increase in the duration of tDNA induced ComEA-mCherry focus persistence (Figure 4.10 A and C). We therefore concluded that Dns is indeed involved in resolution of tDNA induced ComEA-mCherry foci, potentially by cleaving periplasmic DNA.

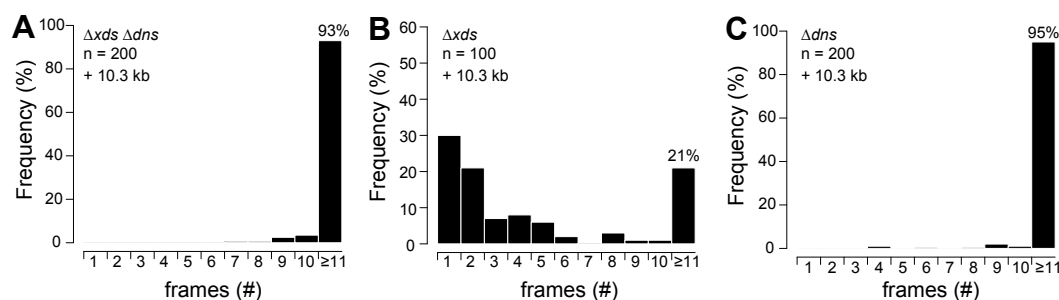


Figure 4.10: The absence of Dns correlates with a delay in the resolution of ComEA-mCherry foci. Competence-induced strains carrying the *comEA-mCherry* allele were deficient in either *dns* and *xds* (A), *xds* (B) or *dns* (C). All strains were exposed to 10.3 kb PCR fragments. The duration of tDNA induced mCherry focus persistence in n = 200 (A,C) or n = 100 (B) cells was tested as described for Figure 4.8.

4.1.7 Establishing a tool to visualize DNA transport across the inner membrane

From our previous experiments we concluded that at least two proteins are essential for transport of DNA across the inner membrane: ComEC, which is supposed to form a channel

Chapter 4. ComEA and the mechanism of DNA uptake

within the inner membrane, and ComF, of which we currently do not know, how it contributes to inner membrane transport. Deletion of one of those two proteins resulted in accumulation of periplasmic DNA (Figure 2.4). In order to pinpoint the position of cytoplasmic DNA uptake, we created translational fusions of *comEC* and *comF* with *gfp* and replaced the original copies of the respective genes on the chromosome by these constructs. The resulting strains were transformable and showed only a minor ~two-fold decrease in transformation frequencies compared to wildtype (Table 4.1). However, we did not detect any signals by microscopy in competence-induced bacteria. Similar results were obtained by constructing a translational fusion between DprA and GFP (Table 4.1).

Table 4.1: Transformation frequencies of strains expressing translational fusion constructs

Strain ¹	Transformation frequency ²
WT	$9.8 \pm 2.5 \times 10^{-5}$
GFP-ComEC	$5.1 \pm 1.6 \times 10^{-5}$
ComF-GFP	$4.8 \pm 1.5 \times 10^{-5}$
DprA-GFP	$7.0 \pm 3.6 \times 10^{-5}$

¹ All strains carry the *TnfoX* transposon for competence induction.

² The average transformation frequency of at least three independent experiments \pm SD is shown.

Therefore, we decided to study the localization of a protein that is supposed to act directly downstream of the inner membrane transporter, namely RecA. The localization of RecA has already been studied successfully in naturally competent *B. subtilis* [87]. Additionally, the localization of RecA has also been studied in non-competent *E. coli* by Renzette and co-workers [229]. Analogous to Renzette *et al.* [229], we fused GFP to the C-terminus of *V. cholerae* RecA and replaced the wildtype allele of *recA* on the chromosome by the *recA-gfp* version. Before studying the localization of RecA-GFP during DNA uptake, we verified its distribution pattern in non-competent cells and tested its functionality (Figure 4.11).

In non-competence-induced bacteria, RecA-GFP was present either dispersed throughout the cytoplasm or accumulated in strongly fluorescent spots (Figure 4.11 A). Furthermore, some cells depicted morphological abnormalities, such as an elongated cell shape (Figure 4.11 A, white arrowhead). Automatic quantification of the number of RecA-GFP foci per cell, using MicrobeTracker [230], revealed that 59% of the bacteria did not contain fluorescence accumulations (Figure 4.11 B). 37% of all cells showed one fluorescence focus, while less than 5% depicted more than one RecA-GFP spot per cell (Figure 4.11 B).

Renzette *et al.* have previously shown that DAPI might compete with RecA for DNA binding and that labeling of the bacterial chromosome with DAPI decreased the number of RecA-GFP foci [229]. Therefore, we repeated the quantification of RecA-GFP spots in the presence of DAPI. In contrast to Renzette *et al.* [229], we did not detect any difference in the number of RecA-GFP foci upon DAPI staining of the bacterial chromosome (Figure 4.11 B).

Consistent with the observation of morphological cell abnormalities (Figure 4.11 A, white arrowhead), the RecA-GFP expressing strain had a slight growth defect on solid LB plates, similar to a *recA* knock-out strain (Figure 4.11 C). Nevertheless, cells expressing RecA-GFP,

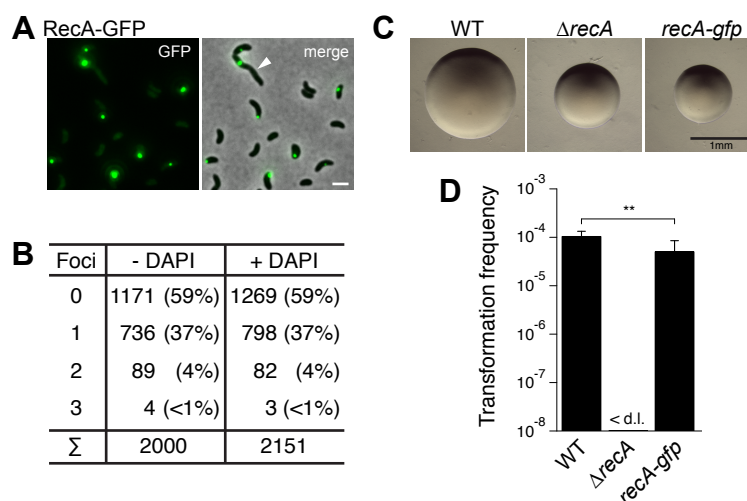


Figure 4.11: Localization and functionality of chromosomally encoded RecA-GFP. The native copy of *recA* on the chromosome was replaced by a translational reporter fusion construct (*recA-gfp*). Localization and functionality of RecA-GFP was tested in live cells. (A) Subcellular localization of RecA-GFP. Depicted is a representative fluorescence image of the green channel (GFP) and an overlay with the phase contrast channel (merge). Some cells show an abnormal morphology (white arrowhead). (B) Quantification of the number of GFP foci per cell in untreated (- DAPI) and DAPI-stained (+ DAPI) cells. (C) Colony morphology and size of a wildtype (WT), $\Delta recA$ and *recA-gfp* strain. (D) Functionality of RecA-GFP in chitin-independent natural transformation assays. All strains contain the *TnfoX* transposon for competence induction. <d.l., below detection limit. Shown are average transformation frequencies of at least three independent experiments \pm SD.

instead of wildtype RecA, retained most of their transformability (Figure 4.11 D; we observed a minor, but significant ~two-fold reduction between WT and RecA-GFP). Therefore, while the RecA-GFP fusion might be partially impaired in some basic cellular processes, it is still functional in terms of promoting transformation-related tasks.

The presence of large RecA-GFP accumulations, even in non-competence-induced cells (Figure 4.11 A), was in line with observations in *E. coli* [229]. Despite this fact, it prompted us to test whether these accumulations might be part of non-functional protein aggregates. To verify this hypothesis, we constructed a translational fusion between the gene encoding Inclusion Body Associated Protein A (IbpA) and mCherry. The small heat-shock protein IbpA has been identified originally in *E. coli* during high-level production of heterologous proteins [231]. Subsequently, the protein has been shown to localize to protein aggregates and inclusion bodies of *E. coli* and to assist chaperone mediated protein disaggregation [232–234]. *V. cholerae* contains a close homolog of *E. coli* IbpA and we thus reasoned that a fusion between IbpA and mCherry would serve as a good indicator for protein aggregation in *V. cholerae*. Therefore, we replaced the original copy of *ibpA* on the chromosome of *V. cholerae* with an *ibpA-mCherry* allele and studied its expression and localization under unstressed conditions (control), or after a 1 h exposure to either a mild heat-shock (40°C) or to inhibitory concentrations of streptomycin (100 μ g/ml) (Figure 4.12 A).

Both stresses, heat-shock exposure and streptomycin treatment, have been shown to induce the formation of protein aggregates that co-localize with IbpA in *E. coli* [232]. While we did not detect accumulations of IbpA-mCherry under control conditions, heat-shock and

Chapter 4. ComEA and the mechanism of DNA uptake

streptomycin treatment induced the formation of IbpA-mCherry foci (Figure 4.12 A). Heat-shock induced clusters of IbpA-mCherry were generally larger and brighter, compared to streptomycin induced foci. Additionally, heat-shock induced clusters progressively increased in size and brightness during microscopy experiments on agarose pads.

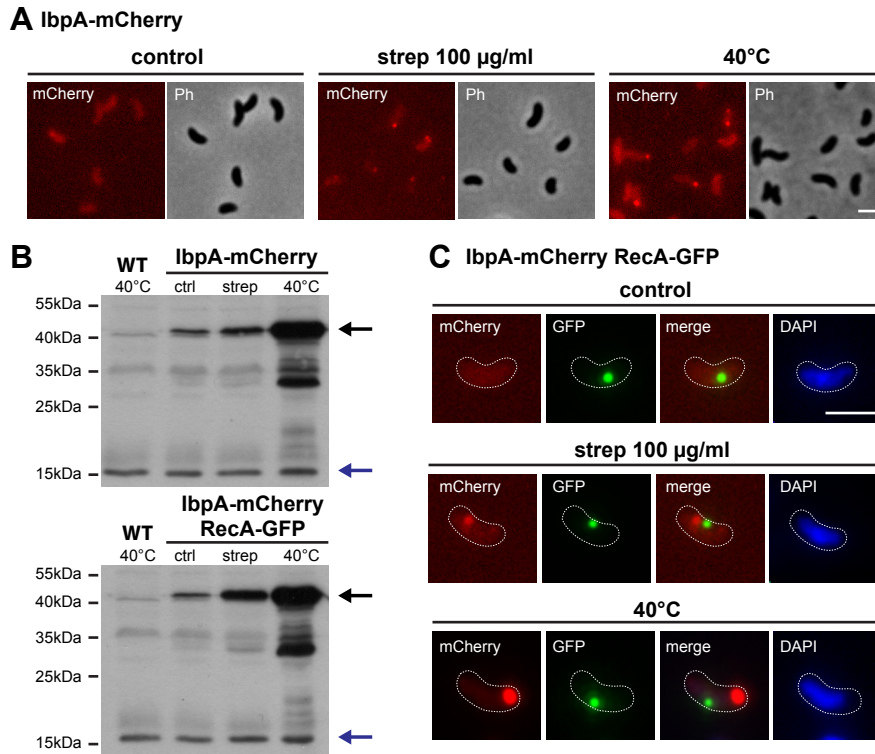


Figure 4.12: RecA-GFP accumulations are not part of misfolded protein aggregates. To visualize misfolded protein aggregates in *V. cholerae*, we exchanged the native copy of *ibpA* with a *ibpA-mCherry* translational fusion. (A) The production and distribution of IbpA-mCherry was tested in unstressed bacterial cultures (control), or after exposure of the bacteria to streptomycin (strep 100 µg/ml) or to a mild heat-shock (40°C). Cells were imaged in the red (mCherry) or phase contrast (Ph) channel. (B) The protein level of IbpA-mCherry was verified by Western blot analysis using polyclonal anti-mCherry antibodies. Cell lysates of a wildtype (WT) strain exposed to a mild heat-shock (40°C), as well as lysates of bacteria carrying the *ibpA-mCherry* alone (upper image), or in combination with the *recA-GFP* allele (lower image) were probed. The predicted size of the IbpA-mCherry construct is indicated (black arrow). Lysates of bacteria producing IbpA-mCherry were either prepared from an unstressed culture (ctrl) or after exposure to streptomycin (strep) or to a mild heat-shock (40°C). An extra band caused by antibody cross-reactivity (blue arrow) served as internal loading control. (C) Absence of co-localization of IbpA-mCherry and RecA-GFP. Representative fluorescence images (mCherry, GFP) and overlays (merge) are shown. Chromosomal DNA was stained with DAPI (DAPI). The cells are outlined with dashed lines. Scale bars, 2 µm.

Next, we tested whether cells carrying the *recA-gfp* allele induce the production of IbpA-mCherry on the protein level, which would be highly indicative of the presence of protein aggregates. However, unstressed cultures of bacteria carrying either the *ibpA-mCherry* construct alone (Figure 4.12 B, upper image, ctrl) or a combination of *ibpA-mCherry* and *recA-GFP* (Figure 4.12 B, lower image, ctrl), both depicted only low levels IbpA-mCherry protein. Exposure to streptomycin led to a slight increase in IbpA-mCherry production for both strains (Figure 4.12 B, strep), which was much more pronounced when bacteria were exposed to a

mild heat-shock (instead of the streptomycin treatment) (Figure 4.12 B, 40°C). We verified these observations by epifluorescence microscopy (Figure 4.12 C). Indeed, we readily observed cells containing large RecA-GFP accumulations, but no IbpA-mCherry foci (Figure 4.12 C, upper row), which would be indicative of protein aggregates. When we induced protein aggregation by a streptomycin treatment or by heat exposure (Figure 4.12 C, middle and lower rows), we detected cells with two distinct fluorescence foci, which strongly suggests that RecA-GFP accumulations are not part of misfolded protein aggregates.

In summary, our results demonstrate that the RecA-GFP fusion is functional with respect to natural transformation (Figure 4.11 D), and although it occasionally formed bright fluorescent spots (Figure 4.11 A, B), it does not aggregate into misfolded protein clusters or inclusion bodies (Figure 4.12).

4.1.8 DNA transport across the outer and inner membrane coincides spatially

After validating the functionality of the RecA-GFP fusion and determining its subcellular distribution pattern in non-competence-induced cells, we continued to use this construct to pinpoint the entry point of tDNA into the cytoplasm. The rationale behind this idea was that RecA would bind to ssDNA entering the cytoplasm (Figure 2.5), thereby changing its localization pattern from a mostly cytoplasmically dispersed distribution to detectable protein accumulations (visible as fluorescent foci) (Figure 4.11 A, B). In order to have an indication of the position of the outer membrane DNA transporter and the localization of periplasmic DNA, we created a strain that carried the *recA-gfp* allele together with the *comEA-mCherry* construct at the respective chromosomal loci.

In the absence of exogenous tDNA, competence-induced cells depicted a uniform distribution pattern of ComEA-mCherry (Figure 4.13 A). Foci of ComEA-mCherry were rare and possibly derived from the release of chromosomal DNA by lysed cells (Figure 4.13 B). Also, the distribution of RecA-GFP was uniform in 66% of the cells and did not show any obvious difference to non-competence-induced bacteria (Figure 4.13 A, B, compared to Figure 4.11). When competence-induced cells were exposed to exogenous tDNA, we frequently observed foci of ComEA-mCherry (10% of all cells) (Figure 4.13 C, D). About half of the cells with ComEA-mCherry foci also contained clusters of RecA-GFP (Figure 4.13 D). Most interestingly, of the 5% of cells which contained both, mCherry and GFP foci, we observed a co-localization of these two fluorescent signals in 67% of the cells (Figure 4.13 E).

Although we detected a clear association between RecA-GFP foci and spots of ComEA-mCherry, these results were not a proof that ssDNA, which enters the cytoplasm, indeed causes RecA-GFP focus formation. On the one hand, exposure of competent cells to exogenous tDNA did not result in an increase in the number of RecA-GFP foci. On the other hand, a substantial fraction of cells, which had foci of both ComEA-mCherry and RecA-GFP, contained non co-localizing spots of the two proteins. In order to further investigate this aspect, we performed time-lapse microscopy experiments. Competence-induced bacteria were exposed to exogenous tDNA and subsequently imaged at 2 min intervals (Figure 4.14).

Cells containing ComEA-mCherry and RecA-GFP foci at some point during time-lapse experiments varied greatly in their phenotypes. Cells, which depicted a uniform distribution

Chapter 4. ComEA and the mechanism of DNA uptake

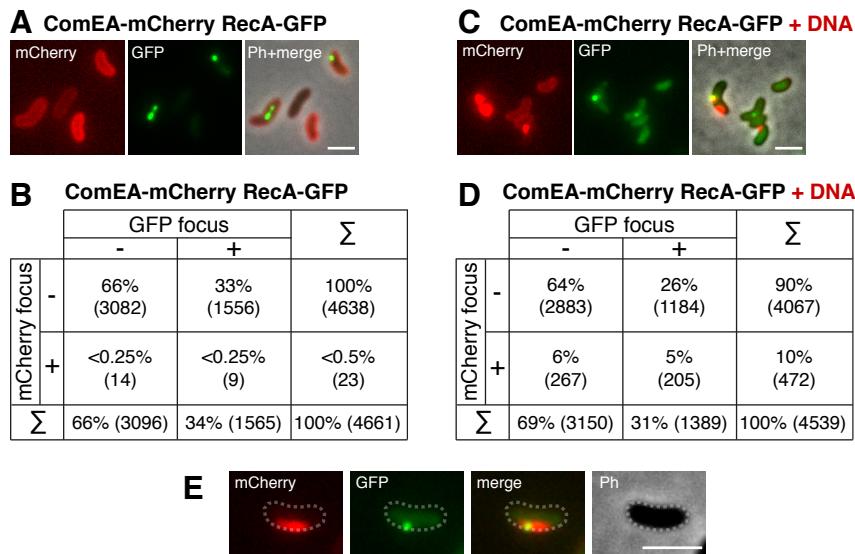


Figure 4.13: Co-localization of ComEA-mCherry and RecA-GFP in competence-induced live cells. The wildtype copies of *comEA* and *recA* were both replaced by translational fusion constructs (*comEA-mCherry* and *recA-GFP*). (A) Fluorescence microscopy images of competent, ComEA-mCherry RecA-GFP expressing bacteria. Shown are fluorescence images (mCherry, GFP) and an overlay of fluorescence images with the phase contrast (Ph) channel (Ph+merge). (B) Quantification of the observed phenotypes in the absence of exogenous tDNA. (C) Fluorescence images as in panel A, but cells were imaged after incubation with exogenous tDNA. (D) Quantification of the observed phenotypes in presence of exogenous tDNA. (E) Representative example of a cell containing a mCherry and a GFP focus. The cells are outlined with dashed lines in panel E. Scale bars, 2 μ m.

pattern of both fusion proteins, followed by the formation of fluorescent foci of ComEA-mCherry and RecA-GFP, were most informative (Figure 4.14 A). In this situation, we exclusively observed co-localization of the two foci (Figure 4.14 E, row a). Furthermore, GFP foci appeared with a certain delay to mCherry foci, even though the duration of this delay was not characteristic and varied between ≤ 2 min and ≤ 18 min. Additionally, in 17 out of 18 events, GFP foci formed exactly at, or close to the position where the mCherry focus appeared first.

Next, we analyzed cases in which mCherry foci were already present at the beginning of the experiment, but GFP foci formed *de novo* during time-lapse imaging (Figure 4.14 B). Again, we exclusively observed co-localization of the two foci (Figure 4.14 E, row b).

In contrast, when we analyzed cells that already contained GFP foci at the beginning of the experiment (Figure 4.14 C, D), co-localization of the two foci was only apparent in approximately 50% of the cases (Figure 4.14 E, rows c-d). It is important to note that the most frequently observed phenotype consisted of cells, which depicted mCherry foci at some point during the time-lapse experiment, but never formed any GFP spots (Figure 4.14 E, row e).

As a control, we repeated the quantification of RecA-GFP and ComEA-mCherry focus formation in time-lapse movies of a *comEC* deficient strain (Figure 4.14 F). Indeed, we detected only very few examples of newly formed GFP foci (<3%, compared to 10% in wildtype cells) (Figure 4.14 F, rows a-b). Furthermore, there was no obvious co-localization pattern observable for these few GFP foci compared with the mCherry foci. Therefore, the newly forming GFP foci in this strain likely represent tDNA-independent spontaneous events, which we also observed

in cells that did not depict ComEA-mCherry foci (data not shown). Notably, we frequently observed cells with pre-existing GFP foci at the beginning of time-lapse experiments, similar to the situation observed for wildtype cells (Figure 4.14 F, rows c-d) and for non-competence-induced bacteria (Figure 4.11).

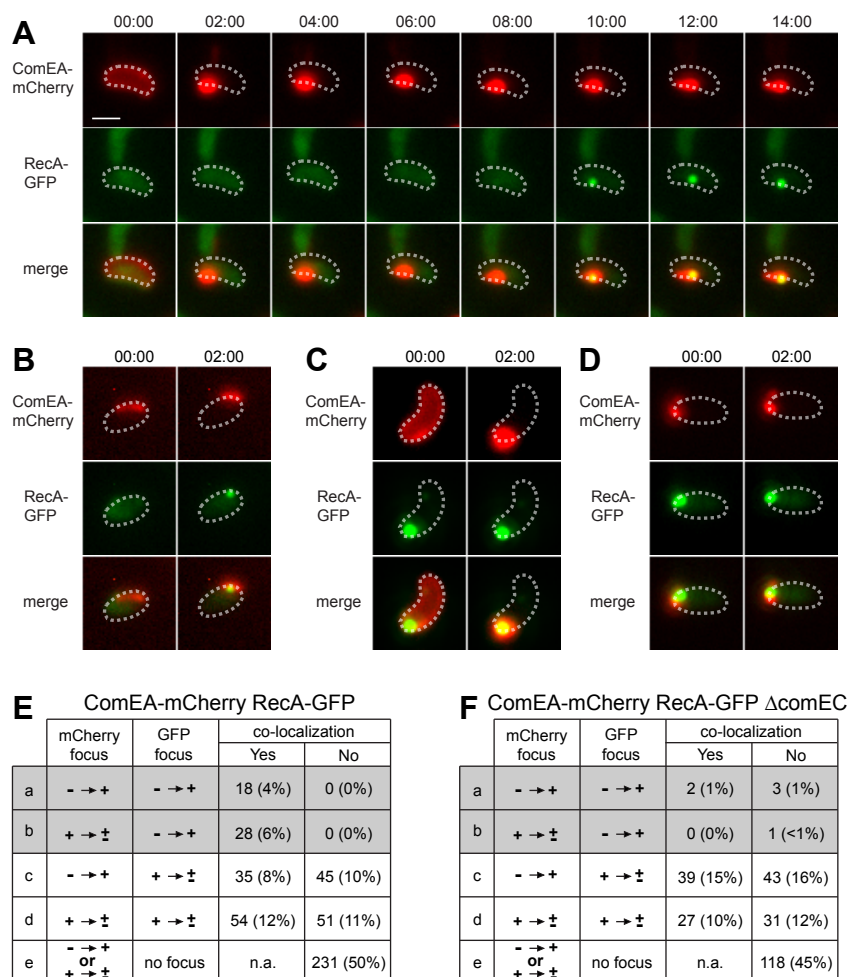


Figure 4.14: Time-lapse microscopy imaging of RecA-GFP ComEA-mCherry expressing bacteria exposed to exogenous tDNA. Competence-induced *V. cholerae* strains expressing chromosomally encoded RecA-GFP and ComEA-mCherry were exposed to exogenous tDNA and imaged at 2 min intervals for a total of 20 min. Time-points (min) relative to the first frame depicted in each panel are indicated above images (Panels A-D). Shown are examples of time-lapse series with distinctive ComEA-mCherry and RecA-GFP foci. Fluorescence channels (mCherry, red; GFP, green) and overlays thereof (merge) are depicted. The cells are outlined with dashed lines. Observed phenotypes comprised cells, which either showed *de novo* formation of mCherry and GFP foci (A), a pre-existing (i.e. present at the beginning of the time-lapse experiment) mCherry focus and a newly formed GFP focus (B), a pre-existing GFP focus and a newly formed mCherry focus (C), or pre-existing foci of both constructs (D). (E) Quantification of the observed phenotypes, as exemplified in Panels A-D. The arrow indicates the change of focus occurrence from a dispersed signal (-), to a focal distribution pattern (+). (±) includes the cases of persisting or disappearing foci. Events with *de novo* GFP focus formation are shaded in grey. n.a., not applicable. (F) As panel E, but in a *comEC* knock-out strain. Scale bar, 2 μ m.

Chapter 4. ComEA and the mechanism of DNA uptake

Since we detected an increase in the duration of ComEA-mCherry focus persistence in the absence of Dns (Figure 4.10), we were wondering whether this would also have an effect on the formation of RecA-GFP foci. To test this, we repeated the experiments shown in Figure 4.14, using strains deficient in *dns* (Figure 4.15). A lack of Dns indeed enhanced the frequency of *de novo* GFP focus formation from 10% in a wildtype strain (Figure 4.14 E, rows a-b), to 21% in the *dns* knock-out strain (Figure 4.15 A, rows a-b). Again, newly forming GFP foci were almost exclusively (94.4%) associated with mCherry foci (Figure 4.15 A, rows a-b). In contrast, deletion of *dns* did not have this effect in a strain that was concomitantly deficient for *comEC* (Figure 4.15 B, rows a-b).

A Δdns ComEA-mCherry RecA-GFP		B $\Delta dns \Delta comEC$ ComEA-mCherry RecA-GFP			
	mCherry focus	GFP focus	co-localization		
			Yes	No	
a	- → +	- → +	22 (4%)	4 (1%)	
b	+ → ±	- → +	79 (16%)	2 (<1%)	
c	- → +	+ → ±	29 (6%)	34 (7%)	
d	+ → ±	+ → ±	76 (15%)	47 (9%)	
e	- → + or + → ±	no focus	n.a.	206 (41%)	
a	- → +	- → +	2 (<1%)	0 (0%)	
b	+ → ±	- → +	6 (1%)	5 (1%)	
c	- → +	+ → ±	22 (5%)	35 (8%)	
d	+ → ±	+ → ±	48 (11%)	74 (17%)	
e	- → + or + → ±	no focus	n.a.	243 (56%)	

Figure 4.15: Strains deficient in *dns* show an increased frequency of *de novo* RecA-GFP focus formation. Quantification of time-lapse microscopy experiments of ComEA-mCherry RecA-GFP expressing strains that have been exposed to exogenous transforming DNA. The imaged strains were deficient in *dns* (A) or lacked *dns* and *comEC* (B). The observed phenotypes were quantified as in Figure 4.14.

4.2 Discussion

4.2.1 Periplasmic ComEA contributes to DNA uptake across the outer membrane

In the previous parts of this thesis, we have shown that the tightly regulated and highly conserved competence protein ComEA is essential for natural transformation of *V. cholerae* (Table 2.2, Figure 2.2). In addition, while being dispensable for the formation of competence-induced type IV pili (Figure 3.3), it is needed for the uptake of DNA across the outer membrane (as detected by PCR, Figure 2.4). However, how ComEA contributes to natural transformation in *V. cholerae* has not yet been studied. To address this question experimentally, we created a translation fusion between ComEA and mCherry and determined its subcellular localization under different conditions.

First, we showed that the C-terminal ComEA-mCherry fusion displays a uniform distribution pattern in competent *V. cholerae* cells (Figure 4.4). This pattern was similar to the distribution of a fusion between the predicted N-terminal 25 amino acid sec-signal peptide of ComEA (SignalP 4.0 [235]) and mCherry, which strongly suggested that ComEA is indeed exported to the periplasm of naturally competent *V. cholerae* cells (Figure 4.1). The periplasmic localization of ComEA was later confirmed by the finding that a functional translational fusion between *comEA* and the gene encoding beta-lactamase conferred full resistance to ampicillin, which is only possible, if the construct is successfully transported to the periplasm [221].

The uniform periplasmic distribution of ComEA is in contrast to observations on *B. subtilis* ComEA (ComEA_{B.s.}) [88, 89]. In *B. subtilis*, it has been shown by immunofluorescence microscopy that ComEA_{B.s.} displays a non-uniform, punctuated staining pattern [88]. These findings have been confirmed by live cell imaging of a fluorescently labeled ComEA_{B.s.} fusion protein [89]. It is important to note, however, that this *comEA*_{B.s.} fusion was not under control of its native promoter and that the amount of inducer used to drive expression of the construct had an impact on the protein's localization [89]. In contrast, we consistently observed a uniform distribution pattern for plasmid encoded *comEA-mCherry* (Figure 4.1) and chromosomally encoded *comEA-mCherry* (Figure 4.4), the latter being expressed from its native promoter. Additionally, replacing mCherry with sfGFP did not change the localization of the fusion construct (data not shown).

Kaufenstein and colleagues have shown that the distinct ComEA_{B.s.} assemblies that were detectable even in the absence of tDNA, were not static but that they changed their position along the membrane [89]. In line with this finding, ComEA of *V. cholerae* was shown to be highly mobile within the periplasm (Figure 4.2). Additionally, we observed a dynamic change in the ComEA distribution upon exposure of competent bacteria to exogenous tDNA (Figure 4.6); uniformly distributed ComEA relocalized and accumulated in fluorescence foci that co-localized with fluorescently labeled tDNA (Figure 4.5). Such *in vivo* binding of ComEA to DNA has not been observed before, although purified ComEA homologs of a number of naturally competent bacterial species, such as *B. subtilis*, *N. gonorrhoeae* or *C. jejuni*, have been shown to bind to DNA *in vitro* [91, 95, 223].

In summary, we have demonstrated that ComEA forms a pool of mobile DNA binding proteins within the periplasm of competent *V. cholerae*. But how does this relate to DNA transport across the outer membrane? One could imagine that by binding to DNA within

Chapter 4. ComEA and the mechanism of DNA uptake

the periplasm, ComEA could act as a ratchet to prevent retrograde movement of DNA during rounds of pilus elongation and retraction [32, 35, 56, 236]. However, such rounds of pilus elongation and retraction are very energy consuming. Craig *et al.* proposed a model for type IV pilus assembly, in which one molecule of ATP is needed by hexameric PilB for the incorporation of one pilus subunit into the growing fiber [237]. Incorporation of this subunit would then lead to elongation of the pilus by ~ 1 nm [237]. Given the fact that *V. cholerae* can take up DNA fragments of ≥ 42 kb [137], which equals to 13.9 nm of DNA in solution [238], many rounds of pilus elongation and retraction would be needed for the uptake of such long stretches of DNA. Recent review articles, which were published while this work was ongoing, suggested that other competence proteins, such as ComEA, might be involved in the DNA uptake process [56, 57] (though without experimental evidence). By experimentally showing that ComEA is indeed binding to DNA within the periplasm of competent *V. cholerae*, we strongly reinforce this hypothesis. We suggest that occasional stochastic retraction of the competence pilus opens the PilQ secretin pore, thereby allowing short stretches of DNA to enter the periplasm (either through Brownian motion or through partial binding to the pilus structure) (Figure 4.16). Within the periplasm, binding of ComEA to DNA would then prevent retrograde movements of the DNA, thereby acting as rectifier of Brownian motion (Figure 4.16). This would ultimately drive transport of DNA across the outer membrane, without the need for any external energy source.

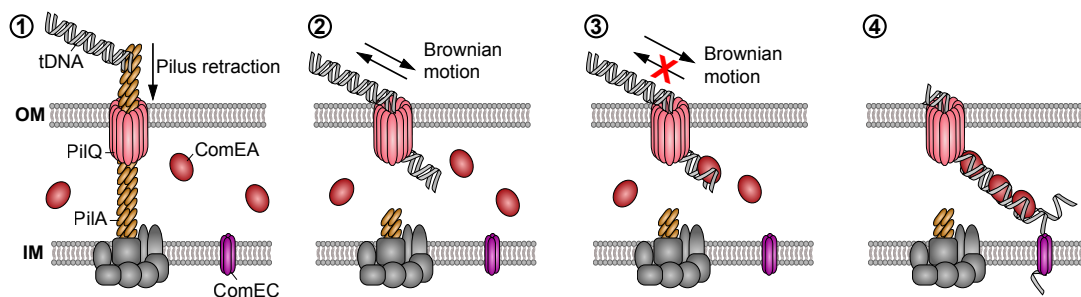


Figure 4.16: Working model of how DNA translocation across the outer membrane might occur in *V. cholerae*. A single retraction event of the competence pilus (with its major subunit PilA) might open the secretin pore (PilQ) in the outer membrane (OM), so that short stretches of the tDNA can enter the periplasm by Brownian motion, or through partial binding to the pilus structure. ComEA would then bind to the tDNA, thereby favoring translocation via a Brownian ratchet mechanism, which is modulated by the effective ComEA DNA-binding kinetics, binding spacing, and concentration. The ComEA-loaded tDNA might eventually interact with the inner membrane transporter ComEC, which would mediate ssDNA transport into the cytoplasm. The model is based on our results and on [32, 35, 56, 57, 84].

The kinetics of this process would depend on a number of parameters, as recently described for DNA transport into the cytoplasm of *E. coli* during phage mediated DNA injection [239]. The authors of this study concluded that binding of *E. coli* host proteins to partially translocated phage DNA would significantly speed up the transport process by providing a ratcheting mechanism (Brownian ratchet) that ultimately creates a net pulling force [239]. This force is dependent on different factors, such as the binding affinity of DNA binding proteins or the number of binding sites [239]. Even though we currently do not have experimental

data, the ratio between periplasmic ComEA protein and the incoming tDNA should be high, which would greatly favor rapid DNA internalization. Indeed, it has been stated in a study on *B. subtilis* ComEA that this protein “is present in greater abundance than other competence proteins [...]” [88], with an estimated 4000-5000 monomers per cell [88]. The concept that binding of a protein can drive the translocation of the protein’s substrate through a pore is a fundamental biological mechanism, and has been described for both DNA [239–241], as well as protein transport [242, 243]. However, so far there was no experimental evidence that directly supported such a model in the context of DNA uptake during natural transformation.

Consistent with our proposed model for DNA transport across the outer membrane (Figure 4.16) was the finding that the position of ComEA focus formation was strongly associated with clusters of the outer membrane secretin PilQ (Figure 4.7). Furthermore, our model predicts that ComEA homologs of other naturally competent bacteria should be able to replace ComEA of *V. cholerae*. Indeed we could show that ComEA of *B. subtilis* was able to efficiently compensate for the absence of ComEA of *V. cholerae* [221]. Moreover, even the C-terminal (HhH)₂ motif of ComEA of *B. subtilis* alone, which was shown to bind DNA *in vitro* [91], was sufficient to restore natural transformation of a *comEA* negative *V. cholerae* strain, as were the ComEA homologs from *N. gonorrhoeae*, *H. influenzae*, and *Pasteurella multocida* [221].

These findings do not only strongly support our hypothesis on the function of ComEA (Figure 4.16), but they also highlight the fact that ComEA-mediated DNA transport could be a highly conserved mechanism. One could even speculate a similar role for the membrane-anchored ComEA of Gram-positive bacteria, such as *B. subtilis* or *S. pneumoniae*. Even though these organisms are not surrounded by an outer membrane, their cell wall might constitute a similar diffusion barrier, and thereby create a space between the peptidoglycan layer and the cell membrane that is reminiscent of the periplasm of Gram-negative bacteria [244]. Once short stretches of DNA reach this space through pseudopilus induced cell wall holes, membrane-anchored ComEA of *B. subtilis* or *S. pneumoniae* might then act as a DNA ratchet and subsequently drive DNA transport in a similar manner as soluble periplasmic ComEA of *V. cholerae*. This idea is supported by the finding that ComEA clusters frequently co-localize with fluorescently labeled DNA fragments in competent *S. pneumoniae* [245].

4.2.2 Specification of ComEA’s DNA binding capacity

Our initial results on *in vivo* binding of ComEA to DNA prompted a series of experiments that aimed to better characterize this interaction. Matteo Dal Peraro (EPFL) and colleagues used a comparative modeling approach to predict the three-dimensional structure of ComEA, based on the ComEA-related protein of *T. thermophilus* [221] (Figure 4.17).

Two residues were identified as candidate residues for DNA binding interactions: K62 and K63 (Figure 4.17, [221]). To validate this model, we used site-directed mutagenesis to create a plethora of ComEA variants with single or double amino acid substitutions [221]. Consistent with the *in silico* predictions, K63, which is suggested to interact with both strands of the dsDNA through H-bonding (Figure 4.17), was of major importance for efficient DNA transport and natural transformation. Furthermore, K62/63 were shown to be required for *in vitro* binding of ComEA to DNA [221]. To test whether ComEA binds DNA in a cooperative manner,

Chapter 4. ComEA and the mechanism of DNA uptake

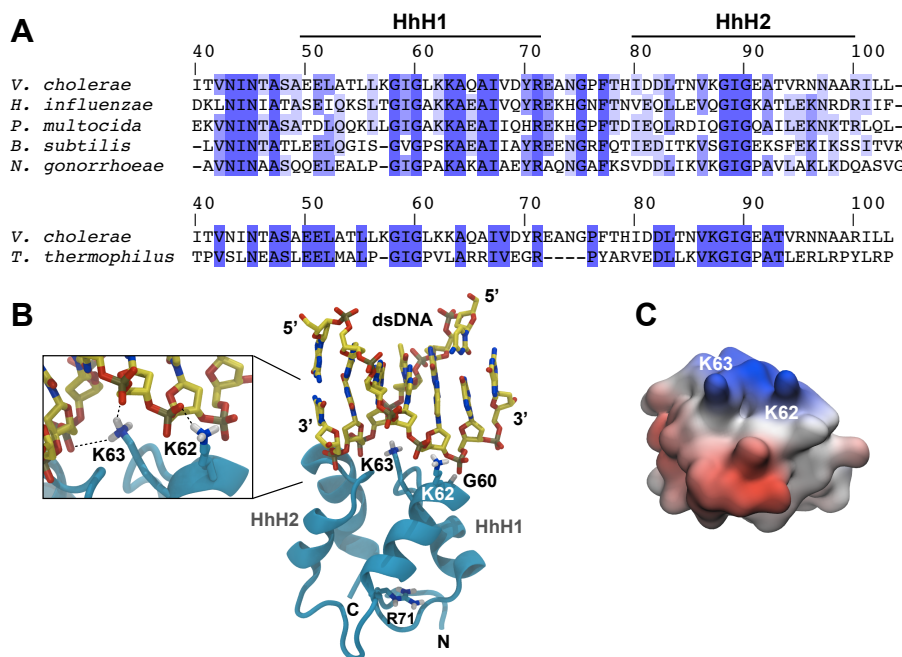


Figure 4.17: *In silico*-prediction of the ComEA-DNA complex. (A) Protein sequence alignment of the two helix-hairpin-helix motifs (HhH1-2) of ComEA/ComE homologs from the indicated organisms (using the ComEA residue numbering). The sequence conservation is shown in tones of blue (dark blue = highly conserved). (B) 3D model of ComEA and its predicted DNA binding mode based on comparative modeling using the ComEA-related protein of *T. thermophilus* HB8 (PDB ID: 2DUY) as template. The non-sequence-specific DNA backbone phosphate interactions with K62 and K63 are shown (inset). (C) The electrostatic potential at the molecular surface of ComEA is reported within a ± 160 $k_B T/e$ range (negative values in red, positive values in blue). Figure adopted from [221].

short PCR fragments (809 bp) were pre-incubated with ComEA-mCherry and visualized by atomic force microscopy [221]. We did not detect cooperative binding of the ComEA protein to DNA under the tested conditions, which again contradicts the hypothesis that ComEA's main function is the protection of the tDNA against nuclease mediated degradation [221].

In summary, these results suggested that ComEA is binding to DNA *in vivo*, as well as *in vitro*, through interactions of residues K62/63 with the DNA backbone [221]. The correlation between DNA uptake, transformability, and the presence of those two crucial residues [221] fully supported our ComEA-mediated ratcheting model (Figure 4.16). It is also important to note that the lack of evidence of cooperative binding of ComEA to DNA does not contradict our hypothesis, since such a mode of binding is not a prerequisite for the rectification of Brownian motion, and would merely speed up the internalization process (as outlined in [239]).

4.2.3 The role of the secreted nucleases Dns and Xds

Surface exposed nucleases have been shown to play an important role in natural transformation of the two Gram-positive bacteria *B. subtilis* and *S. pneumoniae* [102, 246, 247]. The integral membrane protein NucA of *B. subtilis* is expressed during competence and cleaves tDNA at the extracellular side [102]. A *nucA* deficient *B. subtilis* strain displayed reduced transformation frequencies [102]. The authors of this study attributed this observation to the

reduced number of free DNA termini, which are substrates for the subsequent transport into the cytoplasm [102].

Although *S. pneumoniae* does not contain a close homolog of *B. subtilis* NucA, its constitutively expressed membrane-anchored nuclease EndA [248, 249], which is also an important virulence factor [250], is needed for efficient natural transformation in this species [246, 247]. In contrast to NucA, EndA is thought to be responsible for the degradation of one strand of dsDNA during its transport into the cytoplasm as ssDNA [105, 249].

In *V. cholerae*, two secreted nucleases have been identified: Xds and Dns [227]. Both have been shown to be important for biofilm formation and its architecture [251]. Dns, but not Xds, has a major impact on *V. cholerae* transformation, most probably by degrading the extracellular DNA substrate, thereby counteracting natural transformation [178]. We confirmed these results in our chitin-independent transformation assay by showing that transformation frequencies are significantly higher in a *dns* knock-out strain (Figure 4.9). Additionally we could show that Dns might also be present in the periplasm of competent *V. cholerae*, since a *dns* deficient strain displayed a striking delay in ComEA focus resolution during DNA uptake (Figure 4.10). The fact that Dns might be transiently present in the periplasm has been reported earlier [228], and detection of Dns in bacterial cell lysates is in line with this finding [160].

Currently, we can only speculate on the role of Dns within the periplasm. Our observations suggest that it contributes to resolution of ComEA foci (Figure 4.10), possibly through cleavage of ComEA-bound DNA. In the absence of Dns, longer fragments would therefore reach the cytoplasm, which could explain the significant increase in *de novo* focus formation of RecA-GFP (Figure 4.15). Because of this latter observation, we do not favor the hypothesis that Dns specifically degrades one strand of DNA. If this was the case in *V. cholerae*, a *dns* deficient strain should either be blocked for inner membrane transport or it should transfer dsDNA into the cytoplasm, which would not favor the formation of ssDNA-RecA nucleoprotein clusters. In contrast, we suggest that Dns-mediated cleavage of DNA within the periplasm plays a similar role as NucA in *B. subtilis*. By cleavage of long DNA fragments, Dns might provide a higher number of DNA termini, which would have an effect on the rate of inner membrane DNA transport, but not necessarily on the absolute transformation frequency. In fact, occasional cleavage within the selection marker and the transport of shorter DNA fragments across the inner membrane would lower transformation frequencies, even though quantitatively more DNA might enter the cytoplasm.

4.2.4 Transport of DNA across the inner membrane

To pinpoint the localization of ssDNA entry into the cytoplasm, we have engineered a fluorescent fusion between *recA* and *gfp*, which we used to replace the wildtype copy of *recA* on the bacterial chromosome. Studies on *B. subtilis* RecA (RecA_{B,s}) have revealed that this protein co-localizes with other components of the polar DNA uptake complex in competent cells, and suggested that it binds to ssDNA during its polar entry into the cytoplasm of *B. subtilis* [87, 89]. In this organism, polar accumulations of RecA_{B,s} were only observed in competent cells, while the protein localized more uniformly in noncompetent cells [87]. In contrast, we observed

RecA-GFP foci in 41% of noncompetent *V. cholerae* cells (Figure 4.11 A, B). We speculated that these competence-independent RecA foci might represent DNA-less storage structures of RecA, as described for RecA of noncompetent *E. coli* (RecA_{E.c}) [229]. Renzette *et al.* described two types of RecA_{E.c} foci [229]: one type of focus was sensitive to DAPI staining and disappeared upon staining of the bacterial chromosome and the other type was insensitive to DAPI staining. The latter type of focus was attributed to DNA-less RecA_{E.c} aggregates, since a mutation that has been shown to prevent *in vitro* formation of these structures [252], also decreased the number of mutant RecA_{E.c}-GFP foci *in vivo* [229]. Since DAPI staining of the *V. cholerae* chromosome did not have any effect on the number of RecA-GFP foci (Figure 4.11 B), we concluded that they might represent similar DNA-less aggregates or storage structures. By constructing a translational fusion between the gene encoding Inclusion Body Associated Protein A (IbpA) of *V. cholerae* (VC0018) and *mCherry* we could additionally show that these RecA-GFP clusters are not part of misfolded protein aggregates or inclusion bodies (Figure 4.12).

Signals of RecA-GFP almost exclusively appeared as round fluorescent spots (Figure 4.11 A) and only rarely as elongated threads. This was independent of competence induction or exposure of competent cells to exogenous DNA (Figure 4.13 A). In contrast, RecA_{B.s} has been shown by Kidane and Graumann to relocalize in competent cells upon provision of external DNA, and to form long filamentous structures, termed “threads”, in approximately one third of all competent *B. subtilis* cells [87]. Yet the authors of this study reported that RecA_{B.s} threads could only be observed in *B. subtilis* cells that expressed a N-terminal YFP or GFP fusion protein [87]. Replacement of the YFP/GFP-tag with a RFP-tag (and a 5 aa shorter linker) rendered the protein almost non-functional (~1,000 fold reduction in transformation frequencies) and prevented the formation of threads, despite the fact that the protein retained its polar localization [87]. Moreover, it is important to note that Kidane and Graumann maintained the wildtype copy of *recA* on the chromosome and induced expression of the *yfp/gfp* fusion constructs from a xylose inducible promoter [87]. In contrast, we exchanged the wildtype allele of *recA* with the *recA-gfp* version in *V. cholerae*. This strain was almost fully transformable (Figure 4.11 D), although it exhibited a growth defect similar to a complete deletion of *recA* (Figure 4.11 C). We can therefore currently not exclude that the C-terminal GFP tag interferes with thread-formation during transformation, even though the fusion protein retains most of its functionality in the context of natural transformation.

The observation of RecA_{B.s} dynamics [87] prompted us to use RecA-GFP to localize the inner membrane transport process. Thus, we performed time-lapse microscopy experiments in a *recA-gfp comEA-mCherry* expressing strain, shortly after competent *V. cholerae* cells have been exposed to exogenous DNA (Figure 4.14). Although we rarely observed thread-like structures, we readily observed the formation of new GFP foci in cells that were taking up DNA (as judged by the presence of distinctive ComEA-mCherry foci)(Figure 4.14 A, B). In such cells, newly formed RecA-GFP foci consistently co-localized with ComEA-mCherry foci (Figure 4.14 E, rows a, b). Notably, we did not observe such a co-localization in a *comEC* knock-out strain, which is blocked for inner membrane transport of DNA (Figure 4.14 F, rows a, b). This highly suggests that ssDNA entering the cytoplasm is indeed causing the formation of new RecA foci at the

site of inner membrane transport. This is further supported by the finding that a deletion in *dns* not only caused ComEA foci to persist longer (Figure 4.10 C), but also increased the frequency of newly appearing RecA foci in cells that are taking up DNA (Figure 4.15 A). Again, this was efficiently blocked by a deletion of *comEC* (Figure 4.15 B). In contrast, cells with a pre-existing RecA-GFP focus did not necessarily show a co-localization between this and the ComEA-mCherry focus (Figure 4.14 E, F, rows a, b). From these observations we concluded that pre-existing RecA-GFP foci, which likely represent DNA-less aggregates, exist and localize independently from uptake of exogenous tDNA, but that newly appearing RecA-GFP foci in cells with distinctive ComEA-mCherry accumulations indeed indicate the position of ssDNA entry into the cytoplasm. Such events can only be captured in time-lapse experiments, which explains our inconsistent results from image analysis of snapshots (Figure 4.13).

Interestingly, in cells that displayed *de novo* formation of RecA-GFP and ComEA-mCherry foci we could indirectly determine the position of the outer membrane DNA transporter and the position of DNA entry into the cytoplasm by studying the localization of both newly formed foci. In 17/18 cases DNA entered the cytoplasm exactly at, or very close by the position where it crossed the outer membrane. Only in 1/18 cases did we observe the formation of a new ComEA-mCherry focus that moved away from its initial position, before a new RecA-GFP focus appeared. We can therefore not exclude that DNA might enter the cytoplasm occasionally away from the spot where it initially enters the periplasm. It is important to note, however, that this exceptional example was also special in that the RecA-GFP focus first formed without overlapping with the ComEA-mCherry focus and depicted a stable co-localization only with a delay between 2 and 4 min. Given the fact that we also rarely observed spontaneous formation of new RecA-GFP foci in the absence of inner membrane DNA transport (Figure 4.14 F), the exceptional observation of a new RecA-GFP focus that developed away from the initial site of ComEA-mCherry accumulation is not conclusive. In contrast, the observation that 17/18 RecA-GFP foci developed in close proximity to the position where the ComEA-mCherry foci had formed initially and the fact that the GFP and mCherry signals consistently overlapped, suggests that the DNA uptake machinery of *V. cholerae* constitutes one large complex.

5 Conclusion and perspectives

5.1 Conclusion

Natural transformation of any competent bacterial species requires the efficient transport of extracellular DNA into the cytoplasm of the respective organism. Many genes that are associated with natural transformability are strikingly conserved between different species. Yet, there is a lack of experimental data on the mechanism of DNA uptake during natural transformation. The events that take place during transport of DNA from the extracellular side into the cytoplasm have only been studied experimentally in relatively few organisms, and are far from being fully understood. In fact, Rosemary Redfield and coworkers recently stated that “our knowledge of the proteins responsible for DNA uptake and transformation is piecemeal” [207]. By establishing a first model of the DNA uptake complex in naturally competent *V. cholerae*, we contributed substantially to the current understanding of this process. We presented experimental data suggesting that type IV pili, which correlate with transformability in almost all naturally competent bacteria studied so far, also mediate transport of DNA across the outer membrane of *V. cholerae*. In this context, we identified 14 proteins that are essential for the formation of a surface exposed type IV pilus that is not associated with a specific position along the length of the cell. This finding is interesting, because competence-related type IV pili have not been visualized before in living Gram-negative bacteria. Our results showed in particular that the competence pilus is not predominantly localizing to cell poles, as has been shown for the Gram-positive, rod-shaped bacterium *B. subtilis* [87–89], thereby indicating that DNA uptake does not require any particular cellular localization in *V. cholerae*. Although the competence-specific pilus of *V. cholerae* was needed for high frequency transformation, we also showed that rare transformation events occur in its absence. Our findings would therefore be in line with the provocative speculation “that DNA uptake by bacteria is an accidental by-product of bacterial adhesion and twitching motility” [211], although the molecular basis of pilus-independent DNA transport across the outer membrane remains elusive. Moreover, we identified genes that are strictly required for natural transformation, and that are not related to the biogenesis or function of a type IV pilus. One of these genes encodes a predicted periplasmic DNA binding protein named ComEA. Homologs of ComEA have been purified from a number of naturally competent bacterial species, and they have been characterized for *in vitro* DNA binding [91, 95, 223]. Here we showed for the first time that the ComEA protein also binds to DNA *in vivo* and that it indeed is localized to the periplasm

of competent *V. cholerae* cells. These two characteristics might allow it to actively drive DNA uptake by preventing retrograde Brownian motion of DNA that crossed the outer membrane through pilus retraction (or potentially even by pilus expulsion [253]), or in rare cases, through a pilus-independent mechanism. This would provide a means to efficiently translocate DNA without the need of any external energy source. Given the fact that ComEA is a highly conserved protein amongst naturally competent bacteria, we propose that it might fulfill a similar function in a broad range of other bacterial species. Finally, we identified two proteins that mediate transport of DNA across the inner membrane. Since DNA transport across the outer membrane was not prevented in strains that were blocked for inner membrane transport, we concluded that the DNA uptake process across the two membranes of *V. cholerae* is a multi-step process. Although this has been previously demonstrated for *H. pylori* [104], our results are very informative, since *H. pylori* is exceptional in that it does not possess a bona fide T4P-related DNA uptake machinery, but it uses a type IV secretion system for DNA transport across the outer membrane and lacks the ComEA protein [104, 106, 107]. Therefore, our results suggest that the multi-step nature of the DNA uptake process might be a universal feature in all naturally competent Gram-negative bacteria, independent of the precise mode by which DNA crosses the outer membrane.

In summary, our findings provide first insights into the mechanism of DNA uptake in naturally competent *V. cholerae*. By comparing our results with predicted functions of proteins from other competent bacteria, we shed light on conserved aspects of this basic biological process. Thereby we contribute to a better general understanding of the DNA uptake process in naturally competent organisms, including many important human pathogens.

5.2 Perspectives

Although our findings allowed us to develop a basic understanding of the DNA uptake process during natural transformation in *V. cholerae*, a number of important questions remained unanswered. A short selection of these questions is discussed in this paragraph.

What exactly is the role of the competence pilus? We have shown that a competence type IV pilus is needed for efficient DNA uptake and transformation. Still it remains unclear whether DNA is interacting directly with this pilus or whether the pilus merely serves as a placeholder in the outer membrane secretin through which DNA can diffuse passively, once the pore opens upon pilus retraction or even pilus expulsion. Thus far, direct interaction of DNA with competence pili has only been observed in *N. meningitidis* and *S. pneumoniae* [86, 254]. While in *N. meningitidis* the minor pilin ComP is mediating sequence specific DNA binding [86], the exact mechanism by which competence pili of *S. pneumoniae* interact with DNA remains unclear [254]. Moreover, direct binding of *S. pneumoniae* competence pili to DNA, as described by Laurenceau *et al.* [254], has recently been questioned by Balaban and colleagues, who were not able to detect such an interaction *in vitro* [253]. Given the limited experimental evidence on the interaction between DNA and competence pili, it would be highly informative to further analyze this aspect in *V. cholerae*. Interestingly, three of the proteins encoded by the VC0857-VC0861 gene cluster are annotated as putative pilins. Considering the role of the minor pilin ComP in *N. meningitidis* [86], for which we did not identify a homologous protein in *V. cholerae*,

we can speculate that these genes might not only be important for the production of surface exposed pili (as we have shown in this thesis), but that they might fulfill a secondary function, potentially related to DNA binding. Yet it is important to note that DNA uptake in *V. cholerae* is not restricted to the uptake of species-specific DNA (Figure 2.1) and that the potential DNA binding mechanism therefore likely differs from the one observed in *N. meningitidis*.

What are the forces generated by ComEA driven DNA transport? Our model suggests that translocation of DNA across the outer membrane is mainly driven by periplasmic binding to ComEA. The forces against which ComEA could pull DNA into the periplasm are difficult to estimate theoretically, because the parameters that define this force, such as the spacing of ComEA molecules on the incoming DNA or the strength of DNA binding, are currently unknown. Even though no cooperative binding of purified ComEA to DNA was detected by atomic force microscopy *in vitro* under the tested conditions [221], such a binding mode could nevertheless occur *in vivo*, due to the vast excess of protein compared to DNA that enters the periplasm. Cooperative binding and eventually compaction of DNA by ComEA could indeed generate strong forces, as has been previously shown for the unrelated ssDNA binding protein VirE2 of *Agrobacterium tumefaciens* [255]. *A. tumefaciens* injects the VirE2 protein into plant cells, where it cooperatively binds to and compacts ssDNA during DNA translocation. In this way, DNA can be transported into host plant cells against external forces of up to 50 pN [255]. Determining the forces against which DNA can be pulled into *V. cholerae* cells would clarify the contribution of ComEA and/or pili to the DNA uptake process.

Does Dns directly cleave periplasmic transforming DNA? So far we only have indirect evidence for the interaction between Dns and DNA within the periplasm. A *dns* deficient strain showed a significantly increased duration of ComEA focus persistence during DNA uptake and an increase in the frequency with which new RecA-GFP foci appeared within the cytoplasm. Both observations are consistent with the hypothesis that in the absence of Dns no cleavage of periplasmic DNA occurs and therefore longer ssDNA fragments reach the cytoplasm. This predicts that Dns is at least transiently co-localizing and interacting with ComEA bound DNA within the periplasm. While this study was ongoing, Bergé *et al.* observed foci of the membrane-anchored ComEA homolog of *S. pneumoniae*, the pneumococcal nuclease EndA and fluorescently labeled DNA, which all predominantly accumulated at the mid-cell position in competent cells. Based on this, the authors speculated on a direct interaction between ComEA and EndA, during which ComEA might modulate the nuclease activity of EndA to specifically degrade one strand of dsDNA. However, a direct interaction between these proteins has not yet been demonstrated in *S. pneumoniae*. It might therefore be interesting to investigate the potential interaction between ComEA and Dns in *V. cholerae*. Moreover, given the fact that the number of newly formed RecA-GFP foci increased in a *dns* deficient *V. cholerae* strain, as shown in this work, we currently do not favor the hypothesis that the Dns nuclease is responsible to specifically degrade one strand of dsDNA, as suggested for EndA of *S. pneumoniae*. It remains to be seen, to what extent EndA of *S. pneumoniae* and Dns of *V. cholerae* functionally correspond to each other and what constitutes their precise role in DNA uptake.

How is DNA transported across the inner membrane? Currently we identified only two

proteins that are involved in the inner membrane transport process: ComEC and ComF. ComEC most probably forms a channel, through which DNA can enter the cytoplasm, as has been suggested for the *B. subtilis* homolog of this protein [97, 256]. In contrast, the role of ComF remains unclear. The protein contains a C-terminal phosphoribosyl-transferase domain and is strikingly conserved between competent bacterial species. Despite its conservation, no function could be identified so far. Our results demonstrated that the protein is indeed essential for inner membrane transport, as is ComEC. However, how ComF contributes to the inner membrane transport process is still elusive. With its phosphoribosyl-transferase domain, the protein might contribute to nucleotide salvage, by regenerating nucleotides from liberated nucleosides/bases that are potentially released by the degradation of one strand of DNA during inner membrane transport. The recycled nucleotides could then be used to energize inner membrane transport. Yet such a model is purely speculative and it is therefore of great interest to better characterize the protein ComF, as well as re-examine the role of the ssDNA binding protein PriA, which could not be deleted in *V. cholerae* due to its essentiality, thereby indicating that PriA's main role is vital for the cells. Still, this protein has been proposed to be involved in transformation of naturally competent *N. gonorrhoeae* [101].

With the results from this thesis as a starting point and with the excellent genetic tools to experimentally address biological questions in *V. cholerae* at hand, future studies will certainly contribute to the solution of the above questions, and thereby will provide new insights into the conserved mechanism of DNA uptake in a broad range of naturally competent bacteria.

6 Materials and methods

6.1 Culture media and growth conditions

All bacterial strains were grown aerobically in LB-medium (Luria/Miller, purchased from Carl Roth) at 30°C or 37°C. If not stated otherwise, cultures were incubated in 14-ml round-bottom polypropylene tubes under agitation. Solid LB-agar plates contained 1.5% (wt/vol) agar (LB-Agar (Luria/Miller), Carl Roth). For *tfoX* expression and induction of other constructs under control of the P_{BAD} promoter the LB-medium was supplemented with 0.02% L-(+)-arabinose (L-ara). Thiosulfate Citrate Bile Salts Sucrose (TCBS) agar plates were prepared as suggested by the manufacturer (Fluka) and used to counterselect *E. coli* after bacterial conjugation. For sucrose-based *sacB* counterselection, NaCl-free LB-medium containing 6% (wt/vol) sucrose was used. Defined artificial seawater medium (DASW) [112] supplemented with vitamins (MEM, Gibco) was used for natural transformation experiments on chitin flakes. Glycerol stock cultures contained 20% glycerol (vol/vol) and were stored at -80°C. If required, LB-medium and LB-agar plates were supplemented with antibiotics at final concentrations of 50 µg/mL, 75 µg/mL, and 100 µg/mL for gentamicin, kanamycin, and ampicillin, respectively. The ampicillin concentration was lowered to 50 µg/mL for competence-induced *V. cholerae* strains.

6.2 Plasmid and strain construction

Standard molecular-biology based methods were used for DNA manipulations. Restriction enzymes and DNA modifying enzymes were obtained from New England Biolabs. For cloning purposes, the high-fidelity DNA polymerases Pwo (Roche), KOD (Merck, Novagen) and Expand High Fidelity (Roche) were used. Taq DNA polymerase (GoTaq, Promega) was used for all other PCR reactions. Modified DNA sequences were verified using Sanger sequencing (Microsynth, CH).

Plasmid construction

All inducible plasmid constructs were based on pBAD/Myc-HisA (Invitrogen), which contains the *araBAD* (P_{BAD}) promoter followed by a multiple cloning site (MCS) for dose-dependent protein expression. A derivative of pBAD/Myc-HisA, pBAD(kan), was created through substitution of the ampicillin resistance cassette (*bla*) by a kanamycin resistance cassette (*aph*).

The genes and translational fusion constructs were PCR amplified and cloned into the MCS of pBAD/Myc-HisA or pBAD(kan). For the amplification of *V. cholerae* genes, the genomic DNA (gDNA) of strain A1552 [257] served as a template. GFP, mCherry and sfGFP were amplified from plasmids pBKdsGFP [160], pROD17 [258] and pET21-sfGFP, respectively. Site-directed mutagenesis was performed through inverse PCR. All plasmids used in this work are listed in Table A.2. A brief description of the respective cloning procedures is included in Table A.2. *E. coli* strain DH5 α [259] was used as host for cloning purposes.

***V. cholerae* strain construction**

Genes were deleted from the parental strain A1552, using either a gene disruption method based on the counter-selectable suicide plasmid pGP704-Sac28 [158], or on natural transformation and FLP recombination, as recently described (TransFLP method, [182, 183, 260]). Strains carrying chromosomally encoded gene fusions were created by replacing wildtype copies of the respective genes with fusion constructs using the TransFLP method [182, 183, 260]. The general procedure is exemplified in Figure 6.1 for the construction of the A1552-PilA-Strep::FRT strain, which carries a translational fusion between the 8 aa Strep-tag® II (IBA) and the *pilA* gene. Fluorescent protein fusion constructs were integrated into the chromosome analogously. gDNA sequences of strains carrying chromosomally encoded fusions were consistently verified through sequencing. *V. cholerae* strains containing arabinose-inducible *tfoX* on the chromosome were constructed by triparental mating between the respective *V. cholerae* strains (Table A.1) and *E. coli* S17 λ pir strains containing either plasmid pUX-BF13 (providing the transposase function; [261]), or pGP704-mTn7-*araC-tfoX* (providing the Tn*tfoX* transposon; [160]). All *V. cholerae* strains used in this work are listed in Table A.1.

6.3 Homology search and sequence alignment

For the identification of competence gene homologs in different bacterial species we used the Basic Local Alignment Search Tool (BLAST) of the Comprehensive Microbial Resource (CMR) [262] web page (<http://cmr.jcvi.org>) or from the GenoList [263] webpage (<http://genodb.pasteur.fr/cgi-bin/WebObjects/GenoList>). Organisms included in the query were: *V. cholerae* N16961, *Neisseria gonorrhoeae* FA 1090, *Haemophilus influenzae* Rd KW20, *Bacillus subtilis* 168, *Vibrio parahaemolyticus* RIMD 2210633, *Vibrio vulnificus* CMCP6, and *Vibrio fischeri* ES114. PilB protein sequences homologous to PilB of *V. cholerae* N16961 were retrieved from the CMR webpage (<http://cmr.jcvi.org>) for the following bacteria: *Myxococcus xanthus* DK1622 (locus: MXAN_5788), *N. gonorrhoeae* FA1090 (locus: NGO1673), *H. influenzae* Rd KW20 (locus: HI_0298), and *B. subtilis* 168 (locus: BSU24730). The four protein sequences were aligned using Clustal Omega (<http://www.ebi.ac.uk/Tools/msa/clustalo>). The Walker B region in Figure 3.6 was highlighted according to [217].

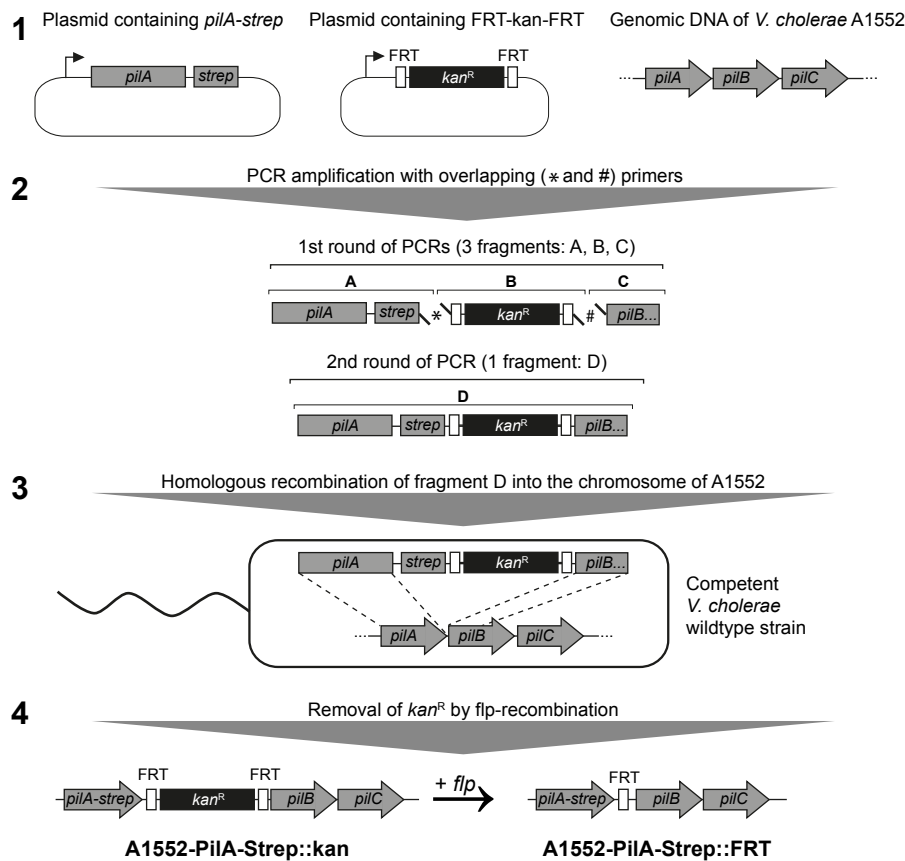


Figure 6.1: Replacement of chromosomal *pilA* through TransFLP. The TransFLP method [182, 183, 260] was used to replace the native copy of *pilA* on the chromosome by the *pilA-strep* allele. The procedure involved four steps: (1) preparation of a plasmid containing the *pilA-strep* construct, isolation of the pBR-FRT-kan-FRT plasmid [182] and purification of genomic DNA of the A1552 wildtype strain. (2) PCR amplification of three fragments (A, B, C), using DNA from step (1) as templates. Primers used to amplify fragments A and B, as well as B and C, were designed to be partially complementary, which allowed ligation of the three fragments (A, B, C) in a subsequent PCR reaction (yielding fragment D). (3) Fragment D was mixed with the competent wildtype strain A1552. Due to sequence homologies between fragment D and the bacterial chromosome, homologous recombination could mediate integration of fragment D, yielding kanamycin-resistant transformants. (4) The kanamycin-resistance cassette, flanked by FRT-sites, was removed by providing the *flp*-recombinase *in trans*.

6.4 Natural transformation assays

Chitin-mediated transformation assay

The natural transformability of bacteria grown on chitin flakes was determined as described in [182]. Briefly, overnight pre-cultures of *V. cholerae* were diluted 1/100 in LB-medium and grown aerobically at 30° until an OD₆₀₀ of ~0.5. Cells were washed once and resuspended in DASW. Autoclaved chitin flakes (50-80 mg, Sigma) were subsequently inoculated with 0.5 ml washed bacterial culture plus 0.5 ml fresh medium, mixed thoroughly and incubated at 30°C for 18-20 h without agitation. 2 µg gDNA of strain A1552-LacZ-kan [182] was added as transforming material. Samples were further incubated for 24 h. Bacteria were then detached from chitin flakes by vigorous vortexing and transformants were selected on kanamycin containing LB-agar plates. Transformation frequencies were calculated as ratios between

numbers of kanamycin resistant colony forming units (CFUs) and the total number of CFU.

Chitin-independent transformation assay

Chitin-independent transformation assays were performed as described in [160]. All strains tested for natural transformability in the chitin-independent setting carried an arabinose-inducible copy of *tfoX* on the chromosome (referred to as Tn*tfoX*) [160]. Overnight pre-cultures of *V. cholerae* were diluted 1/100 in LB-medium supplemented with 0.02% L-ara and grown aerobically at 30°C until an OD₆₀₀ of ~1.0. At that point, aliquots of 0.5 ml culture were transferred to 1.5 ml Eppendorf tubes and mixed with 1 µg gDNA of strain A1552-LacZ-kan [182]. Tubes were incubated under agitation at 30° for 5 h. Transformation frequencies were determined as for chitin-mediated transformation assays. To test natural transformability in different growth phases, bacteria were exposed to transforming DNA solely for 30 min (instead of the 5 h incubation period used in the standard protocol). Cells were subsequently treated with DNaseI (Roche) in PBS supplemented with 10 mM MgCl₂ for 10 min at 37°C. Serial dilutions were plated, and the CFU were enumerated as in the standard protocol.

Statistical analysis

Each experiment was repeated at least three independent times, and the averages of all experiments ± standard deviation (SD) are given in the respective figures. Statistical analysis of transformation frequencies was conducted in 'R' [264]. Differences were considered significant when P-values of Welch's t tests on log-transformed data were below 0.05 (*) or 0.01 (**).

6.5 Detection of DNA uptake by PCR

gDNA used for DNA uptake assays was isolated from *V. cholerae* strain A1552-LacZ-kan [182], *E. coli* BL21(DE3) and *B. subtilis* 168 using bacterial genomic DNA preparation kits (GenElute, Sigma; Genomic-tip 100/G or 500/G, Qiagen). Three approaches, which differed in their nature of competence induction, were used to study the uptake of DNA into a DNase-resistant state (e.g. at least into the periplasmic space) [43, 176, 221]. All centrifugation steps were carried out at 20,000 g for 3 min.

Chitin-based DNA uptake assay

Cells of strains A1552, A1552ΔcomEC, A1552ΔpilQ, A552ΔrecA, and A1552ΔdprA (Table A.1) were induced for natural competence by growing them on chitin flakes (as outlined for chitin-mediated transformation assays, section 6.4). A total of 2 µg donor gDNA of either the *V. cholerae* strain A1552-LacZ-kan, *E. coli* strain BL21(DE3), or *B. subtilis* 168 was added 22 h after inoculation of chitin flakes. After 24 h of incubation (statically, 30°C), the cells were detached from the chitin surface by extensive vortexing (~30 s). Flakes were allowed to settle for 1 min, before 500 µl of supernatant were transferred to a new 1.5 ml Eppendorf tube and pelleted by centrifugation. The bacteria were resuspended in 500 µl PBS containing 10 mM MgCl₂ and treated with 10 units DNase I (Roche) for 15 min at 37°C. Excess nuclease was removed by 3 rounds of washing in 1 ml PBS before the bacterial pellet was resuspended in 20 µl PBS. 1 µl of this bacterial suspension served as a template in a whole-cell duplex PCR

reaction. The primer pair LacZ-missing-fw and -bw (Table 6.1) was used at a 10-fold-lower concentration and served as a control for the total amount of acceptor cells released from the chitin flakes' surface. The second primer pair used in the duplex PCR was Kan-start-inwards/Kan-end-inwards, T7RNA-pol-750 up/T7RNA-Pol#3, and SpoIIIE-fw/SpoIIIE-bw to detect DNA uptake of donor gDNA derived from *V. cholerae*, *E. coli*, and *B. subtilis*, respectively (Table 6.1). Results of chitin-based DNA uptake assays are depicted in Figure 2.1.

DNA uptake assay based on expression of *tfoX* in trans

For a more quantitative measurement of the DNA uptake process, overnight pre-cultures of *V. cholerae* strains harboring the plasmid pBAD-*tfoX*-stop (Table A.2) were diluted to an OD₆₀₀ of 0.05 in LB-medium containing 0.02% L-ara. Cultures were grown aerobically at 30°C to an OD₆₀₀ of 0.8-1.0 and 1 ml aliquots were transferred to 1.5 ml Eppendorf tubes. 2 µg of gDNA was added to the samples and bacteria were further incubated statically for 2 h at 30°C. The bacteria were harvested by centrifugation, washed once in 1 ml PBS and subjected to DNase I treatment as described above. Washing, resuspension and PCR detection were then performed as described for the chitin-based DNA uptake assay. Results of plasmid-based DNA uptake assays are depicted in Figure 2.1.

Tn*tfoX*-based DNA uptake assay

In order to detect DNA uptake in a quantitative manner and independent of plasmids, overnight pre-cultures of *V. cholerae* strains carrying the Tn*tfoX* transposon were diluted 1/100 in 2.5 ml LB-medium supplemented with 0.02% L-ara for competence induction. Cultures were incubated under agitation until they reached an OD₆₀₀ of 1.0-1.5. Aliquots of 0.5 ml culture were transferred to 1.5 ml Eppendorf tubes and mixed with 1 µg gDNA of *E. coli* strain BL21(DE3). Tubes were incubated under agitation for 2 h at 30°C. Bacteria were then harvested and resuspended in 500 µl PBS containing 10 mM MgCl₂ and 10 units of DNaseI (Roche). After incubation for 15 min at 37°C, cells were washed twice in 1 ml PBS and resuspended in 100 µl PBS. The OD₆₀₀ of this bacterial suspension was determined and ~ 3 × 10⁶ bacteria served as a template in whole-cell duplex PCR reactions. Primer pairs were specific to the transforming DNA derived from *E. coli* strain BL21(DE3) (T7RNAP-start-dw and -bw, Table 6.1; expected PCR fragment size: 2,652 bp) and to the chromosome of the *V. cholerae* acceptor strain (LacZ-missing-fw and -bw, Table 6.1; expected PCR fragment size: 474 bp; primers used at a 10-fold lower concentration). This procedure was later slightly optimized, by changing the washing procedure and the primers used for the detection of transforming DNA [221]: cells were washed once in 1 ml PBS before the DNaseI treatment and once in 1 ml PBS after the treatment (instead of two washes after the DNaseI treatment step). For the detection of *E. coli* strain BL21(DE3) gDNA the primers T7RNA-pol-750-down and T7RNAP-end-bw (Table 6.1; expected PCR fragment size: 1,902 bp) were used.

Chapter 6. Materials and methods

Table 6.1: Primers used for the detection of DNA uptake by PCR

Primer name	Comment(s)	Sequence (5' to 3')
LacZ-missing-fw	Specific for <i>V. cholerae</i> A1552 and <i>lacZ</i> ⁺ derivatives of it; #1 in Figure 2.1	GCCGACTTTCCAATGATCCACAATGGG
LacZ-missing-bw	Specific for <i>V. cholerae</i> A1552 and <i>lacZ</i> ⁺ derivatives of it; #2 in Figure 2.1	CCCTCGCTATCCCATTGGAAATGCC
Kan-start-inwards	<i>V. cholerae</i> A1552-LacZ-kan specific; #3 in Figure 2.1;	ATGAGCCATATCAACGGGAAACGTC
Kan-end-inwards	<i>V. cholerae</i> A1552-LacZ-kan specific; #4 in Figure 2.1;	TTAGAAAACTCATCGAGCATCAAATG
T7RNA-pol-750 up	<i>E. coli</i> BL21(DE3) specific; #5 in Figure 2.1;	GCACGGGTTGCGATAGCCTCAGC
T7RNA-pol#3	<i>E. coli</i> BL21(DE3) specific; #6 in Figure 2.1;	ATGAACACGATTAACATCGCTAAGAAC-GACTTCTC
SpoIIIE-fw	<i>B. subtilis</i> 168 specific; #7 in Figure 2.1;	GGTAGTCGGGCAAACGTTTATC-TATTTGTTCCG
SpoIIIE-bw	<i>B. subtilis</i> 168 specific; #8 in Figure 2.1;	GCTAACCTTCACTCCGACATCAGGATAT-ACTTC
T7RNAP-start-dw	<i>E. coli</i> BL21(DE3) specific	ATGAACACGATTAACATCGCTAAGAACG
T7RNAP-end-bw	<i>E. coli</i> BL21(DE3) specific	TTACGCGAACGCGAAGTCCGACTCTAAG
T7RNA-pol-750-down	<i>E. coli</i> BL21(DE3) specific	GCTGAGGCTATCGCAACCCGTGC

6.6 Fluorescence microscopy

Widefield fluorescence microscopy experiments were performed using a Zeiss Axio Imager M2 epifluorescence microscope. Images were acquired with the Zeiss AxioVision software and a high-resolution AxioCam MRm camera. A Plan-Apochromat 100×/1.4 Oil objective was used throughout this work. For illumination, an HXP120 lamp was used. Filter sets were purchased from Zeiss and included: 63 HE mRFP shift free, 38 Endow GFP shift free and 49 DAPI shift free. All bacterial samples were mounted on 2% (wt/vol) agarose/PBS pads. For time-lapse experiments, coverslips were sealed with a heated 1:1:1 (wt/wt/wt) mixture of Vaseline, lanolin, and parafin (VALAP). During sample preparation, centrifugation steps were carried out for 3 min at 20,000 g. For all experiments, overnight pre-cultures were prepared and diluted in fresh LB-medium (dilution 1/100 if not stated otherwise).

Visualization of competence pili and flagellar staining

Pili were visualized by immunofluorescence microscopy, targeting the major pilus subunit, PilA [43]. More precisely, *V. cholerae* strains used to study piliation carried a translational fusion between the major pilus subunit-encoding gene *pilA* and the sequence coding for the 8 aa Strep-tag® II affinity tag (IBA) at the endogenous locus of *pilA* (*pilA-strep*) (Figure 6.1). The strains were grown aerobically in LB-medium supplemented with 0.02% L-ara for 6-7 h. For live cell imaging, culture aliquots were incubated under agitation for 10 min at 30°C with a Strep-tag-recognizing antibody (StrepMAB classic conjugated to Oyster 488; IBA) at a dilution of 1:250. Cells were washed once in PBS (centrifugation speed lowered to 12,000 g) and imaged immediately. Through a serendipitous finding, we discovered that the SNAP-Cell

TMR-Star substrate (New England Biolabs) stains the membrane of *V. cholerae*, including the sheathed flagellum. Thus, for co-staining of pili and flagella, bacteria were placed in a shaking incubator for 30 min with SNAP-Cell TMR-Star at a final dilution of 1 mM. Next, the bacteria were pelleted, resuspended in PBS, and fixed for 30 min with 2% (wt/vol) paraformaldehyde. After three rounds of washing in PBS, the cells were incubated for 1 h with the anti-*Strep*-tag antibody (StrepMAB Oyster 488; diluted 1:250 in PBS) under gentle agitation. The bacteria were mounted after four additional wash steps and visualized by fluorescence microscopy.

Microscopy of strains expressing fluorescent fusion proteins

V. cholerae strains carrying chromosomally encoded translational fusions between PilB, PilT, or PilQ and the respective fluorescent proteins were grown aerobically at 30°C in LB-medium (2.5 ml culture in 14 ml round-bottom polypropylene tubes) supplemented with 0.02% L-ara for 6-7h (OD₆₀₀ 1.9-2.4, Figure 3.1). The samples were washed once in PBS and imaged immediately. To determine co-localization between PilQ and competence pili, a strain carrying the *mCherry-pilQ* and *pilA-strep* alleles was tested for piliation as described above. Quantification was performed manually in 80 randomly picked pilated cells that showed distinctive mCherry-PilQ clusters.

E. coli strains containing plasmids encoding *tat-gfp* and *tat-comEA-gfp* were grown under agitation at 37°C in LB-medium (5 ml LB-medium in a 50 ml Erlenmeyer flask) containing 0.002% L-ara for 5 h.

The staining of chromosomal DNA was performed through the addition of DAPI (final concentration 5 µg/ml) to bacterial cultures for at least 5 min.

To characterize ComEA-mCherry localization in the presence of exogenous DNA, *comEA-mCherry* expressing cells were grown as described above. A total of 50 µl washed culture was mixed with 1 µg of gDNA derived either from *V. cholerae* strain A1552-LacZ-kan [182], commercially available phage-λ DNA (Roche) or a 10.3 kb fragment amplified through PCR. The PCR fragment was amplified from A1552 gDNA and spans the region between the ends of *recN* and *VC0861*. After 5 min of incubation in presence of exogenous DNA the bacteria were mounted on agarose pads and imaged. To visualize the DNA during the relocation of ComEA-mCherry, phage-λ DNA (Roche) was pre-stained with 10 µM YoYo-1 (Molecular Probes/Invitrogen) at 4°C in LB-medium (corresponding to a base pair to dye ratio of 15:1). 180 µl washed bacterial culture was mixed with 20 µl of pre-stained DNA and incubated for 20 min under gentle agitation. The cells were washed once in PBS and imaged immediately.

For time-lapse microscopy of *comEA-mCherry* expressing cells, the samples were prepared as described above, but immediately imaged after the addition of DNA. Images were taken at 3 sec to 120 sec intervals, as indicated in the figure and movie legends. To determine co-localization between ComEA-mCherry and sfGFP-PilQ, cells were exposed to exogenous phage-λ DNA (Roche) as described above and imaged at 30 sec intervals. Co-localization of foci was then quantified manually in 69 randomly chosen cells that showed distinctive sfGFP-PilQ clusters and that depicted ComEA-mCherry focus formation from a previously uniform distribution pattern. Only the first frame showing a distinctive ComEA-mCherry focus was analyzed.

The duration of ComEA-focus persistence was analyzed in time-lapse experiments of *comEA-mCherry* expressing strains that were exposed to 10.3 kb PCR fragments or ~48.5 kb phage- λ DNA (Roche) as indicated in the figure legends. 21 frames were imaged at 2 min intervals (\approx 40 min per experiment). Only cells that depicted a newly formed ComEA-mCherry focus from a previously uniform distribution pattern between frames 2 and 10 were analyzed. The frames (\approx time) in which these cells contained distinctive ComEA-mCherry foci were counted manually.

For the detection of IbpA containing protein aggregates, strains carrying chromosomally encoded *ibpA-mCherry* (Figure 4.12A) or *ibpA-mCherry* and *recA-gfp* (Figure 4.12C) were grown in plain LB-medium for 6 h at 30°C. At this time-point, cultures were either further incubated for 1 h at 30°C or exposed to 100 μ g/ml streptomycin for 1 h at 30°C or incubated for 1 h at 40°C, as indicated in the figure legends.

The distribution of RecA-GFP foci in non-competence-induced cells (Figure 4.11A, B) was tested by diluting overnight pre-cultures of strains carrying the *recA-gfp* allele to an OD₆₀₀ of 0.02 in plain LB-medium. Cultures were incubated under agitation for 7 h at 30°C, washed once in PBS and imaged immediately. Alternatively, cells were washed once in PBS and incubated for 15 min in PBS containing 5 μ g/ml DAPI prior to microscopy imaging. The distribution of RecA-GFP foci was evaluated using MirobeTracker (see below).

To test co-localization of ComEA-mCherry and RecA-GFP foci, strains expressing both fluorescent fusion constructs were diluted from overnight pre-cultures to an OD₆₀₀ of 0.02 in LB-medium supplemented with 0.02% L-ara. The cultures were incubated for 7 h at 30°C under agitation and washed once in PBS. 50 μ l of washed culture were exposed to 1 μ g phage- λ DNA as described above. Images were taken after a 5 min incubation period in Eppendorf tubes, followed by a 10 min incubation period on agarose pads (snapshots, Figure 4.13). Quantification of cells with ComEA-mCherry foci and/or RecA-GFP foci was performed manually in random-fields of view. To test for co-localization, only cells exposed to external transforming DNA were analyzed (Figure 4.13E). Counts from three independent experiments were checked for consistency and pooled for statistical analysis. For time-lapse imaging of *recA-gfp* expressing bacteria (Figures 4.14, 4.15), cells were imaged at 2 min intervals for 20 min (\approx 11 frames) immediately after exposure to exogenous phage- λ DNA. Phenotypes were scored manually in random fields of view. As for the analysis of snapshots, results from three independent experiments were checked for consistency and pooled for statistical analysis.

Fluorescence loss in photobleaching

Fluorescence loss in photobleaching (FLIP) experiments were performed on a Zeiss LSM710 microscope equipped with a 561 nm solid-state laser (20 mW). A Plan-Apochomat 63 \times /1.40 Oil objective was used. The microscope was controlled with the Zen 2009 software suite (Zeiss). Images were acquired using 1% of the maximum laser power at a 1024 \times 1024 pixel resolution and using a 1.5 \times zoomfactor. The pinhole was opened completely (600 nm). Amplifier offset and detector gain were set to 180 and 800-850, respectively. Time intervals during image acquisition ranged from 104 to 120 ms/frame for live cells to max. 160 ms/frame for fixed cells. The maximum (100%) laser power was used for bleaching.

6.7. Cell lysates, SDS-PAGE and western blot analysis

V. cholerae strains Δ comEA-TntfoX harboring pBAD(kan)-comEA-mCherry or pBAD(kan)-ss[ComEA]-mCherry were grown aerobically for 5 h in LB-medium supplemented with 0.02% arabinose and 75 mg/ml of kanamycin at 30°C. After the cells were mounted on agarose pads, the slides were sealed with VALAP and the bacteria were imaged immediately (live samples; Figure 4.2A, B). Alternatively, the cells were fixed for 30 min at room temperature in 4% paraformaldehyde/150 mM phosphate buffer, before imaging (fixed samples; Figure 4.2C).

For FLIP data acquisition a circular bleaching region of ~440 nm width was defined at one cell pole (region of interest (ROI) 1; labeled as 1 in Figure 4.2). A circular ROI of the same size was defined at the opposite cell pole of the same bacterium (labeled as 2 in Figure 4.2) and in an adjacent cell (labeled as 3 in Figure 4.2). The average fluorescence intensity of all regions was recorded. Bleaching of ROI 1 was initiated after a lag of 20 frames and repeated after each frame. The acquired data were exported and processed in 'R' [264]. The recorded fluorescence intensities were normalized to the average fluorescence intensity of the first 10 frames. Trendlines were calculated as moving averages using the SMA(x, n = 5) function from the 'TTR' package [264].

MicrobeTracker

The MicrobeTracker Suite [230] was used for the statistical analysis of piliation (Figure 3.2) and to determine the number of RecA-GFP foci per cell (Figure 4.11). The parameters of Alg4 were altered slightly (splitTreshold set to 0.2 and split1 set to 1) to outline *V. cholerae* cells. For the quantification of piliated cells, the spotFinderM tool was used and a total of 401 piliated cells was analyzed. To determine the position of the pilus along the cell, the attachment point of the pilus was marked manually. The relative l-coordinates of the spots were used for statistics. RecA-GFP foci were detected automatically in non-competence-induced cells using the spotFinderZ tool. For the statistical analysis of piliation and the number of RecA-GFP foci per cell, data from three biological replicates were checked for consistency and pooled for analysis.

Image processing and annotation

Image processing and manual quantification of co-localization was performed using ImageJ. Linear adjustments of the contrast and brightness of microscopy images were applied to whole images (never restricted to a particular region of an image) throughout this work, and only used to optimally display gray-values within the observed range. Adobe Illustrator was used for image annotation. Cells were outlined with Bézier-curves according to the size and shape of bacteria in phase-contrast images.

6.7 Cell lysates, SDS-PAGE and western blot analysis

For the preparation of cell lysates, bacteria expressing IbpA-mCherry were grown as for microscopical analysis (see section 6.6). Cells were harvested by centrifugation at 20,000 g for 5 min and resuspended in 2×Laemmli buffer. The volume of 2×Laemmli buffer used for resuspension was adjusted to the OD₆₀₀ of the bacterial culture (yielding a theoretical OD₆₀₀ of 10 for cells resuspended in Laemmli buffer). The cell-suspension was then boiled for 15 min

Chapter 6. Materials and methods

at 98°C and stored at -20°C.

Separation of proteins under denaturing conditions was conducted by SDS-PAGE using 11% acrylamide gels [265, 266]. Equal amounts of protein samples were loaded in all lanes. For western blot analysis, the proteins were transferred onto PVDF western blotting membranes (Roche) in a Peqlab PerfecBlue™ tank-electroblotter at 100 V for one hour at 4°C. PVDF membranes were subsequently incubated in blocking buffer (2.5% (wt/vol) skim milk in TBS + 0.1% (vol/vol) tween-20 (TBST)), and exposed to primary antibodies against mCherry (Biovision 5993-100) at a dilution of 1:5,000 in blocking buffer for one hour at room temperature. After extensive washing in TBST, primary antibodies were detected using a secondary goat anti-rabbit antibody conjugated to peroxidase (Sigma A9169; used at a 1:20,000 dilution in blocking buffer for one hour at room temperature). Immunoblots were developed using the Western Lightning-ECL (Perkin Elmer) substrate and signals were detected on chemiluminescence-films (Amersham Hyperfilm ECL, GE Healthcare).

A Appendix

A.1 Strain list

Table A.1: List of *V. cholerae* strains used in this work

Strain	Genotype ¹	Source
A1552	Wildtype, O1 El Tor Inaba; Rif ^R	[257]
A1552-LacZ-kan	A1552 strain with <i>aph</i> cassette in <i>lacZ</i> gene; Rif ^R , Kan ^R	[182]
A1552-Tn ϕ X	A1552 containing mini-Tn7- <i>araC</i> -P _{BAD} - <i>tfoX</i> ; Rif ^R , Gent ^R	[160]
ComEA-mCherry-Tn ϕ X	A1552-Tn ϕ X with <i>comEA</i> - <i>mCherry</i> ::FRT replacing <i>comEA</i> ; Rif ^R , Gent ^R	[221]
ComEA-sfGFP-Tn ϕ X	A1552-Tn ϕ X with <i>comEA</i> - <i>sfGFP</i> ::FRT replacing <i>comEA</i> ; Rif ^R , Gent ^R	†
ComEA-mCherry Δ comEC-Tn ϕ X	A1552- <i>comEA</i> - <i>mCherry</i> ::FRT Δ VC1879-Tn ϕ X; Rif ^R , Gent ^R	[221]
ComEA-mCherry Δ dns Δ xds-Tn ϕ X	A1552- <i>comEA</i> - <i>mCherry</i> Δ VC0470 Δ VC2621-Tn ϕ X; Rif ^R , Gent ^R	†
ComEA-mCherry Δ dns-Tn ϕ X	A1552- <i>comEA</i> - <i>mCherry</i> Δ VC0470-Tn ϕ X; Rif ^R , Gent ^R	†
ComEA-mCherry Δ pilQ-Tn ϕ X	A1552- <i>comEA</i> - <i>mCherry</i> ::FRT Δ VC2630-Tn ϕ X; Rif ^R , Gent ^R	[221]
ComEA-mCherry Δ xds-Tn ϕ X	A1552- <i>comEA</i> - <i>mCherry</i> Δ VC2621-Tn ϕ X; Rif ^R , Gent ^R	†
ComF-GFP-Tn ϕ X	A1552-Tn ϕ X with <i>comF</i> - <i>gfp</i> ::FRT replacing <i>comF</i> ; Rif ^R , Gent ^R	†
DprA-GFP-Tn ϕ X	A1552-Tn ϕ X with <i>dprA</i> - <i>gfp</i> ::FRT replacing <i>dprA</i> ; Rif ^R , Gent ^R	†
GFP-ComEC-Tn ϕ X	A1552-Tn ϕ X with <i>gfp</i> - <i>comEC</i> ::FRT replacing <i>comEC</i> ; Rif ^R , Gent ^R	†
IbpA-mCherry-Tn ϕ X	A1552-Tn ϕ X with <i>ibpA</i> - <i>mCherry</i> ::FRT replacing <i>ibpA</i> (VC0018); Rif ^R , Gent ^R	†
mCherry-pilQ-Tn ϕ X	A1552-Tn ϕ X with <i>mCherry</i> - <i>pilQ</i> ::FRT replacing <i>pilQ</i> ; Rif ^R , Gent ^R	[43]
mCherry-pilQ PilA-Strep::kan-Tn ϕ X	A1552- <i>pilA</i> - <i>strep</i> ::FRT-kan-FRT <i>mCherry</i> - <i>pilQ</i> ::FRT-Tn ϕ X; Rif ^R , Gent ^R , Kan ^R	[43]
mCherry-pilQ pilB-GFP-Tn ϕ X	A1552- <i>mCherry</i> - <i>pilQ</i> ::FRT (replacing <i>pilQ</i>) <i>pilB</i> - <i>gfp</i> ::FRT (replacing <i>pilB</i>) Tn ϕ X; Rif ^R , Gent ^R	[43]
PilA-Strep::FRT-Tn ϕ X	A1552-Tn ϕ X with <i>pilA</i> - <i>strep</i> ::FRT replacing <i>pilA</i> ; Rif ^R , Gent ^R	[43]
PilA-Strep::kan-Tn ϕ X	A1552-Tn ϕ X with <i>pilA</i> - <i>strep</i> ::FRT-kan-FRT replacing <i>pilA</i> ; Rif ^R , Gent ^R , Kan ^R	[43]
PilA::FRT-Tn ϕ X	A1552-Tn ϕ X with <i>pilA</i> ::FRT replacing <i>pilA</i> ; Rif ^R , Gent ^R	[43]
PilA-Strep::kan Δ comEA-Tn ϕ X	A1552- <i>pilA</i> - <i>strep</i> ::FRT-kan-FRT Δ VC1917-Tn ϕ X; Rif ^R , Gent ^R , Kan ^R	[43]
PilA-Strep::kan Δ comEC-Tn ϕ X	A1552- <i>pilA</i> - <i>strep</i> ::FRT-kan-FRT Δ VC1879-Tn ϕ X; Rif ^R , Gent ^R , Kan ^R	[43]
PilA-Strep::kan Δ comF-Tn ϕ X	A1552- <i>pilA</i> - <i>strep</i> ::FRT-kan-FRT Δ VC2719-Tn ϕ X; Rif ^R , Gent ^R , Kan ^R	[43]
PilA-Strep::kan Δ pilB-Tn ϕ X	A1552- <i>pilA</i> - <i>strep</i> ::FRT-kan-FRT Δ VC2424-Tn ϕ X; Rif ^R , Gent ^R , Kan ^R	[43]
PilA-Strep::kan Δ pilC-Tn ϕ X	A1552- <i>pilA</i> - <i>strep</i> ::FRT-kan-FRT Δ VC2425::FRT-Tn ϕ X; Rif ^R , Gent ^R , Kan ^R	[43]
PilA-Strep::kan Δ pilM-Tn ϕ X	A1552- <i>pilA</i> - <i>strep</i> ::FRT-kan-FRT Δ VC2634::FRT-Tn ϕ X; Rif ^R , Gent ^R , Kan ^R	[43]
PilA-Strep::kan Δ pilN-Tn ϕ X	A1552- <i>pilA</i> - <i>strep</i> ::FRT-kan-FRT Δ VC2633::FRT-Tn ϕ X; Rif ^R , Gent ^R , Kan ^R	[43]
PilA-Strep::kan Δ pilO-Tn ϕ X	A1552- <i>pilA</i> - <i>strep</i> ::FRT-kan-FRT Δ VC2632::FRT-Tn ϕ X; Rif ^R , Gent ^R , Kan ^R	[43]
PilA-Strep::kan Δ pilP-Tn ϕ X	A1552- <i>pilA</i> - <i>strep</i> ::FRT-kan-FRT Δ VC2631::FRT-Tn ϕ X; Rif ^R , Gent ^R , Kan ^R	[43]

Continued on next page

Table A.1: continued

Strain	Genotype ¹	Source
PilA-Strep::kan ΔpilQ-Tn foX	A1552- <i>pilA-strep</i> ::FRT-kan-FRT ΔVC2630-Tn foX ; Rif ^R , Gent ^R , Kan ^R	[43]
PilA-Strep::kan ΔpilT-Tn foX	A1552- <i>pilA-strep</i> ::FRT-kan-FRT ΔVC0462-Tn foX ; Rif ^R , Gent ^R , Kan ^R	[43]
PilA-Strep::kan ΔrecA-Tn foX	A1552- <i>pilA-strep</i> ::FRT-kan-FRT ΔVC0543-Tn foX ; Rif ^R , Gent ^R , Kan ^R	[43]
PilA-Strep::kan ΔVC0857-Tn foX	A1552- <i>pilA-strep</i> ::FRT-kan-FRT ΔVC0857-Tn foX ; Rif ^R , Gent ^R , Kan ^R	[43]
PilA-Strep::kan ΔVC0858-Tn foX	A1552- <i>pilA-strep</i> ::FRT-kan-FRT ΔVC0858-Tn foX ; Rif ^R , Gent ^R , Kan ^R	[43]
PilA-Strep::kan ΔVC0859-Tn foX	A1552- <i>pilA-strep</i> ::FRT-kan-FRT ΔVC0859-Tn foX ; Rif ^R , Gent ^R , Kan ^R	[43]
PilA-Strep::kan ΔVC0860-Tn foX	A1552- <i>pilA-strep</i> ::FRT-kan-FRT ΔVC0860-Tn foX ; Rif ^R , Gent ^R , Kan ^R	[43]
PilA-Strep::kan ΔVC0861-Tn foX	A1552- <i>pilA-strep</i> ::FRT-kan-FRT ΔVC0861-Tn foX ; Rif ^R , Gent ^R , Kan ^R	[43]
PilA-Strep::kan ΔpilF-Tn foX	A1552- <i>pilA-strep</i> ::FRT-kan-FRT ΔVC1612-Tn foX ; Rif ^R , Gent ^R , Kan ^R	[43]
PilB-GFP	A1552 with <i>pilB-gfp</i> ::FRT replacing <i>pilB</i> ; Rif ^R , Gent ^R	[43]
PilB-GFP-Tn foX	A1552-Tn foX with <i>pilB-gfp</i> ::FRT replacing <i>pilB</i> ; Rif ^R , Gent ^R	[43]
PilB ^{E394A} -GFP-Tn foX	A1552-Tn foX with <i>pilB^{E394A}-gfp</i> ::FRT replacing <i>pilB</i> ; Rif ^R , Gent ^R	[43]
PilT-GFP	A1552 with <i>pilT-gfp</i> ::FRT replacing <i>pilT</i> ; Rif ^R , Gent ^R	[43]
PilT-GFP-Tn foX	A1552-Tn foX with <i>pilT-gfp</i> ::FRT replacing <i>pilT</i> ; Rif ^R , Gent ^R	[43]
RecA-GFP-Tn foX	A1552-Tn foX with <i>recA-gfp</i> ::FRT replacing <i>recA</i> ; Rif ^R , Gent ^R	†
RecA-GFP IbpA-mCherry-Tn foX	A1552-Tn foX with <i>recA-gfp</i> ::FRT (replacing <i>recA</i>) <i>ibpA-mCherry</i> ::FRT (replacing <i>ibpA</i>); Rif ^R , Gent ^R	†
RecA-GFP ComEA-mCherry ΔcomEC	A1552-Tn foX with <i>recA-gfp</i> ::FRT (replacing <i>recA</i>) <i>comEA-mCherry</i> ::FRT (replacing <i>comEA</i>) ΔVC1879::FRT ΔVC0470; Rif ^R , Gent ^R	†
RecA-GFP ComEA-mCherry ΔcomEC-Tn foX	A1552-Tn foX with <i>recA-gfp</i> ::FRT (replacing <i>recA</i>) <i>comEA-mCherry</i> ::FRT (replacing <i>comEA</i>) ΔVC1879::FRT; Rif ^R , Gent ^R	†
RecA-GFP ComEA-mCherry Δdns-Tn foX	A1552-Tn foX with <i>recA-gfp</i> ::FRT (replacing <i>recA</i>) <i>comEA-mCherry</i> ::FRT (replacing <i>comEA</i>) ΔVC0470; Rif ^R , Gent ^R	†
RecA-GFP ComEA-mCherry-Tn foX	A1552-Tn foX with <i>recA-gfp</i> ::FRT (replacing <i>recA</i>) <i>comEA-mCherry</i> ::FRT (replacing <i>comEA</i>); Rif ^R , Gent ^R	†
sfGFP-PilQ-Tn foX	A1552-Tn foX with <i>sfgfp-pilQ</i> ::FRT replacing <i>pilQ</i> ; Rif ^R , Gent ^R	†
sfGFP-PilQ ComEA-mCherry-Tn foX	A1552-Tn foX with <i>sfgfp-pilQ</i> ::FRT (replacing <i>pilQ</i>) <i>comEA-mCherry</i> ::FRT (replacing <i>comEA</i>); Rif ^R , Gent ^R	†
ss[ComEA]-mCherry-Tn foX	A1552-Tn foX carrying ss[ComEA]- <i>mCherry</i> encoding a translational fusion between the signal sequence of <i>comEA</i> and <i>mCherry</i> ; replacing <i>comEA</i> ; Rif ^R , Gent ^R	[221]
ΔcomEA	A1552 ΔVC1917; Rif ^R	[112]
ΔcomEA ΔcomEC-Tn foX	A1552 ΔVC1917 ΔVC1879-Tn foX ; Rif ^R , Gent ^R	[43]

Continued on next page

Table A.1.: continued

Strain	Genotype ¹	Source
Δ comEA Δ comEC::FRT-Kan-FRT-Tn <i>foX</i>	AI552 Δ VCI1917 Δ VCI1879::FRT-Kan-FRT-Tn <i>foX</i> ; Kan ^R , Rif ^R , Gent ^R	[221]
Δ comEA-Tn <i>foX</i>	AI552 Δ VCI1917-Tn <i>foX</i> ; Rif ^R , Gent ^R	[164]
Δ comEC	AI552 Δ VCI1879; Rif ^R	[176]
Δ comEC-Tn <i>foX</i>	AI552 Δ VCI1879-Tn <i>foX</i> ; Rif ^R , Gent ^R	[43]
Δ comEC::FRT-Kan-FRT-Tn <i>foX</i>	AI552 Δ VCI1879::FRT-Kan-FRT-Tn <i>foX</i> ; Kan ^R , Rif ^R , Gent ^R	[221]
Δ comF	AI552 Δ VCI2719; Rif ^R	[43]
Δ comF Δ comEC::kan-Tn <i>foX</i>	AI552 Δ VCI2719 Δ VCI1879::FRT-kan-FRT-Tn <i>foX</i> ; Rif ^R , Gent ^R , Kan ^R	[43]
Δ comF-Tn <i>foX</i>	AI552 Δ VCI2719-Tn <i>foX</i> ; Rif ^R , Gent ^R	[43]
Δ dns	AI552 Δ VCI0470; Rif ^R	[178]
Δ dns Δ comEC	AI552 Δ VCI0470 Δ VCI1879; Rif ^R	[176]
Δ dns Δ pilQ	AI552 Δ VCI0470 Δ VCI2630; Rif ^R	[176]
Δ dns Δ xdS Δ comEA	AI552 Δ VCI0470 Δ VCI2621 Δ VCI1917 Δ VCI1879::FRT-Kan-FRT-Tn <i>foX</i> ; Kan ^R , Rif ^R , Gent ^R	[221]
Δ comEC::FRT-Kan-FRT-Tn <i>foX</i>		
Δ dns Δ xdS Δ comEA-Tn <i>foX</i>	AI552 Δ VCI0470 Δ VCI2621 Δ VCI1917-Tn <i>foX</i> ; Rif ^R , Gent ^R	[221]
Δ dns Δ xdS Δ comEC::FRT-Kan-FRT-Tn <i>foX</i>	AI552 Δ VCI0470 Δ VCI2621 Δ VCI1879::FRT-Kan-FRT-Tn <i>foX</i> ; Kan ^R , Rif ^R , Gent ^R	[221]
Δ dns Δ xdS-Tn <i>foX</i>	AI552 Δ VCI0470 Δ VCI2621-Tn <i>foX</i> ; Rif ^R , Gent ^R	[221]
Δ dns-Tn <i>foX</i>	AI552 Δ VCI0470-Tn <i>foX</i> ; Rif ^R , Gent ^R	[221]
Δ dprA	AI552 Δ VCI0048; Rif ^R	[176]
Δ dprA Δ comEC-Tn <i>foX</i>	AI552 Δ VCI0048 Δ VCI1879-Tn <i>foX</i> ; Rif ^R , Gent ^R	[221]
Δ dprA-Tn <i>foX</i>	AI552 Δ VCI0048-Tn <i>foX</i> ; Rif ^R , Gent ^R	[221]
Δ epsD-Tn <i>foX</i>	AI552 Δ VCI2733::FRT-Tn <i>foX</i> ; Rif ^R , Gent ^R	#
Δ mshL Δ pilA-Tn <i>foX</i>	AI552 Δ VCI0402::FRT Δ VCI2423-Tn <i>foX</i> ; Rif ^R , Gent ^R	#
Δ mshL-Tn <i>foX</i>	AI552 Δ VCI0402::FRT-Tn <i>foX</i> ; Rif ^R , Gent ^R	#
Δ pilA	AI552 Δ VCI2423; Rif ^R	[112]
Δ pilA Δ comEC-Tn <i>foX</i>	AI552 Δ VCI2423 Δ VCI1879-Tn <i>foX</i> ; Rif ^R , Gent ^R	[43]
Δ pilA-Tn <i>foX</i>	AI552 Δ VCI2423-Tn <i>foX</i> ; Rif ^R , Gent ^R	[43]
Δ pilB	AI552 Δ VCI2424; Rif ^R	[112]
Δ pilB Δ comEC::kan-Tn <i>foX</i>	AI552 Δ VCI2424 Δ VCI1879::FRT-kan-FRT-Tn <i>foX</i> ; Rif ^R , Gent ^R , Kan ^R	[43]
Δ pilB-Tn <i>foX</i>	AI552 Δ VCI2424-Tn <i>foX</i> ; Rif ^R , Gent ^R	[43]
Δ pilC	AI552 Δ VCI2425::FRT; Rif ^R	[43]
Δ pilC Δ comEC::kan-Tn <i>foX</i>	AI552 Δ VCI2425::FRT Δ VCI1879::FRT-kan-FRT-Tn <i>foX</i> ; Rif ^R , Gent ^R , Kan ^R	[43]

Continued on next page

Table A.1: continued

Strain	Genotype ¹	Source
Δ pilC-Tn <i>foX</i>	A1552 Δ VC2425::FRT-Tn <i>foX</i> ; Rif ^R , Gent ^R	[43]
Δ pilD	A1552 Δ VC2426::FRT; Rif ^R	[43]
Δ pilM	A1552 Δ VC2634::FRT; Rif ^R	[43]
Δ pilM Δ comEC::kan-Tn <i>foX</i>	A1552 Δ VC2634::FRT Δ VC1879::FRT-kan-FRT-Tn <i>foX</i> ; Rif ^R , Gent ^R , Kan ^R	[43]
Δ pilM-Tn <i>foX</i>	A1552 Δ VC2634::FRT-Tn <i>foX</i> ; Rif ^R , Gent ^R	[43]
Δ pilN	A1552 Δ VC2633::FRT; Rif ^R	[43]
Δ pilN Δ comEC-Tn <i>foX</i>	A1552 Δ VC2633::FRT Δ VC1879-Tn <i>foX</i> ; Rif ^R , Gent ^R	[43]
Δ pilN-Tn <i>foX</i>	A1552 Δ VC2633::FRT-Tn <i>foX</i> ; Rif ^R , Gent ^R	[43]
Δ pilO	A1552 Δ VC2632::FRT; Rif ^R	[43]
Δ pilO Δ comEC::kan-Tn <i>foX</i>	A1552 Δ VC2632::FRT Δ VC1879::FRT-kan-FRT-Tn <i>foX</i> ; Rif ^R , Gent ^R , Kan ^R	[43]
Δ pilO-Tn <i>foX</i>	A1552 Δ VC2632::FRT-Tn <i>foX</i> ; Rif ^R , Gent ^R	[43]
Δ pilP	A1552 Δ VC2631::FRT; Rif ^R	[43]
Δ pilP Δ comEC-Tn <i>foX</i>	A1552 Δ VC2631::FRT Δ VC1879-Tn <i>foX</i> ; Rif ^R , Gent ^R	[43]
Δ pilP-Tn <i>foX</i>	A1552 Δ VC2631::FRT-Tn <i>foX</i> ; Rif ^R , Gent ^R	[43]
Δ pilQ	A1552 Δ VC2630; Rif ^R	[112]
Δ pilQ Δ comEC-Tn <i>foX</i>	A1552 Δ VC2630 Δ VC1879-Tn <i>foX</i> ; Rif ^R , Gent ^R	[43]
Δ pilQ-Tn <i>foX</i>	A1552 Δ VC2630-Tn <i>foX</i> ; Rif ^R , Gent ^R	[43]
Δ pilT	A1552 Δ VC0462::FRT; Rif ^R	[43]
Δ pilT Δ comEC::kan-Tn <i>foX</i>	A1552 Δ VC0462::FRT Δ VC1879::FRT-kan-FRT-Tn <i>foX</i> ; Rif ^R , Gent ^R , Kan ^R	[43]
Δ pilT-Tn <i>foX</i>	A1552 Δ VC0462::FRT-Tn <i>foX</i> ; Rif ^R , Gent ^R	[43]
Δ pilU	A1552 Δ VC0463::FRT; Rif ^R	[43]
Δ recA	A1552 Δ VC0543; Rif ^R	[176]
Δ recA Δ comEC::kan-Tn <i>foX</i>	A1552 Δ VC0543 Δ VC1879::FRT-kan-FRT-Tn <i>foX</i> ; Rif ^R , Gent ^R , Kan ^R	[43]
Δ recA-Tn <i>foX</i>	A1552 Δ VC0543-Tn <i>foX</i> ; Rif ^R , Gent ^R	[43]
Δ VC0857	A1552 Δ VC0857; Rif ^R	[43]
Δ VC0857 Δ comEC::kan-Tn <i>foX</i>	A1552 Δ VC0857 Δ VC1879::FRT-kan-FRT-Tn <i>foX</i> ; Rif ^R , Gent ^R , Kan ^R	[43]
Δ VC0857-Tn <i>foX</i>	A1552 Δ VC0857-Tn <i>foX</i> ; Rif ^R , Gent ^R	[43]
Δ VC0858	A1552 Δ VC0858; Rif ^R	[43]
Δ VC0858 Δ comEC-Tn <i>foX</i>	A1552 Δ VC0858 Δ VC1879-Tn <i>foX</i> ; Rif ^R , Gent ^R	[43]
Δ VC0858-Tn <i>foX</i>	A1552 Δ VC0858-Tn <i>foX</i> ; Rif ^R , Gent ^R	[43]
Δ VC0859	A1552 Δ VC0859; Rif ^R	[43]

Continued on next page

Table A.1: continued

Strain	Genotype ¹	Source
Δ VCO859 Δ comEC::kan-Tn <i>foX</i>	A1552 Δ VCO859 Δ VCI879::FRT-kan-FRT-Tn <i>foX</i> ; Rif ^R , Gent ^R , Kan ^R	[43]
Δ VCO859-Tn <i>foX</i>	A1552 Δ VCO859-Tn <i>foX</i> ; Rif ^R , Gent ^R	[43]
Δ VCO860	A1552 Δ VCO860; Rif ^R	[43]
Δ VCO860 Δ comEC-Tn <i>foX</i>	A1552 Δ VCO860 Δ VCI879-Tn <i>foX</i> ; Rif ^R , Gent ^R	[43]
Δ VCO860-Tn <i>foX</i>	A1552 Δ VCO860-Tn <i>foX</i> ; Rif ^R , Gent ^R	[43]
Δ VCO861	A1552 Δ VCO861; Rif ^R	[43]
Δ VCO861 Δ comEC::kan-Tn <i>foX</i>	A1552 Δ VCO861 Δ VCI879::FRT-kan-FRT-Tn <i>foX</i> ; Rif ^R , Gent ^R , Kan ^R	[43]
Δ VCO861-Tn <i>foX</i>	A1552 Δ VCO861-Tn <i>foX</i> ; Rif ^R , Gent ^R	[43]
Δ pilF	A1552 Δ VCI1612; Rif ^R	[43]
Δ pilF Δ comEC::kan-Tn <i>foX</i>	A1552 Δ VCI1612 Δ VCI879::FRT-kan-FRT-Tn <i>foX</i> ; Rif ^R , Gent ^R , Kan ^R	[43]
Δ pilF-Tn <i>foX</i>	A1552 Δ VCI1612-Tn <i>foX</i> ; Rif ^R , Gent ^R	[43]
Δ VC1886	A1552 Δ VCI886::FRT; Rif ^R	#
Δ xds-Tn <i>foX</i>	A1552 Δ VCI2621-Tn <i>foX</i> ; Rif ^R , Gent ^R	[221]

¹ VC numbers according to [115]

Seitz & Blokesch, in preparation

unpublished

A.2 Plasmid list

Table A.2: List of plasmids used in this work

Plasmid	Description	Source
pBAD/Myc-HisA	pBR322-derived arabinose inducible expression vector; <i>araBAD</i> promoter (P_{BAD}); Amp ^R	Invitrogen
pUX-BF13	<i>oriR6K</i> , helper plasmid with Tn7 transposition function; Amp ^R	[261]
pGP704-Sac28	Suicide vector; <i>oriR6K</i> ; <i>sacB</i> ; Amp ^R	[158]
pGP704-28-SacB- Δ VVC0470	pGP704-Sac28 with a gene fragment resulting in a deletion within VVC0470; Amp ^R	[178]
pGP704-28-SacB- Δ VVC0857	pGP704-Sac28 with a gene fragment resulting in a deletion within VVC0857; Amp ^R	[43]
pGP704-28-SacB- Δ VVC0858	pGP704-Sac28 with a gene fragment resulting in a deletion within VVC0858; Amp ^R	[43]
pGP704-28-SacB- Δ VVC0859	pGP704-Sac28 with a gene fragment resulting in a deletion within VVC0859; Amp ^R	[43]
pGP704-28-SacB- Δ VVC0860	pGP704-Sac28 with a gene fragment resulting in a deletion within VVC0860; Amp ^R	[43]
pGP704-28-SacB- Δ VVC0861	pGP704-Sac28 with a gene fragment resulting in a deletion within VVC0861; Amp ^R	[43]
pGP704-28-SacB- Δ VVC1612	pGP704-Sac28 with a gene fragment resulting in a deletion within VVC1612; Amp ^R	[43]
pGP704-28-SacB- Δ VVC1879	pGP704-Sac28 with a gene fragment resulting in a deletion within VVC1879; Amp ^R	[176]
pGP704-28-SacB- Δ VVC2719	pGP704-Sac28 with a gene fragment resulting in a deletion within VVC2719; Amp ^R	[43]
pGP704-mTn7- <i>araC-fox</i>	pGP704 with mini-Tn7 carrying <i>araC</i> and P_{BAD} -driven <i>fox</i> ; Amp ^R	[164]
pBAD-pilA	<i>pilA</i> cloned into NcoI/EcoRI sites of pBAD/Myc-HisA; Amp ^R	[43]
pBAD-pilA-strep	<i>pilA-strep</i> cloned into NcoI/EcoRI sites of pBAD/Myc-HisA; Amp ^R	[43]
pBAD-pilB	<i>pilB</i> cloned into NcoI/EcoRI sites of pBAD/Myc-HisA; a <i>SmaI</i> site was introduced before the <i>pilB</i> stop codon; Amp ^R	[43]
pBAD-pilB ^{E394A}	derived from pBAD- <i>pilB</i> ; E394A point mutation encoding sequence was introduced in <i>pilB</i> by inverse PCR; Amp ^R	[43]
pBAD-pilB-gfp	<i>gfp</i> preceded by a sequence encoding a 5-aa linker cloned into the <i>SmaI</i> site of pBAD- <i>pilB</i> ; Amp ^R	[43]
pBAD-pilB ^{E394A} -gfp	derived from pBAD- <i>pilB-gfp</i> ; E394A point mutation encoding sequence was introduced in <i>pilB</i> by inverse PCR; Amp ^R	[43]
pBAD-pilC	<i>pilC</i> cloned into NcoI/EcoRI sites of pBAD/Myc-HisA; Amp ^R	[43]
pBAD-pilT	<i>pilT</i> cloned into blunted NcoI/EcoRI sites of pBAD/Myc-HisA; a <i>SmaI</i> site was introduced before the <i>pilT</i> stop codon; Amp ^R	[43]
pBAD-pilT-gfp	<i>gfp</i> preceded by a sequence encoding a 5-aa linker cloned into <i>SmaI</i> site of pBAD- <i>pilT</i> ; Amp ^R	[43]
pBAD-pilF	VVC1612 cloned into NcoI/XhoI sites of pBAD/Myc-HisA; Amp ^R	[43]
pBAD-pilM	<i>pilM</i> cloned into NcoI/EcoRI sites of pBAD/Myc-HisA; Amp ^R	[43]
pBAD-pilN	<i>pilN</i> ¹ cloned into NcoI/EcoRI sites of pBAD/Myc-HisA; Amp ^R	[43]
pBAD-pilO	<i>pilO</i> ¹ cloned into blunted NcoI/EcoRI sites of pBAD/Myc-HisA; Amp ^R	[43]
pBAD-pilP	<i>pilP</i> cloned into NcoI/EcoRI sites of pBAD/Myc-HisA; Amp ^R	[43]

Continued on next page

Table A.2: continued

Plasmid	Description	Source
pBAD-pilQ	<i>pilQ</i> ¹ cloned into NcoI/XhoI sites of pBAD/Myc-HisA; Amp ^R	[43]
pBAD-SacI-pilQ	derived from pBAD-pilQ by inverse PCR; a SacI site was introduced after the sequence predicted to encode the PilQ sec-dependent signal peptide cleavage site; Amp ^R	[43]
pBAD-mCherry-pilQ	<i>mCherry</i> preceded by a SacI site and followed by a sequence encoding a 3-aa linker plus a second SacI site was cloned into pBAD-SacI-pilQ; Amp ^R	[43]
pBAD-VC0857	VC0857 cloned into NcoI/EcoRI sites of pBAD/Myc-HisA; Amp ^R	[43]
pBAD-VC0858	VC0858 ¹ cloned into NcoI/EcoRI sites of pBAD/Myc-HisA; Amp ^R	[43]
pBAD-VC0859	VC0859 cloned into NcoI/EcoRI sites of pBAD/Myc-HisA; Amp ^R	[43]
pBAD-VC0860	VC0860 ¹ cloned into NcoI/EcoRI sites of pBAD/Myc-HisA; Amp ^R	[43]
pBAD-VC0861	VC0861 cloned into NcoI/EcoRI sites of pBAD/Myc-HisA; Amp ^R	[43]
pBAD-comEC	<i>comEC</i> ¹ cloned into blunted NcoI/EcoRI sites of pBAD/Myc-HisA; a SmaI site was introduced before the <i>comEC</i> stop codon; a SacI site was introduced before the <i>comEC</i> start codon; Amp ^R	[43]
pBAD-comEA	<i>comEA</i> cloned into NcoI/EcoRI sites of pBAD/Myc-HisA; Amp ^R	[164]
pBAD-comF	<i>comF</i> cloned into blunted NcoI/EcoRI sites of pBAD/Myc-HisA; Amp ^R	[43]
pBAD-recA	<i>recA</i> cloned into NcoI/EcoRI sites of pBAD/Myc-HisA; Amp ^R	[43]
pBAD(kan)	<i>bla</i> replaced by <i>aph</i> in pBAD/Myc-HisA; promoter region and MCS maintained; Kan ^R	[221]
pBAD(kan)-comEA	<i>comEA</i> gene cloned into pBAD(kan), arabinose inducible; Kan ^R	[221]
pBAD(kan)-comEA-mCherry	<i>comEA-mCherry</i> gene cloned into pBAD(kan), arabinose inducible; Kan ^R	[221]
pBAD(kan)-ss[ComEA]-mCherry	<i>ss[ComEA]-mCherry</i> gene cloned into pBAD(kan), arabinose inducible; Kan ^R	[221]
pBAD-tat-gfp	tat-dependent signal sequence of <i>torA</i> (VC1692) followed by a MCS translationally fused to <i>gfp</i> ; cloned into NcoI/HindIII sites of pBAD/Myc-HisA; arabinose inducible; Amp ^R	[221]
pBAD-tat-comEA-gfp	<i>comEA</i> lacking its native sec-dependent signal sequence cloned in frame into the MCS of pBAD-tat- <i>gfp</i> ; arabinose inducible; Amp ^R	[221]
pBAD- <i>tfoot</i> -stop	VC1153 (<i>tfoot</i>) in pBAD/Myc-HisA; arabinose inducible	[176]

¹ The predicted noncanonical start codon was exchanged for the canonical start codon ATG

References

- [1] Dunning Hotopp, J. C. (2011) Horizontal gene transfer between bacteria and animals. *Trends Genet* **27**, 157–63.
- [2] Ochman, H, Lawrence, J. G, & Groisman, E. A. (2000) Lateral gene transfer and the nature of bacterial innovation. *Nature* **405**, 299–304.
- [3] Boucher, Y, Douady, C. J, Papke, R. T, Walsh, D. A, Boudreau, M. E. R, Nesbø, C. L, Case, R. J, & Doolittle, W. F. (2003) Lateral gene transfer and the origins of prokaryotic groups. *Annu Rev Genet* **37**, 283–328.
- [4] Koonin, E. V & Wolf, Y. I. (2008) Genomics of bacteria and archaea: the emerging dynamic view of the prokaryotic world. *Nucleic Acids Res* **36**, 6688–719.
- [5] Cohan, F. M & Koeppel, A. F. (2008) The origins of ecological diversity in prokaryotes. *Curr Biol* **18**, R1024–34.
- [6] Wiedenbeck, J & Cohan, F. M. (2011) Origins of bacterial diversity through horizontal genetic transfer and adaptation to new ecological niches. *FEMS Microbiol Rev* **35**, 957–76.
- [7] Blattner, F. R, Plunkett III, G, Bloch, C. A, Perna, N, Burland, V, Riley, M, Collado-Vides, J, Glasner, J. D, Rode, C. K, Mayhew, G. F, Gregor, J, Davis, N. W, Kirkpatrick, H. A, Goeden, M. A, Rose, D. J, Mau, B, & Shao, Y. (1997) The Complete Genome Sequence of *Escherichia coli* K-12. *Science* **277**, 1453–1462.
- [8] Lawrence, J. G & Ochman, H. (1998) Molecular archaeology of the *Escherichia coli* genome. *Proc Natl Acad Sci U S A* **95**, 9413–7.
- [9] Griffith, F. (1928) The Significance of Pneumococcal Types. *J Hyg (Lond)* **27**, 113–159.
- [10] Avery, O. T, MacLeod, C. M, & McCarty, M. (1944) Studies on the chemical nature of the substance inducing transformatin of pneumococcal types: induction of transformation by a desoxyribonucleic acid fraction isolated from pneumococcus type III. *J Exp Med* **79**, 137–158.
- [11] Hacker, J, Bender, L, Ott, M, Wingender, J, Lund, B, Marre, R, & Goebel, W. (1990) Deletions of chromosomal regions coding for fimbriae and hemolysins occur *in vitro* and *in vivo* in various extraintestinal *Escherichia coli* isolates. *Microb Pathog* **8**, 213–225.
- [12] Hacker, J, Blum-Oehler, G, Mühldorfer, I, & Tschäpe, H. (1997) Pathogenicity islands of virulent bacteria: structure, function and impact on microbial evolution. *Mol Microbiol* **23**, 1089–1097.
- [13] Dobrindt, U, Hochhut, B, Hentschel, U, & Hacker, J. (2004) Genomic islands in pathogenic and environmental microorganisms. *Nat Rev Microbiol* **2**, 414–424.
- [14] Gal-Mor, O & Finlay, B. B. (2006) Pathogenicity islands: a molecular toolbox for bacterial virulence. *Cell Microbiol* **8**, 1707–1719.
- [15] Davies, J. (1995) Vicious circles: looking back on resistance plasmids. *Genetics* **139**, 1465–1468.
- [16] Davies, J & Davies, D. (2010) Origins and evolution of antibiotic resistance. *Microbiol Mol Biol Rev* **74**, 417–433.
- [17] Stokes, H. W & Gillings, M. R. (2011) Gene flow, mobile genetic elements and the recruitment of antibiotic resistance genes into Gram-negative pathogens. *FEMS Microbiol Rev* **35**, 790–819.
- [18] He, M, Sebahia, M, Lawley, T. D, Stabler, R. A, Dawson, L. F, Martin, M. J, Holt, K. E, Seth-Smith, H. M. B, Quail, M. A, Rance, R, Brooks, K, Churcher, C, Harris, D, Bentley, S. D, Burrows, C, Clark, L, Corton, C, Murray, V, Rose, G, Thurston, S, van Tonder, A, Walker, D, Wren, B. W, Dougan, G, & Parkhill, J. (2010) Evolutionary dynamics of *Clostridium difficile* over short and long time scales. *Proc Natl Acad Sci U S A* **107**, 7527–7532.

References

- [19] Ohnishi, M, Watanabe, Y, Ono, E, Takahashi, C, Oya, H, Kuroki, T, Shimuta, K, Okazaki, N, Nakayama, S, & Watanabe, H. (2010) Spread of a chromosomal cefixime-resistant *penA* gene among different *Neisseria gonorrhoeae* lineages. *Antimicrob Agents Chemother* **54**, 1060–1067.
- [20] Marri, P. R, Paniscus, M, Weyand, N. J, Rendon, M. A, Calton, C. M, Hernandez, D. R, Higashi, D. L, Sodergren, E, Weinstock, G. M, Rounsley, S. D, & So, M. (2010) Genome sequencing reveals widespread virulence gene exchange among human *Neisseria* species. *PLoS One* **5**, e11835.
- [21] Goren, M. G, Carmeli, Y, Schwaber, M. J, Chmelnitsky, I, Schechner, V, & Navon-Venezia, S. (2010) Transfer of carbapenem-resistant plasmid from *Klebsiella pneumoniae* ST258 to *Escherichia coli* in patient. *Emerg Infect Dis* **16**, 1014–1017.
- [22] Mathers, A. J, Cox, H. L, Kitchel, B, Bonatti, H, Brassinga, A. K. C, Carroll, J, Scheld, W. M, Hazen, K. C, & Sifri, C. D. (2011) Molecular dissection of an outbreak of carbapenem-resistant enterobacteriaceae reveals intergenus KPC carbapenemase transmission through a promiscuous plasmid. *MBio* **2**, e00204–11.
- [23] Lederberg, J & Tatum, E. L. (1946) Gene recombination in *Escherichia coli*. *Nature* **158**, 558.
- [24] Arutyunov, D & Frost, L. S. (2013) F conjugation: back to the beginning. *Plasmid* **70**, 18–32.
- [25] Madigan, M. T & Brock, T. D. (2009) *Brock biology of microorganisms*. (Pearson/Benjamin Cummings).
- [26] Morse, M. L, Lederberg, E. M, & Lederberg, J. (1956) Transduction in *Escherichia coli* K-12. *Genetics* **41**, 142–156.
- [27] Deflaun, M. F, Paul, J. H, & Jeffrey, W. H. (1987) Distribution and molecular weight of dissolved DNA in subtropical estuarine and oceanic environments. *Marine Ecology - Progress Series* **38**, 65–73.
- [28] Hurt, R. A, Qiu, X, Wu, L, Roh, Y, Palumbo, A. V, Tiedje, J. M, & Zhou, J. (2001) Simultaneous recovery of RNA and DNA from soils and sediments. *Appl Environ Microbiol* **67**, 4495–4503.
- [29] Tsai, Y. L & Olson, B. H. (1991) Rapid method for direct extraction of DNA from soil and sediments. *Appl Environ Microbiol* **57**, 1070–1074.
- [30] Fleischhacker, M, Schmidt, B, Weickmann, S, Fersching, D. M. I, Leszinski, G. S, Siegele, B, Stötzer, O. J, Nagel, D, & Holdenrieder, S. (2011) Methods for isolation of cell-free plasma DNA strongly affect DNA yield. *Clin Chim Acta* **412**, 2085–2088.
- [31] Thomas, C. M & Nielsen, K. M. (2005) Mechanisms of, and barriers to, horizontal gene transfer between bacteria. *Nat Rev Microbiol* **3**, 711–721.
- [32] Chen, I & Dubnau, D. (2004) DNA uptake during bacterial transformation. *Nat Rev Microbiol* **2**, 241–249.
- [33] Mortier-Barrière, I, Velten, M, Dupaigne, P, Mirouze, N, Piétremont, O, McGovern, S, Fichant, G, Martin, B, Noirot, P, Le Cam, E, Polard, P, & Claverys, J.-P. (2007) A key presynaptic role in transformation for a widespread bacterial protein: DprA conveys incoming ssDNA to RecA. *Cell* **130**, 824–836.
- [34] Majewski, J, Zawadzki, P, Pickerill, P, Cohan, F. M, & Dowson, C. G. (2000) Barriers to genetic exchange between bacterial species: *Streptococcus pneumoniae* transformation. *J Bacteriol* **182**, 1016–1023.
- [35] Claverys, J.-P, Martin, B, & Polard, P. (2009) The genetic transformation machinery: composition, localization, and mechanism. *FEMS Microbiol Rev* **33**, 643–656.
- [36] Prudhomme, M, Libante, V, & Claverys, J.-P. (2002) Homologous recombination at the border: insertion-deletions and the trapping of foreign DNA in *Streptococcus pneumoniae*. *Proc Natl Acad Sci U S A* **99**, 2100–2105.
- [37] de Vries, J & Wackernagel, W. (2002) Integration of foreign DNA during natural transformation of *Acinetobacter* sp. by homology-facilitated illegitimate recombination. *Proc Natl Acad Sci U S A* **99**, 2094–2099.
- [38] Meier, P & Wackernagel, W. (2003) Mechanisms of homology-facilitated illegitimate recombination for foreign DNA acquisition in transformable *Pseudomonas stutzeri*. *Mol Microbiol* **48**, 1107–1118.
- [39] Hülter, N & Wackernagel, W. (2008) Double illegitimate recombination events integrate DNA segments through two different mechanisms during natural transformation of *Acinetobacter baylyi*. *Mol Microbiol* **67**, 984–995.

- [40] Domingues, S, Harms, K, Fricke, W. F, Johnsen, P. J, da Silva, G. J, & Nielsen, K. M. (2012) Natural transformation facilitates transfer of transposons, integrons and gene cassettes between bacterial species. *PLoS Pathog* **8**, e1002837.
- [41] Johnsborg, O, Eldholm, V, & Håvarstein, L. S. (2007) Natural genetic transformation: prevalence, mechanisms and function. *Res Microbiol* **158**, 767–778.
- [42] Claverys, J.-P & Martin, B. (2003) Bacterial "competence" genes: signatures of active transformation, or only remnants? *Trends Microbiol* **11**, 161–165.
- [43] Seitz, P & Blokesch, M. (2013) Cues and regulatory pathways involved in natural competence and transformation in pathogenic and environmental Gram-negative bacteria. *FEMS Microbiol Rev* **37**, 336–363.
- [44] Redfield, R. J. (2001) Do bacteria have sex? *Nat Rev Genet* **2**, 634–639.
- [45] Finkel, S. E & Kolter, R. (2001) DNA as a nutrient: novel role for bacterial competence gene homologs. *J Bacteriol* **183**, 6288–6293.
- [46] Vos, M. (2009) Why do bacteria engage in homologous recombination? *Trends Microbiol* **17**, 226–232.
- [47] Otto, S. P & Lenormand, T. (2002) Resolving the paradox of sex and recombination. *Nat Rev Genet* **3**, 252–261.
- [48] Danner, D. B, Deich, R. A, Sisco, K. L, & Smith, H. O. (1980) An eleven-base-pair sequence determines the specificity of DNA uptake in *Haemophilus* transformation. *Gene* **11**, 311–318.
- [49] Elkins, C, Thomas, C. E, Seifert, H. S, & Sparling, P. F. (1991) Species-specific uptake of DNA by gonococci is mediated by a 10-base-pair sequence. *J Bacteriol* **173**, 3911–3913.
- [50] Aas, F. E, Wolfgang, M, Frye, S, Dunham, S, Løvold, C, & Koomey, M. (2002) Competence for natural transformation in *Neisseria gonorrhoeae*: components of DNA binding and uptake linked to type IV pilus expression. *Mol Microbiol* **46**, 749–760.
- [51] Claverys, J.-P & Håvarstein, L. S. (2007) Cannibalism and fratricide: mechanisms and raisons d'être. *Nat Rev Microbiol* **5**, 219–229.
- [52] Prudhomme, M, Attaiech, L, Sanchez, G, Martin, B, & Claverys, J.-P. (2006) Antibiotic stress induces genetic transformability in the human pathogen *Streptococcus pneumoniae*. *Science* **313**, 89–92.
- [53] Dorer, M. S, Fero, J, & Salama, N. R. (2010) DNA damage triggers genetic exchange in *Helicobacter pylori*. *PLoS Pathog* **6**, e1001026.
- [54] Charpentier, X, Kay, E, Schneider, D, & Shuman, H. A. (2011) Antibiotics and UV radiation induce competence for natural transformation in *Legionella pneumophila*. *J Bacteriol* **193**, 1114–1121.
- [55] Averhoff, B. (2009) Shuffling genes around in hot environments: the unique DNA transporter of *Thermus thermophilus*. *FEMS Microbiol Rev* **33**, 611–626.
- [56] Burton, B & Dubnau, D. (2010) Membrane-associated DNA transport machines. *Cold Spring Harb Perspect Biol* **2**, a000406.
- [57] Krüger, N.-J & Stingl, K. (2011) Two steps away from novelty - principles of bacterial DNA uptake. *Mol Microbiol* **80**, 860–867.
- [58] Allemand, J.-F, Maier, B, & Smith, D. E. (2012) Molecular motors for DNA translocation in prokaryotes. *Curr Opin Biotechnol* **23**, 503–509.
- [59] Craig, L, Pique, M. E, & Tainer, J. A. (2004) Type IV pilus structure and bacterial pathogenicity. *Nat Rev Microbiol* **2**, 363–378.
- [60] Melville, S & Craig, L. (2013) Type IV pili in Gram-positive bacteria. *Microbiol Mol Biol Rev* **77**, 323–341.
- [61] Giltner, C. L, Nguyen, Y, & Burrows, L. L. (2012) Type IV pilin proteins: versatile molecular modules. *Microbiol Mol Biol Rev* **76**, 740–772.
- [62] Peabody, C. R, Chung, Y. J, Yen, M.-R, Vidal-Ingigliardi, D, Pugsley, A. P, & Saier, M. H. J. (2003) Type II protein secretion and its relationship to bacterial type IV pili and archaeal flagella. *Microbiology* **149**, 3051–3072.

References

- [63] Korotkov, K. V, Sandkvist, M, & Hol, W. G. J. (2012) The type II secretion system: biogenesis, molecular architecture and mechanism. *Nat Rev Microbiol* **10**, 336–351.
- [64] Burrows, L. L. (2012) *Pseudomonas aeruginosa* twitching motility: type IV pili in action. *Annu Rev Microbiol* **66**, 493–520.
- [65] Cianciotto, N. P. (2005) Type II secretion: a protein secretion system for all seasons. *Trends Microbiol* **13**, 581–588.
- [66] Sandkvist, M. (2001) Type II secretion and pathogenesis. *Infect Immun* **69**, 3523–3535.
- [67] Pelicic, V. (2008) Type IV pili: e pluribus unum? *Mol Microbiol* **68**, 827–837.
- [68] Hazes, B, Sastry, P. A, Hayakawa, K, Read, R. J, & Irvin, R. T. (2000) Crystal structure of *Pseudomonas aeruginosa* PAK pilin suggests a main-chain-dominated mode of receptor binding. *J Mol Biol* **299**, 1005–1017.
- [69] Craig, L, Taylor, R. K, Pique, M. E, Adair, B. D, Arvai, A. S, Singh, M, Lloyd, S. J, Shin, D. S, Getzoff, E. D, Yeager, M, Forest, K. T, & Tainer, J. A. (2003) Type IV pilin structure and assembly: X-ray and EM analyses of *Vibrio cholerae* toxin-coregulated pilus and *Pseudomonas aeruginosa* PAK pilin. *Mol Cell* **11**, 1139–1150.
- [70] Nunn, D, Bergman, S, & Lory, S. (1990) Products of three accessory genes, *pilB*, *pilC*, and *pilD*, are required for biogenesis of *Pseudomonas aeruginosa* pili. *J Bacteriol* **172**, 2911–2919.
- [71] Marsh, J. W & Taylor, R. K. (1998) Identification of the *Vibrio cholerae* type 4 prepilin peptidase required for cholera toxin secretion and pilus formation. *Mol Microbiol* **29**, 1481–1492.
- [72] Collins, R. F, Frye, S. A, Kitmitto, A, Ford, R. C, Tønjum, T, & Derrick, J. P. (2004) Structure of the *Neisseria meningitidis* outer membrane PilQ secretin complex at 12 Å resolution. *J Biol Chem* **279**, 39750–39756.
- [73] Frye, S. A, Assalkhou, R, Collins, R. F, Ford, R. C, Petersson, C, Derrick, J. P, & Tønjum, T. (2006) Topology of the outer-membrane secretin PilQ from *Neisseria meningitidis*. *Microbiology* **152**, 3751–3764.
- [74] Berry, J.-L, Phelan, M. M, Collins, R. F, Adomavicius, T, Tønjum, T, Frye, S. A, Bird, L, Owens, R, Ford, R. C, Lian, L.-Y, & Derrick, J. P. (2012) Structure and assembly of a trans-periplasmic channel for type IV pili in *Neisseria meningitidis*. *PLoS Pathog* **8**, e1002923.
- [75] Collins, R. F, Frye, S. A, Balasingham, S, Ford, R. C, Tønjum, T, & Derrick, J. P. (2005) Interaction with type IV pili induces structural changes in the bacterial outer membrane secretin PilQ. *J Biol Chem* **280**, 18923–18930.
- [76] Wolfgang, M, van Putten, J. P, Hayes, S. F, Dorward, D, & Koomey, M. (2000) Components and dynamics of fiber formation define a ubiquitous biogenesis pathway for bacterial pili. *EMBO J* **19**, 6408–6418.
- [77] Carbonnelle, E, Hélaine, S, Prouvensier, L, Nassif, X, & Pelicic, V. (2005) Type IV pilus biogenesis in *Neisseria meningitidis*: PilW is involved in a step occurring after pilus assembly, essential for fibre stability and function. *Mol Microbiol* **55**, 54–64.
- [78] Merz, A. J, So, M, & Sheetz, M. P. (2000) Pilus retraction powers bacterial twitching motility. *Nature* **407**, 98–102.
- [79] Morand, P. C, Bille, E, Morelle, S, Eugene, E, Beretti, J.-L, Wolfgang, M, Meyer, T. F, Koomey, M, & Nassif, X. (2004) Type IV pilus retraction in pathogenic *Neisseria* is regulated by the PilC proteins. *EMBO J* **23**, 2009–2017.
- [80] Satyshur, K. A, Worzalla, G. A, Meyer, L. S, Heiniger, E. K, Aukema, K. G, Mistic, A. M, & Forest, K. T. (2007) Crystal structures of the pilus retraction motor PilT suggest large domain movements and subunit cooperation drive motility. *Structure* **15**, 363–376.
- [81] Mistic, A. M, Satyshur, K. A, & Forest, K. T. (2010) *P. aeruginosa* PilT structures with and without nucleotide reveal a dynamic type IV pilus retraction motor. *J Mol Biol* **400**, 1011–1021.
- [82] Maier, B, Potter, L, So, M, Long, C. D, Seifert, H. S, & Sheetz, M. P. (2002) Single pilus motor forces exceed 100 pN. *Proc Natl Acad Sci U S A* **99**, 16012–16017.
- [83] Clausen, M, Jakovljevic, V, Søgaard-Andersen, L, & Maier, B. (2009) High-force generation is a conserved property of type IV pilus systems. *J Bacteriol* **191**, 4633–4638.

- [84] Allemand, J.-F & Maier, B. (2009) Bacterial translocation motors investigated by single molecule techniques. *FEMS Microbiol Rev* **33**, 593–610.
- [85] Hamilton, H. L & Dillard, J. P. (2006) Natural transformation of *Neisseria gonorrhoeae*: from DNA donation to homologous recombination. *Mol Microbiol* **59**, 376–385.
- [86] Cehovin, A, Simpson, P J, McDowell, M. A, Brown, D. R, Noschese, R, Pallett, M, Brady, J, Baldwin, G. S, Lea, S. M, Matthews, S. J, & Pelicic, V. (2013) Specific DNA recognition mediated by a type IV pilin. *Proc Natl Acad Sci U S A* **110**, 3065–3070.
- [87] Kidane, D & Graumann, P. L. (2005) Intracellular protein and DNA dynamics in competent *Bacillus subtilis* cells. *Cell* **122**, 73–84.
- [88] Hahn, J, Maier, B, Haijema, B. J, Sheetz, M, & Dubnau, D. (2005) Transformation proteins and DNA uptake localize to the cell poles in *Bacillus subtilis*. *Cell* **122**, 59–71.
- [89] Kaufenstein, M, van der Laan, M, & Graumann, P. L. (2011) The three-layered DNA uptake machinery at the cell pole in competent *Bacillus subtilis* cells is a stable complex. *J Bacteriol* **193**, 1633–1642.
- [90] Pugsley, A. P. (1993) The complete general secretory pathway in gram-negative bacteria. *Microbiol Rev* **57**, 50–108.
- [91] Provvedi, R & Dubnau, D. (1999) ComEA is a DNA receptor for transformation of competent *Bacillus subtilis*. *Mol Microbiol* **31**, 271–280.
- [92] Maier, B, Chen, I, Dubnau, D, & Sheetz, M. P. (2004) DNA transport into *Bacillus subtilis* requires proton motive force to generate large molecular forces. *Nat Struct Mol Biol* **11**, 643–649.
- [93] Maier, B, Koomey, M, & Sheetz, M. P. (2004) A force-dependent switch reverses type IV pilus retraction. *Proc Natl Acad Sci U S A* **101**, 10961–10966.
- [94] Inamine, G. S & Dubnau, D. (1995) ComEA, a *Bacillus subtilis* integral membrane protein required for genetic transformation, is needed for both DNA binding and transport. *J Bacteriol* **177**, 3045–3051.
- [95] Chen, I & Gotschlich, E. C. (2001) ComE, a competence protein from *Neisseria gonorrhoeae* with DNA-binding activity. *J Bacteriol* **183**, 3160–3168.
- [96] Kramer, N, Hahn, J, & Dubnau, D. (2007) Multiple interactions among the competence proteins of *Bacillus subtilis*. *Mol Microbiol* **65**, 454–464.
- [97] Draskovic, I & Dubnau, D. (2005) Biogenesis of a putative channel protein, ComEC, required for DNA uptake: membrane topology, oligomerization and formation of disulphide bonds. *Mol Microbiol* **55**, 881–896.
- [98] Facius, D, Fussenegger, M, & Meyer, T. F. (1996) Sequential action of factors involved in natural competence for transformation of *Neisseria gonorrhoeae*. *FEMS Microbiol Lett* **137**, 159–164.
- [99] Londoño-Vallejo, J. A & Dubnau, D. (1994) Mutation of the putative nucleotide binding site of the *Bacillus subtilis* membrane protein ComFA abolishes the uptake of DNA during transformation. *J Bacteriol* **176**, 4642–4645.
- [100] Marians, K. J. (2000) PriA-directed replication fork restart in *Escherichia coli*. *Trends Biochem Sci* **25**, 185–189.
- [101] Kline, K. A & Seifert, H. S. (2005) Mutation of the *priA* gene of *Neisseria gonorrhoeae* affects DNA transformation and DNA repair. *J Bacteriol* **187**, 5347–5355.
- [102] Provvedi, R, Chen, I, & Dubnau, D. (2001) NucA is required for DNA cleavage during transformation of *Bacillus subtilis*. *Mol Microbiol* **40**, 634–644.
- [103] Chaussee, M. S & Hill, S. A. (1998) Formation of single-stranded DNA during DNA transformation of *Neisseria gonorrhoeae*. *J Bacteriol* **180**, 5117–5122.
- [104] Stingl, K, Müller, S, Scheidgen-Kleyboldt, G, Clausen, M, & Maier, B. (2010) Composite system mediates two-step DNA uptake into *Helicobacter pylori*. *Proc Natl Acad Sci U S A* **107**, 1184–1189.
- [105] Bergé, M, Moscoso, M, Prudhomme, M, Martin, B, & Claverys, J.-P. (2002) Uptake of transforming DNA in Gram-positive bacteria: a view from *Streptococcus pneumoniae*. *Mol Microbiol* **45**, 411–421.

References

- [106] Hofreuter, D, Odenbreit, S, & Haas, R. (2001) Natural transformation competence in *Helicobacter pylori* is mediated by the basic components of a type IV secretion system. *Mol Microbiol* **41**, 379–391.
- [107] Karnholz, A, Hoefler, C, Odenbreit, S, Fischer, W, Hofreuter, D, & Haas, R. (2006) Functional and topological characterization of novel components of the *comB* DNA transformation competence system in *Helicobacter pylori*. *J Bacteriol* **188**, 882–893.
- [108] Cascales, E & Christie, P. J. (2003) The versatile bacterial type IV secretion systems. *Nat Rev Microbiol* **1**, 137–149.
- [109] Hornick, R. B, Music, S. I, Wenzel, R, Cash, R, Libonati, J. P, Snyder, M. J, & Woodward, T. E. (1971) The Broad Street pump revisited: response of volunteers to ingested cholera vibrios. *Bull NY Acad Med* **47**, 1181–1191.
- [110] Chun, J, Grim, C. J, Hasan, N. A, Lee, J. H, Choi, S. Y, Haley, B. J, Taviani, E, Jeon, Y.-S, Kim, D. W, Lee, J.-H, Brettin, T. S, Bruce, D. C, Challacombe, J. F, Detter, J. C, Han, C. S, Munk, A. C, Chertkov, O, Meincke, L, Saunders, E, Walters, R. A, Huq, A, Nair, G. B, & Colwell, R. R. (2009) Comparative genomics reveals mechanism for short-term and long-term clonal transitions in pandemic *Vibrio cholerae*. *Proc Natl Acad Sci U S A* **106**, 15442–15447.
- [111] Cho, Y.-J, Yi, H, Lee, J. H, Kim, D. W, & Chun, J. (2010) Genomic evolution of *Vibrio cholerae*. *Curr Opin Microbiol* **13**, 646–651.
- [112] Meibom, K. L, Blokesch, M, Dolganov, N. A, Wu, C.-Y, & Schoolnik, G. K. (2005) Chitin induces natural competence in *Vibrio cholerae*. *Science* **310**, 1824–1827.
- [113] Koch, R. (1884) An Address on Cholera and its Bacillus. *Br Med J* **2**, 403–407.
- [114] Harris, J. B, LaRocque, R. C, Qadri, F, Ryan, E. T, & Calderwood, S. B. (2012) Cholera. *Lancet* **379**, 2466–2476.
- [115] Heidelberg, J. F, Eisen, J. A, Nelson, W. C, Clayton, R. A, Gwinn, M. L, Dodson, R. J, Haft, D. H, Hickey, E. K, Peterson, J. D, Umayam, L, Gill, S. R, Nelson, K. E, Read, T. D, Tettelin, H, Richardson, D, Ermolaeva, M. D, Vamathevan, J, Bass, S, Qin, H, Dragoi, I, Sellers, P, McDonald, L, Utterback, T, Fleishmann, R. D, Nierman, W. C, White, O, Salzberg, S. L, Smith, H. O, Colwell, R. R, Mekalanos, J. J, Venter, J. C, & Fraser, C. M. (2000) DNA sequence of both chromosomes of the cholera pathogen *Vibrio cholerae*. *Nature* **406**, 477–483.
- [116] Walton, D. A & Ivers, L. C. (2011) Responding to cholera in post-earthquake Haiti. *N Engl J Med* **364**, 3–5.
- [117] Sack, D. A, Sack, R. B, Nair, G. B, & Siddique, A. K. (2004) Cholera. *Lancet* **363**, 223–233.
- [118] World Health Organization. (2012) Cholera fact sheet No. 107.
- [119] Nelson, E. J, Nelson, D. S, Salam, M. A, & Sack, D. A. (2011) Antibiotics for both moderate and severe cholera. *N Engl J Med* **364**, 5–7.
- [120] Okeke, I. N, Aboderin, O. A, Byarugaba, D. K, Ojo, K. K, & Opintan, J. A. (2007) Growing problem of multidrug-resistant enteric pathogens in Africa. *Emerg Infect Dis* **13**, 1640–1646.
- [121] Vanden Broeck, D, Horvath, C, & De Wolf, M. J. S. (2007) *Vibrio cholerae*: cholera toxin. *Int J Biochem Cell Biol* **39**, 1771–1775.
- [122] Sánchez, J & Holmgren, J. (2008) Cholera toxin structure, gene regulation and pathophysiological and immunological aspects. *Cell Mol Life Sci* **65**, 1347–1360.
- [123] Taylor, R. K, Miller, V. L, Furlong, D. B, & Mekalanos, J. J. (1987) Use of *phoA* gene fusions to identify a pilus colonization factor coordinately regulated with cholera toxin. *Proc Natl Acad Sci U S A* **84**, 2833–2837.
- [124] Herrington, D. A, Hall, R. H, Losonsky, G, Mekalanos, J. J, Taylor, R. K, & Levine, M. M. (1988) Toxin, toxin-coregulated pili, and the *toxR* regulon are essential for *Vibrio cholerae* pathogenesis in humans. *J Exp Med* **168**, 1487–1492.
- [125] Krebs, S. J & Taylor, R. K. (2011) Protection and attachment of *Vibrio cholerae* mediated by the toxin-coregulated pilus in the infant mouse model. *J Bacteriol* **193**, 5260–5270.
- [126] Kirn, T. J, Lafferty, M. J, Sandoe, C. M, & Taylor, R. K. (2000) Delineation of pilin domains required for bacterial association into microcolonies and intestinal colonization by *Vibrio cholerae*. *Mol Microbiol* **35**, 896–910.

- [127] Faruque, S. M & Mekalanos, J. J. (2003) Pathogenicity islands and phages in *Vibrio cholerae* evolution. *Trends Microbiol* **11**, 505–510.
- [128] Karaolis, D. K, Johnson, J. A, Bailey, C. C, Boedeker, E. C, Kaper, J. B, & Reeves, P. R. (1998) A *Vibrio cholerae* pathogenicity island associated with epidemic and pandemic strains. *Proc Natl Acad Sci U S A* **95**, 3134–3139.
- [129] Waldor, M. K & Mekalanos, J. J. (1996) Lysogenic conversion by a filamentous phage encoding cholera toxin. *Science* **272**, 1910–1914.
- [130] World Health Organization. (2013) Cholera, 2012. *Wkly Epidemiol Rec* **88**, 321–334.
- [131] Ali, M, Lopez, A. L, You, Y. A, Kim, Y. E, Sah, B, Maskery, B, & Clemens, J. (2012) The global burden of cholera. *Bull World Health Organ* **90**, 209–218.
- [132] Chatterjee, S. N & Chaudhuri, K. (2003) Lipopolysaccharides of *Vibrio cholerae*. I. Physical and chemical characterization. *Biochim Biophys Acta* **1639**, 65–79.
- [133] Barua, D. (1972) The global epidemiology of cholera in recent years. *Proc R Soc Med* **65**, 423–428.
- [134] Ryan, E. T. (2011) The cholera pandemic, still with us after half a century: time to rethink. *PLoS Negl Trop Dis* **5**, e1003.
- [135] Ramamurthy, T, Garg, S, Sharma, R, Bhattacharya, S. K, Nair, G. B, Shimada, T, Takeda, T, Karasawa, T, Kurazano, H, & Pal, A. (1993) Emergence of novel strain of *Vibrio cholerae* with epidemic potential in southern and eastern India. *Lancet* **341**, 703–704.
- [136] Bik, E. M, Bunschoten, A. E, Gouw, R. D, & Mooi, F. R. (1995) Genesis of the novel epidemic *Vibrio cholerae* O139 strain: evidence for horizontal transfer of genes involved in polysaccharide synthesis. *EMBO J* **14**, 209–216.
- [137] Blokesch, M & Schoolnik, G. K. (2007) Serogroup conversion of *Vibrio cholerae* in aquatic reservoirs. *PLoS Pathog* **3**, e81.
- [138] Colwell, R. R, Kaper, J, & Joseph, S. W. (1977) *Vibrio cholerae*, *Vibrio parahaemolyticus*, and other vibrios: occurrence and distribution in Chesapeake Bay. *Science* **198**, 394–396.
- [139] Colwell, R. R, Seidler, R. J, Kaper, J, Joseph, S. W, Garges, S, Lockman, H, Maneval, D, Bradford, H, Roberts, N, Remmers, E, Huq, I, & Huq, A. (1981) Occurrence of *Vibrio cholerae* serotype O1 in Maryland and Louisiana estuaries. *Appl Environ Microbiol* **41**, 555–558.
- [140] Huq, A, Small, E. B, West, P. A, Huq, M. I, Rahman, R, & Colwell, R. R. (1983) Ecological relationships between *Vibrio cholerae* and planktonic crustacean copepods. *Appl Environ Microbiol* **45**, 275–283.
- [141] Huq, A, West, P. A, Small, E. B, Huq, M. I, & Colwell, R. R. (1984) Influence of water temperature, salinity, and pH on survival and growth of toxigenic *Vibrio cholerae* serovar O1 associated with live copepods in laboratory microcosms. *Appl Environ Microbiol* **48**, 420–424.
- [142] Tamplin, M. L, Gauzens, A. L, Huq, A, Sack, D. A, & Colwell, R. R. (1990) Attachment of *Vibrio cholerae* serogroup O1 to zooplankton and phytoplankton of Bangladesh waters. *Appl Environ Microbiol* **56**, 1977–1980.
- [143] Colwell, R. R. (1996) Global climate and infectious disease: the cholera paradigm. *Science* **274**, 2025–2031.
- [144] Lipp, E. K, Huq, A, & Colwell, R. R. (2002) Effects of global climate on infectious disease: the cholera model. *Clin Microbiol Rev* **15**, 757–770.
- [145] Pruzzo, C, Vezzulli, L, & Colwell, R. R. (2008) Global impact of *Vibrio cholerae* interactions with chitin. *Environ Microbiol* **10**, 1400–1410.
- [146] Colwell, R. R, Huq, A, Islam, M. S, Aziz, K. M. A, Yunus, M, Khan, N. H, Mahmud, A, Sack, R. B, Nair, G. B, Chakraborty, J, Sack, D. A, & Russek-Cohen, E. (2003) Reduction of cholera in Bangladeshi villages by simple filtration. *Proc Natl Acad Sci U S A* **100**, 1051–1055.
- [147] Alam, M, Hasan, N. A, Sadique, A, Bhuiyan, N. A, Ahmed, K. U, Nusrin, S, Nair, G. B, Siddique, A. K, Sack, R. B, Sack, D. A, Huq, A, & Colwell, R. R. (2006) Seasonal cholera caused by *Vibrio cholerae* serogroups O1 and O139 in the coastal aquatic environment of Bangladesh. *Appl Environ Microbiol* **72**, 4096–4104.

References

- [148] Glass, R. I, Becker, S, Huq, M. I, Stoll, B. J, Khan, M. U, Merson, M. H, Lee, J. V, & Black, R. E. (1982) Endemic cholera in rural Bangladesh, 1966-1980. *Am J Epidemiol* **116**, 959–970.
- [149] Lobitz, B, Beck, L, Huq, A, Wood, B, Fuchs, G, Faruque, A. S, & Colwell, R. (2000) Climate and infectious disease: use of remote sensing for detection of *Vibrio cholerae* by indirect measurement. *Proc Natl Acad Sci U S A* **97**, 1438–1443.
- [150] Longini, I. M. J, Yunus, M, Zaman, K, Siddique, A. K, Sack, R. B, & Nizam, A. (2002) Epidemic and endemic cholera trends over a 33-year period in Bangladesh. *J Infect Dis* **186**, 246–251.
- [151] Colwell, R. R & Huq, A. (1994) Environmental reservoir of *Vibrio cholerae*. The causative agent of cholera. *Ann NY Acad Sci* **740**, 44–54.
- [152] Xu, H.-S, Roberts, N, Singleton, F. L, Attwell, R. W, Grimes, D. J, & Colwell, R. R. (1982) Survival and Viability of Nonculturable Escherichia coli and *Vibrio cholerae* in the Estuarine and Marine Environment. *Microbial Ecology* **8**, pp. 313–323.
- [153] Brayton, P. R, Tamplin, M. L, Huq, A, & Colwell, R. R. (1987) Enumeration of *Vibrio cholerae* O1 in Bangladesh waters by fluorescent-antibody direct viable count. *Appl Environ Microbiol* **53**, 2862–2865.
- [154] Vezzulli, L, Pruzzo, C, Huq, A, & Colwell, R. R. (2010) Environmental reservoirs of *Vibrio cholerae* and their role in cholera. *Environ Microbiol Rep* **2**, 27–33.
- [155] Baron, S, Lesne, J, Moore, S, Rossignol, E, Rebaudet, S, Gazin, P, Barraix, R, Magloire, R, Boncy, J, & Piarroux, R. (2013) No evidence of significant levels of toxigenic *V. cholerae* O1 in the Haitian aquatic environment during the 2012 rainy season. *PLoS Curr* **5**.
- [156] Keyhani, N. O & Roseman, S. (1999) Physiological aspects of chitin catabolism in marine bacteria. *Biochim Biophys Acta* **1473**, 108–122.
- [157] Connell, T. D, Metzger, D. J, Lynch, J, & Folster, J. P. (1998) Endochitinase is transported to the extracellular milieu by the eps-encoded general secretory pathway of *Vibrio cholerae*. *J Bacteriol* **180**, 5591–5600.
- [158] Meibom, K. L, Li, X. B, Nielsen, A. T, Wu, C.-Y, Roseman, S, & Schoolnik, G. K. (2004) The *Vibrio cholerae* chitin utilization program. *Proc Natl Acad Sci U S A* **101**, 2524–2529.
- [159] Sun, Y, Bernardy, E. E, Hammer, B. K, & Miyashiro, T. (2013) Competence and natural transformation in vibrios. *Mol Microbiol* **89**, 583–595.
- [160] Lo Scudato, M & Blokesch, M. (2012) The regulatory network of natural competence and transformation of *Vibrio cholerae*. *PLoS Genet* **8**, e1002778.
- [161] Li, X & Roseman, S. (2004) The chitinolytic cascade in *Vibrios* is regulated by chitin oligosaccharides and a two-component chitin catabolic sensor/kinase. *Proc Natl Acad Sci U S A* **101**, 627–631.
- [162] Yamamoto, S, Morita, M, Izumiya, H, & Watanabe, H. (2010) Chitin disaccharide (GlcNAc)₂ induces natural competence in *Vibrio cholerae* through transcriptional and translational activation of a positive regulatory gene *tfoX_{VC}*. *Gene* **457**, 42–49.
- [163] Yamamoto, S, Izumiya, H, Mitobe, J, Morita, M, Arakawa, E, Ohnishi, M, & Watanabe, H. (2011) Identification of a chitin-induced small RNA that regulates translation of the *tfoX* gene, encoding a positive regulator of natural competence in *Vibrio cholerae*. *J Bacteriol* **193**, 1953–1965.
- [164] Lo Scudato, M & Blokesch, M. (2013) A transcriptional regulator linking quorum sensing and chitin induction to render *Vibrio cholerae* naturally transformable. *Nucleic Acids Res* **41**, 3644–3658.
- [165] Blokesch, M. (2012) Chitin colonization, chitin degradation and chitin-induced natural competence of *Vibrio cholerae* are subject to catabolite repression. *Environ Microbiol* **14**, 1898–1912.
- [166] Deutscher, J. (2008) The mechanisms of carbon catabolite repression in bacteria. *Curr Opin Microbiol* **11**, 87–93.
- [167] Ng, W.-L & Bassler, B. L. (2009) Bacterial quorum-sensing network architectures. *Annu Rev Genet* **43**, 197–222.

- [168] Bassler, B. L, Greenberg, E. P, & Stevens, A. M. (1997) Cross-species induction of luminescence in the quorum-sensing bacterium *Vibrio harveyi*. *J Bacteriol* **179**, 4043–4045.
- [169] Miller, M. B, Skorupski, K, Lenz, D. H, Taylor, R. K, & Bassler, B. L. (2002) Parallel quorum sensing systems converge to regulate virulence in *Vibrio cholerae*. *Cell* **110**, 303–314.
- [170] Xavier, K. B & Bassler, B. L. (2003) LuxS quorum sensing: more than just a numbers game. *Curr Opin Microbiol* **6**, 191–197.
- [171] Lenz, D. H, Mok, K. C, Lilley, B. N, Kulkarni, R. V, Wingreen, N. S, & Bassler, B. L. (2004) The small RNA chaperone Hfq and multiple small RNAs control quorum sensing in *Vibrio harveyi* and *Vibrio cholerae*. *Cell* **118**, 69–82.
- [172] Bardill, J. P, Zhao, X, & Hammer, B. K. (2011) The *Vibrio cholerae* quorum sensing response is mediated by Hfq-dependent sRNA/mRNA base pairing interactions. *Mol Microbiol* **80**, 1381–1394.
- [173] Zhu, J, Miller, M. B, Vance, R. E, Dziejman, M, Bassler, B. L, & Mekalanos, J. J. (2002) Quorum-sensing regulators control virulence gene expression in *Vibrio cholerae*. *Proc Natl Acad Sci U S A* **99**, 3129–3134.
- [174] Zhu, J & Mekalanos, J. J. (2003) Quorum sensing-dependent biofilms enhance colonization in *Vibrio cholerae*. *Dev Cell* **5**, 647–656.
- [175] Hammer, B. K & Bassler, B. L. (2003) Quorum sensing controls biofilm formation in *Vibrio cholerae*. *Mol Microbiol* **50**, 101–104.
- [176] Suckow, G, Seitz, P, & Blokesch, M. (2011) Quorum sensing contributes to natural transformation of *Vibrio cholerae* in a species-specific manner. *J Bacteriol* **193**, 4914–4924.
- [177] Antonova, E. S & Hammer, B. K. (2011) Quorum-sensing autoinducer molecules produced by members of a multispecies biofilm promote horizontal gene transfer to *Vibrio cholerae*. *FEMS Microbiol Lett* **322**, 68–76.
- [178] Blokesch, M & Schoolnik, G. K. (2008) The extracellular nuclease Dns and its role in natural transformation of *Vibrio cholerae*. *J Bacteriol* **190**, 7232–7240.
- [179] Fullner, K. J & Mekalanos, J. J. (1999) Genetic characterization of a new type IV-A pilus gene cluster found in both classical and El Tor biotypes of *Vibrio cholerae*. *Infect Immun* **67**, 1393–1404.
- [180] Kamp, H. D, Patimalla-Dipali, B, Lazinski, D. W, Wallace-Gadsden, F, & Camilli, A. (2013) Gene Fitness Landscapes of *Vibrio cholerae* at Important Stages of Its Life Cycle. *PLoS Pathog* **9**, e1003800.
- [181] Chao, M. C, Pritchard, J. R, Zhang, Y. J, Rubin, E. J, Livny, J, Davis, B. M, & Waldor, M. K. (2013) High-resolution definition of the *Vibrio cholerae* essential gene set with hidden Markov model-based analyses of transposon-insertion sequencing data. *Nucleic Acids Res* **41**, 9033–9048.
- [182] Marvig, R. L & Blokesch, M. (2010) Natural transformation of *Vibrio cholerae* as a tool—optimizing the procedure. *BMC Microbiol* **10**, 155.
- [183] De Souza Silva, O & Blokesch, M. (2010) Genetic manipulation of *Vibrio cholerae* by combining natural transformation with FLP recombination. *Plasmid* **64**, 186–195.
- [184] Jeong, H, Barbe, V, Lee, C. H, Vallenet, D, Yu, D. S, Choi, S.-H, Couloux, A, Lee, S.-W, Yoon, S. H, Cattolico, L, Hur, C.-G, Park, H.-S, Segurens, B, Kim, S. C, Oh, T. K, Lenski, R. E, Studier, F. W, Daegelen, P, & Kim, J. E. (2009) Genome sequences of *Escherichia coli* B strains REL606 and BL21(DE3). *J Mol Biol* **394**, 644–652.
- [185] Martin, B, Garcia, P, Castanie, M. P, & Claverys, J. P. (1995) The *recA* gene of *Streptococcus pneumoniae* is part of a competence-induced operon and controls lysogenic induction. *Mol Microbiol* **15**, 367–379.
- [186] Karudapuram, S, Zhao, X, & Barcak, G. J. (1995) DNA sequence and characterization of *Haemophilus influenzae* *dprA*⁺, a gene required for chromosomal but not plasmid DNA transformation. *J Bacteriol* **177**, 3235–3240.
- [187] Bergé, M, Mortier-Barrière, I, Martin, B, & Claverys, J.-P. (2003) Transformation of *Streptococcus pneumoniae* relies on DprA- and RecA-dependent protection of incoming DNA single strands. *Mol Microbiol* **50**, 527–536.
- [188] Lambertsen, L, Sternberg, C, & Molin, S. (2004) Mini-Tn7 transposons for site-specific tagging of bacteria with fluorescent proteins. *Environ Microbiol* **6**, 726–732.

References

- [189] Koo, J, Tammam, S, Ku, S.-Y, Sampaleanu, L. M, Burrows, L. L, & Howell, P. L. (2008) PilF is an outer membrane lipoprotein required for multimerization and localization of the *Pseudomonas aeruginosa* Type IV pilus secretin. *J Bacteriol* **190**, 6961–6969.
- [190] Koo, J, Tang, T, Harvey, H, Tammam, S, Sampaleanu, L, Burrows, L. L, & Howell, P. L. (2013) Functional mapping of PilF and PilQ in the *Pseudomonas aeruginosa* type IV pilus system. *Biochemistry* **52**, 2914–2923.
- [191] Collins, R. F, Saleem, M, & Derrick, J. P. (2007) Purification and three-dimensional electron microscopy structure of the *Neisseria meningitidis* type IV pilus biogenesis protein PilG. *J Bacteriol* **189**, 6389–6396.
- [192] Karuppiyah, V, Collins, R. F, Thistlethwaite, A, Gao, Y, & Derrick, J. P. (2013) Structure and assembly of an inner membrane platform for initiation of type IV pilus biogenesis. *Proc Natl Acad Sci U S A* **110**, E4638–47.
- [193] Friedrich, C, Bulyha, I, & Sogaard-Andersen, L. (2014) Outside-In Assembly Pathway of the Type IV Pilus System in *Myxococcus xanthus*. *J Bacteriol* **196**, 378–390.
- [194] Tammam, S, Sampaleanu, L. M, Koo, J, Sundaram, P, Ayers, M, Chong, P. A, Forman-Kay, J. D, Burrows, L. L, & Howell, P. L. (2011) Characterization of the PilN, PilO and PilP type IVa pilus subcomplex. *Mol Microbiol* **82**, 1496–1514.
- [195] Balasingham, S. V, Collins, R. F, Assalkhou, R, Homberset, H, Frye, S. A, Derrick, J. P & Tønjum, T. (2007) Interactions between the lipoprotein PilP and the secretin PilQ in *Neisseria meningitidis*. *J Bacteriol* **189**, 5716–5727.
- [196] Cisneros, D. A, Bond, P. J, Pugsley, A. P, Campos, M, & Francetic, O. (2012) Minor pseudopilin self-assembly primes type II secretion pseudopilus elongation. *EMBO J* **31**, 1041–1053.
- [197] Londoño-Vallejo, J. A & Dubnau, D. (1993) *comF*, a *Bacillus subtilis* late competence locus, encodes a protein similar to ATP-dependent RNA/DNA helicases. *Mol Microbiol* **9**, 119–131.
- [198] Cameron, D. E, Urbach, J. M, & Mekalanos, J. J. (2008) A defined transposon mutant library and its use in identifying motility genes in *Vibrio cholerae*. *Proc Natl Acad Sci U S A* **105**, 8736–8741.
- [199] Meyer, R. R & Laine, P. S. (1990) The single-stranded DNA-binding protein of *Escherichia coli*. *Microbiol Rev* **54**, 342–380.
- [200] Cameron, A. D. S & Redfield, R. J. (2008) CRP binding and transcription activation at CRP-S sites. *J Mol Biol* **383**, 313–323.
- [201] Yadav, T, Carrasco, B, Hejna, J, Suzuki, Y, Takeyasu, K, & Alonso, J. C. (2013) *Bacillus subtilis* DprA recruits RecA onto single-stranded DNA and mediates annealing of complementary strands coated by SsbB and SsbA. *J Biol Chem* **288**, 22437–22450.
- [202] Mirouze, N, Bergé, M. A, Soulet, A.-L, Mortier-Barrière, I, Quentin, Y, Fichant, G, Granadel, C, Noirot-Gros, M.-F, Noirot, P, Polard, P, Martin, B, & Claverys, J.-P. (2013) Direct involvement of DprA, the transformation-dedicated RecA loader, in the shut-off of pneumococcal competence. *Proc Natl Acad Sci U S A* **110**, E1035–44.
- [203] Ando, T, Israel, D. A, Kusugami, K, & Blaser, M. J. (1999) HP0333, a member of the *dprA* family, is involved in natural transformation in *Helicobacter pylori*. *J Bacteriol* **181**, 5572–5580.
- [204] Smeets, L. C, Bijlsma, J. J, Kuipers, E. J, Vandenbroucke-Grauls, C. M, & Kusters, J. G. (2000) The *dprA* gene is required for natural transformation of *Helicobacter pylori*. *FEMS Immunol Med Microbiol* **27**, 99–102.
- [205] Ogura, M, Yamaguchi, H, Kobayashi, K, Ogasawara, N, Fujita, Y, & Tanaka, T. (2002) Whole-genome analysis of genes regulated by the *Bacillus subtilis* competence transcription factor ComK. *J Bacteriol* **184**, 2344–2351.
- [206] Tadesse, S & Graumann, P. L. (2007) DprA/Smf protein localizes at the DNA uptake machinery in competent *Bacillus subtilis* cells. *BMC Microbiol* **7**, 105.
- [207] Sinha, S, Mell, J. C, & Redfield, R. J. (2012) Seventeen Sxy-dependent cyclic AMP receptor protein site-regulated genes are needed for natural transformation in *Haemophilus influenzae*. *J Bacteriol* **194**, 5245–5254.
- [208] Seitz, P & Blokesch, M. (2013) DNA-uptake machinery of naturally competent *Vibrio cholerae*. *Proc Natl Acad Sci U S A* **110**, 17987–17992.

- [209] Dubnau, D. (1999) DNA uptake in bacteria. *Annu Rev Microbiol* **53**, 217–244.
- [210] Chiavelli, D. A, Marsh, J. W, & Taylor, R. K. (2001) The mannose-sensitive hemagglutinin of *Vibrio cholerae* promotes adherence to zooplankton. *Appl Environ Microbiol* **67**, 3220–3225.
- [211] Bakkali, M. (2013) Could DNA uptake be a side effect of bacterial adhesion and twitching motility? *Arch Microbiol* **195**, 279–289.
- [212] Duffin, P. M & Seifert, H. S. (2010) DNA uptake sequence-mediated enhancement of transformation in *Neisseria gonorrhoeae* is strain dependent. *J Bacteriol* **192**, 4436–4444.
- [213] Frye, S. A, Nilsen, M, Tønjum, T, & Ambur, O. H. (2013) Dialects of the DNA uptake sequence in *Neisseriaceae*. *PLoS Genet* **9**, e1003458.
- [214] Smith, H. O, Gwinn, M. L, & Salzberg, S. L. (1999) DNA uptake signal sequences in naturally transformable bacteria. *Res Microbiol* **150**, 603–616.
- [215] Henke, J. M & Bassler, B. L. (2004) Three parallel quorum-sensing systems regulate gene expression in *Vibrio harveyi*. *J Bacteriol* **186**, 6902–6914.
- [216] Scott, M. E, Dossani, Z. Y, & Sandkvist, M. (2001) Directed polar secretion of protease from single cells of *Vibrio cholerae* via the type II secretion pathway. *Proc Natl Acad Sci U S A* **98**, 13978–13983.
- [217] Filloux, A. (2004) The underlying mechanisms of type II protein secretion. *Biochim Biophys Acta* **1694**, 163–179.
- [218] Jakovljevic, V, Leonardy, S, Hoppert, M, & Søgaard-Andersen, L. (2008) PilB and PilT are ATPases acting antagonistically in type IV pilus function in *Myxococcus xanthus*. *J Bacteriol* **190**, 2411–2421.
- [219] Lybarger, S. R, Johnson, T. L, Gray, M. D, Sikora, A. E, & Sandkvist, M. (2009) Docking and assembly of the type II secretion complex of *Vibrio cholerae*. *J Bacteriol* **191**, 3149–3161.
- [220] Bulyha, I, Schmidt, C, Lenz, P, Jakovljevic, V, Höne, A, Maier, B, Hoppert, M, & Søgaard-Andersen, L. (2009) Regulation of the type IV pili molecular machine by dynamic localization of two motor proteins. *Mol Microbiol* **74**, 691–706.
- [221] Seitz, P, Pezeshgi Modarres, H, Borgeaud, S, Bulushev, R. D, Steinbock, L. J, Radenovic, A, Dal Peraro, M, & Blokesch, M. (2014) ComeA is essential for the transfer of external DNA into the periplasm in naturally transformable *Vibrio cholerae* cells. *PLoS Genet* **10**, e1004066.
- [222] Ishikawa-Ankerhold, H. C, Ankerhold, R, & Drummen, G. P. C. (2012) Advanced fluorescence microscopy techniques-FRAP, FLIP, FLAP, FRET and FLIM. *Molecules* **17**, 4047–4132.
- [223] Jeon, B & Zhang, Q. (2007) Cj0011c, a periplasmic single- and double-stranded DNA-binding protein, contributes to natural transformation in *Campylobacter jejuni*. *J Bacteriol* **189**, 7399–7407.
- [224] Feilmeier, B. J, Iseminger, G, Schroeder, D, Webber, H, & Phillips, G. J. (2000) Green fluorescent protein functions as a reporter for protein localization in *Escherichia coli*. *J Bacteriol* **182**, 4068–4076.
- [225] Larsson, A, Carlsson, C, Jonsson, M, & Albinsson, B. (1994) Characterization of the binding of the fluorescent dyes YO and YOYO to DNA by polarized light spectroscopy. *J Am Chem Soc* **116**, 8459–8465.
- [226] Dinh, T & Bernhardt, T. G. (2011) Using superfolder green fluorescent protein for periplasmic protein localization studies. *J Bacteriol* **193**, 4984–4987.
- [227] Focareta, T & Manning, P. A. (1991) Distinguishing between the extracellular DNases of *Vibrio cholerae* and development of a transformation system. *Mol Microbiol* **5**, 2547–2555.
- [228] Focareta, T & Manning, P. A. (1991) Genetic analysis of the export of an extracellular DNase of *Vibrio cholerae* using DNase-beta-lactamase fusions. *Gene* **108**, 31–37.
- [229] Renzette, N, Gumlaw, N, Nordman, J. T, Krieger, M, Yeh, S.-P, Long, E, Centore, R, Boonsombat, R, & Sandler, S. J. (2005) Localization of RecA in *Escherichia coli* K-12 using RecA-GFP. *Mol Microbiol* **57**, 1074–1085.
- [230] Sliusarenko, O, Heinritz, J, Emonet, T, & Jacobs-Wagner, C. (2011) High-throughput, subpixel precision analysis of bacterial morphogenesis and intracellular spatio-temporal dynamics. *Mol Microbiol* **80**, 612–627.

References

- [231] Allen, S. P, Polazzi, J. O, Gierse, J. K, & Easton, A. M. (1992) Two novel heat shock genes encoding proteins produced in response to heterologous protein expression in *Escherichia coli*. *J Bacteriol* **174**, 6938–6947.
- [232] Lindner, A. B, Madden, R, Demarez, A, Stewart, E. J, & Taddei, F. (2008) Asymmetric segregation of protein aggregates is associated with cellular aging and rejuvenation. *Proc Natl Acad Sci U S A* **105**, 3076–3081.
- [233] Ratajczak, E, Zietkiewicz, S, & Liberek, K. (2009) Distinct activities of *Escherichia coli* small heat shock proteins IbpA and IbpB promote efficient protein disaggregation. *J Mol Biol* **386**, 178–189.
- [234] Van der Henst, C, Charlier, C, Deghelt, M, Wouters, J, Matroule, J.-Y, Letesson, J.-J, & De Bolle, X. (2010) Over-produced *Brucella abortus* PdhS-mCherry forms soluble aggregates in *Escherichia coli*, partially associating with mobile foci of IbpA-YFP. *BMC Microbiol* **10**, 248.
- [235] Petersen, T. N, Brunak, S, von Heijne, G, & Nielsen, H. (2011) SignalP 4.0: discriminating signal peptides from transmembrane regions. *Nat Methods* **8**, 785–786.
- [236] Chen, I, Christie, P. J, & Dubnau, D. (2005) The ins and outs of DNA transfer in bacteria. *Science* **310**, 1456–1460.
- [237] Craig, L, Volkmann, N, Arvai, A. S, Pique, M. E, Yeager, M, Egelman, E. H, & Tainer, J. A. (2006) Type IV pilus structure by cryo-electron microscopy and crystallography: implications for pilus assembly and functions. *Mol Cell* **23**, 651–662.
- [238] Mandelkern, M, Elias, J. G, Eden, D, & Crothers, D. M. (1981) The dimensions of DNA in solution. *J Mol Biol* **152**, 153–161.
- [239] Inamdar, M. M, Gelbart, W. M, & Phillips, R. (2006) Dynamics of DNA ejection from bacteriophage. *Biophys J* **91**, 411–420.
- [240] Salman, H, Zbaida, D, Rabin, Y, Chatenay, D, & Elbaum, M. (2001) Kinetics and mechanism of DNA uptake into the cell nucleus. *Proc Natl Acad Sci U S A* **98**, 7247–7252.
- [241] Peskin, C. S, Odell, G. M, & Oster, G. F. (1993) Cellular motions and thermal fluctuations: the Brownian ratchet. *Biophys J* **65**, 316–324.
- [242] Simon, S. M, Peskin, C. S, & Oster, G. F. (1992) What drives the translocation of proteins? *Proc Natl Acad Sci U S A* **89**, 3770–3774.
- [243] Ambjörnsson, Tobias and Metzler, Ralf. (2004) Chaperone-assisted translocation. *Phys Biol* **1**, 77–88.
- [244] Matias, V. R. F & Beveridge, T. J. (2005) Cryo-electron microscopy reveals native polymeric cell wall structure in *Bacillus subtilis* 168 and the existence of a periplasmic space. *Mol Microbiol* **56**, 240–251.
- [245] Bergé, M. J, Kamgoué, A, Martin, B, Polard, P, Campo, N, & Claverys, J.-P. (2013) Midcell recruitment of the DNA uptake and virulence nuclease, EndA, for pneumococcal transformation. *PLoS Pathog* **9**, e1003596.
- [246] Lacks, S, Greenberg, B, & Neuberger, M. (1975) Identification of a deoxyribonuclease implicated in genetic transformation of *Diplococcus pneumoniae*. *J Bacteriol* **123**, 222–232.
- [247] Puyet, A, Greenberg, B, & Lacks, S. A. (1990) Genetic and structural characterization of *endA*. A membrane-bound nuclease required for transformation of *Streptococcus pneumoniae*. *J Mol Biol* **213**, 727–738.
- [248] Lacks, S & Neuberger, M. (1975) Membrane location of a deoxyribonuclease implicated in the genetic transformation of *Diplococcus pneumoniae*. *J Bacteriol* **124**, 1321–1329.
- [249] Rosenthal, A. L & Lacks, S. A. (1980) Complex structure of the membrane nuclease of *Streptococcus pneumoniae* revealed by two-dimensional electrophoresis. *J Mol Biol* **141**, 133–146.
- [250] Beiter, K, Wartha, F, Albiger, B, Normark, S, Zychlinsky, A, & Henriques-Normark, B. (2006) An endonuclease allows *Streptococcus pneumoniae* to escape from neutrophil extracellular traps. *Curr Biol* **16**, 401–407.
- [251] Seper, A, Fengler, V. H. I, Roier, S, Wolinski, H, Kohlwein, S. D, Bishop, A. L, Camilli, A, Reidl, J, & Schild, S. (2011) Extracellular nucleases and extracellular DNA play important roles in *Vibrio cholerae* biofilm formation. *Mol Microbiol* **82**, 1015–1037.
- [252] Eldin, S, Forget, A. L, Lindenmuth, D. M, Logan, K. M, & Knight, K. L. (2000) Mutations in the N-terminal region of RecA that disrupt the stability of free protein oligomers but not RecA-DNA complexes. *J Mol Biol* **299**, 91–101.

- [253] Balaban, M, Battig, P, Muschiol, S, Tirier, S. M, Wartha, F, Normark, S, & Henriques-Normark, B. (2014) Secretion of a pneumococcal type II secretion system pilus correlates with DNA uptake during transformation. *Proc Natl Acad Sci U S A* **111**, E758–65.
- [254] Laurenceau, R, Péhau-Arnaudet, G, Bacconnais, S, Gault, J, Malosse, C, Dujeancourt, A, Campo, N, Chamot-Rooke, J, Le Cam, E, Claverys, J.-P, & Fronzes, R. (2013) A type IV pilus mediates DNA binding during natural transformation in *Streptococcus pneumoniae*. *PLoS Pathog* **9**, e1003473.
- [255] Grange, W, Duckely, M, Husale, S, Jacob, S, Engel, A, & Hegner, M. (2008) VirE2: a unique ssDNA-compacting molecular machine. *PLoS Biol* **6**, e44.
- [256] Hahn, J, Albano, M, & Dubnau, D. (1987) Isolation and characterization of Tn917lac-generated competence mutants of *Bacillus subtilis*. *J Bacteriol* **169**, 3104–3109.
- [257] Yildiz, F. H & Schoolnik, G. K. (1998) Role of *rpoS* in stress survival and virulence of *Vibrio cholerae*. *J Bacteriol* **180**, 773–784.
- [258] Reyes-Lamothe, R, Possoz, C, Danilova, O, & Sherratt, D. J. (2008) Independent positioning and action of *Escherichia coli* replisomes in live cells. *Cell* **133**, 90–102.
- [259] Yanisch-Perron, C, Vieira, J, & Messing, J. (1985) Improved M13 phage cloning vectors and host strains: nucleotide sequences of the M13mp18 and pUC19 vectors. *Gene* **33**, 103–119.
- [260] Blokesch, M. (2012) TransFLP—a method to genetically modify *Vibrio cholerae* based on natural transformation and FLP-recombination. *J Vis Exp*.
- [261] Bao, Y, Lies, D. P, Fu, H, & Roberts, G. P. (1991) An improved Tn7-based system for the single-copy insertion of cloned genes into chromosomes of Gram-negative bacteria. *Gene* **109**, 167–168.
- [262] Peterson, J. D, Umayam, L. A, Dickinson, T, Hickey, E. K, & White, O. (2001) The Comprehensive Microbial Resource. *Nucleic Acids Res* **29**, 123–125.
- [263] Lechat, P, Hummel, L, Rousseau, S, & Moszer, I. (2008) GenoList: an integrated environment for comparative analysis of microbial genomes. *Nucleic Acids Res* **36**, D469–74.
- [264] R Development Core Team. (2008) *R: A Language and Environment for Statistical Computing* (R Foundation for Statistical Computing, Vienna, Austria). ISBN 3-900051-07-0.
- [265] Laemmli, U. K. (1970) Cleavage of structural proteins during the assembly of the head of bacteriophage T4. *Nature* **227**, 680–685.
- [266] Sambrook, J & Russell, D. (2001) *Molecular Cloning: A Laboratory Manual*, Molecular Cloning: A Laboratory Manual. (Cold Spring Harbor Laboratory Press) No. Bd. 1.

Curriculum Vitae

Personal information

Name	Patrick Seitz
Date of birth	August 14 th , 1983
Citizenship	Swiss
Email	ptrk.seitz@gmail.com

Education and research experience

Since May 2010	PhD thesis in molecular microbiology École Polytechnique Fédérale de Lausanne (EPFL) “Mechanistic aspects of DNA uptake in naturally competent <i>Vibrio cholerae</i> ” Supervision: Prof. Melanie Blokesch
2008 - 2010	Master of Science in Biology with major in “Infection Biology” Swiss Tropical and Public Health Institute, Basel “Localization, mode of action and target identification of a new antimalarial compound ” (graded 6.0/6.0) Supervision: Prof. Hans-Peter Beck, Prof. Reto Brun, Dr. Matthias Rottmann
2006 - 2008	Bachelor of Science in Biology, University of Basel Further studies of the mathematical curriculum, University of Basel
2004 - 2006	Basic studies in biology and mathematics, University of Basel

Work experience

Since May 2010	PhD student at the Global Health Institute, EPFL (Lausanne)
2008 - 2009	Teacher of mathematics at the Berufsfachschule (BFS) Basel (part time)
2005 - 2008	Waiter, restaurant Safran Zunft, Basel (part time)
2004	Windsurf instructor, 1 season (Windsurfing Sempachersee)

Languages

German	native
English	fluent
French	fluent (oral), basic (written)
Italian	basic

Key skills

Scientific	Sterile working techniques with biosafety level 2 organisms Genetic engineering of <i>Vibrio cholerae</i> and molecular cloning Immunostaining and fluorescence (time-lapse) microscopy Protein detection by SDS-PAGE/silver staining/western blot analysis Planning, implementation and evaluation of molecular biology experiments Communication of scientific results to expert/non-expert audiences
------------	--

Teaching	Extensive teaching experience at the Berufsfachschule Basel (mathematics) and as a teaching assistant at the EPFL (biology) Sports coach J + S (Jugend und Sport) in gymnastics and windsurfing
IT	Statistical data analysis using 'R' Image editing (ImageJ, Illustrator, Photoshop) Microsoft Office (Word, Excel, Powerpoint) Document typesetting using LaTeX Basic Linux skills

Scientific publications

- **Seitz, P**, Pezeshgi Modarres, H, Borgeaud, S, Bulushev, R. D, Steinbock, L. J, Radenovic, A, Dal Peraro, M, & Blokesch, M. (2014) ComEA is essential for the transfer of external DNA into the periplasm in naturally transformable *Vibrio cholerae* cells. *PLoS Genet* 10, e1004066.
- **Seitz, P** & Blokesch, M. (2013) DNA-uptake machinery of naturally competent *Vibrio cholerae*. *Proc Natl Acad Sci U S A* 110, 17987-17992.
- **Seitz, P**, & Blokesch, M. (2013) Cues and regulatory pathways involved in natural competence and transformation in pathogenic and environmental Gram-negative bacteria. *FEMS Microbiol Rev* 37, 336-363.
- Suckow, G, **Seitz, P**, & Blokesch, M. (2011) Quorum sensing contributes to natural transformation of *Vibrio cholerae* in a species-specific manner. *J Bacteriol* 193, 4914-4924.
- Rottmann, M, McNamara, C, Yeung, B.K.S, Lee, M.C.S, Zou, B, Russell, B, **Seitz, P**, Plouffe, D.M, Dharia, N.V, Tan, J, Cohen, S. B, Spencer, K. R, Gonzalez-Paez, G. E, Lakshminarayana, S. B, Goh, A, Suwanarusk, R, Jegla, T, Schmitt, E. K, Beck, H.-P, Brun, R, Nosten, F, Renia, L, Dartois, V, Keller, T. H, Fidock, D. A, Winzeler, E. A, & Diagana, T. T. (2010) Spiroindolones, a potent compound class for the treatment of malaria. *Science* 329, 1175-1180.

Awards and honors

- "The Erling Seeberg Outstanding Poster Award" (1st price) at the 4th Genome Maintenance Meeting 2013, Oslo, Norway
- Poster prize (3rd place) at the 71st Annual Congress of the Swiss Society of Microbiology (SSM), 2013
- FEMS Young Scientist Meeting Grant (2013)
- "Best Oral Presentation Award" at the CUSO (Conférence Universitaire de Suisse Occidentale) PhD retreat 2011

Interests

- Sports (long distance running, mountaineering, windsurfing)
- Active member and sports coach at the Sportverein Lausen (1991 - 2010)
- Traveling (recent trips to the Middle East and to South East Asia)

Acknowledgements

After exciting years at the EPFL, I would like to express my deepest gratitude to those who made this thesis possible. First of all, I would like to thank my supervisor Prof. Melanie Blokesch, who not only guided me through my PhD project, but who also always took the time to discuss any open question or problem, and who constantly supported me during the last four years. Her unparalleled passion for science was truly inspiring.

Equally I would like to thank all present and former members of the Blokesch-lab, in particular: Gaia Suckow and Mirella Lo Scudato for helping me to get started (both colleagues started their PhD thesis before me); the former and present skilled technicians in the lab, Olga de Souza Silva, Clémentine Thévoz, Tiziana Scignari and Sandrine Borgeaud for keeping the lab running and occasionally assisting in experiments; the post-docs in the lab, Lisa Metzger, Juliane Kühn and Charles Van der Henst for their advice, scientific discussions, many enjoyable coffee/lunch breaks and motivating words, when I needed them; and finally, the lab's secretary Marisa Marciano Wynn for always helping with flight bookings, conference registrations, and with any other administrative issue. Thanks to all of you it was a great pleasure and a true privilege to work in this lab.

I would also like to express my gratitude to all members from neighboring labs who made the GHI a great place to work and who readily provided advice and help, when I had questions. I deeply appreciated the countless chats and the general positive atmosphere on our floor. Furthermore, I would like to acknowledge Arne Seitz and Thierry Laroche from the EPFL BioImaging and Optics Core Facility (BIOP), who were instrumental for the FLIP experiments.

I also thank Peter Seitz, Juliane Kühn, Lalit Kumar, Sachin Kotak and Ruben Hartkoorn for reading parts of this manuscript and providing helpful suggestions.

This thesis would not have been possible without the tremendous support of my family, whom I could always count on and who is always here for me. The same is true for my friends, who encouraged me in difficult times and enjoyed life with me when things were going fine. I owe them my sincere gratitude.

Finally, I would like to thank Christina Baumann for always being by my side, for her endless patience and empathy during difficult periods of my PhD project, and for all the memorable moments that we shared in the last four years.

Lausanne, 03 Mars 2014